

**Regulation der Translation von SAPAP3 mRNA  
Molekülen in *Rattus norvegicus***

**Dissertation**

**zur Erlangung des Doktorgrades  
des Department Biologie  
der Universität Hamburg**

vorgelegt von

**CHUA JIA EN JOHN**  
aus SINGAPORE

Hamburg 2006

**Translational Regulation of mRNAs Encoding  
SAPAP3 in *Rattus norvegicus***

**A DISSERTATION**

SUBMITTED FOR THE DOCTORAL DEGREE  
DEPARTMENT OF BIOLOGY  
UNIVERSITY OF HAMBURG

BY

**CHUA JIA EN JOHN**  
from SINGAPORE

Hamburg 2006

Genehmigt vom Department Biologie  
der Fakultät für Mathematik, Informatik und Naturwissenschaften  
an der Universität Hamburg  
auf Antrag von Herrn Professor Dr. D. RICHTER  
Weiterer Gutachter der Dissertation:  
Herr Professor Dr. K. WIESE  
Tag der Disputation: 12. Mai 2006

Hamburg, den 28. April 2006



A handwritten signature in black ink, consisting of a large 'R' followed by a cursive 'L' and 'e'.

Professor Dr. Reinhard Lieberei  
Leiter des Departments

---

<b><u>TABLE OF CONTENTS</u></b>		<b><u>Page</u></b>
Table of Contents		i
Abbreviations		iv
<b>1</b>	<b>Introduction</b>	
1.1	An Overview of the Cap-dependent Mechanism of Eukaryotic Translation Initiation	1
1.2	Recognizing the Initiator Codon	2
1.3	Regulation of Translation by the 5' Untranslated Region of mRNAs	3
1.3.1	Secondary Structures and RNA binding proteins	4
1.3.2	Upstream Open Reading Frames – Leaky Scanning versus Translational Re-initiation	5
1.4	Variations on a Theme: Alternative Translational Initiation based on Leaky Scanning and Re-initiation Mechanisms	7
1.5	The SAP90/PSD-95-Associated Protein (SAPAP) family of proteins	9
1.6	Purpose of This Study	11
<b>2</b>	<b>Materials and Methods</b>	
2.1	Materials	
2.1.1	Chemicals	13
2.1.2	Microbial Strains, Laboratory Animals and Cell Lines	13
2.1.3	Plasmid DNA	13
2.1.3.1	Basic Vectors	13
2.1.3.2	Vectors generated in this study	14
2.1.4	Antibodies	16
2.1.5	Oligonucleotides	16
2.2	Methods	
2.2.1	Molecular Biology Techniques	17
2.2.1.1	Preparation of Total RNA	17
2.2.1.2	Quantitation of Nucleic Acids	17
2.2.1.3	Synthesis of cDNA and 5' RACE cDNA	17
2.2.1.4	Polymerase Chain Reaction	17
2.2.1.5	Agarose Gel Electrophoresis	18
2.2.1.6	Excision and Purification of DNA bands	19
2.2.1.7	Molecular Cloning	19
2.2.1.8	Site-directed Mutagenesis	19
2.2.1.9	DNA Sequencing	20
2.2.1.10	Northern Blot	20

2.2.2	Cell Biology Techniques	21
2.2.2.1	Culture and Transient Transfection of Established Cell Lines	21
2.2.2.2	Preparation of Primary Hippocampal and Cortical Neuron Cultures	21
2.2.2.3	Stimulation of Neuronal Cultures by Spaced Stimuli Protocol	22
2.2.3	Immunofluorescence Techniques	23
2.2.3.1	Cell Fixation and Permeabilization	23
2.2.3.2	Labeling with Antibodies	23
2.2.3.3	Image Acquisition	24
2.2.4	Biochemical Techniques	24
2.2.4.1	SDS-Polyacrylamide-Gel-Electrophoresis (SDS-PAGE)	24
2.2.4.2	Western Blotting	24
2.2.4.3	Luciferase Assays	25
2.2.4.4	Translation Initiation Assays	25
2.2.4.5	<i>In vitro</i> Competition Experiments	26
2.2.4.6	Biochemical Isolation of Post-Synaptic Densities	27
2.2.4.7	Production and Affinity Purification of Anti-SAPAP antibodies	27
<b>3</b>	<b>Results</b>	
3.1	SAPAP3 Expression Profile	29
3.1.1	SAPAP3 is Specifically Expressed in the Brain and is Strongly Enriched in the Post-Synaptic Density	29
3.1.2	SAPAP3 mRNAs and Proteins are Developmentally Regulated	31
3.2	5' Untranslated Regions (UTRs) of SAPAP3 Transcripts	33
3.2.1	SAPAP3 mRNAs Possess Different 5' UTRs	33
3.2.2	SAPAP3 5' UTR is a Strong Inhibitor of Translational	42
3.2.3	SAPAP3 5' UTR is Sufficient to Confer Translational Inhibition	47
3.2.4	SAPAP3 5' UTR does not function as an IRES	49
3.2.5	Synaptic Activity does not Modulate Translational Inhibition	51
3.3	Mechanisms of Translational Inhibition Mediated by SAPAP3 5' UTR	53
3.3.1	SAPAP3 5' UTR Inhibits Formation of the 80S Ribosome	53
3.3.2	Translational Inhibition is not Mediated by <i>trans</i> -acting Factors	59
3.3.3	An uORF is Responsible for Mediating Translational Inhibition by SAPAP3 5' UTR	61
3.4	Biological Significance of Translational Regulation in SAPAP3	65
3.4.1	SAPAP3 5' UTR Mediates Expression of Two SAPAP3 Isoforms from a Single Transcript	65
3.4.2	SAPAP3 $\beta$ is Synthesized from a Downstream Alternative Start Codon	67
3.4.3	Expression of SAPAP3 Isoforms in Different Regions of the Adult Rat Brain	69

3.4.4	Morphological Changes in Neurons Over-expressing SAPAP3	70
<b>4</b>	<b>Discussion</b>	73
<b>5</b>	<b>Summary</b>	85
<b>6</b>	<b>References</b>	86
<b>7</b>	<b>Appendices</b>	
	Appendix I: Primers synthesized in this study	A1-i
	Appendix II: MFOLD predicted RNA folding structures for E1B variant SAPAP3 5' UTR	A2-i
	<b>Erklärung</b>	
	<b>Bibliography</b>	

**ABBREVIATIONS**

<b>Acc. No.</b>	accession number in GenBank ( <a href="http://www.ncbi.nlm.nih.gov">www.ncbi.nlm.nih.gov</a> )
<b>Amp</b>	Ampicillin
<b>ATI</b>	alternative translational initiation
<b>AUG</b>	start codon
<b>bp</b>	base pair(s)
<b>BSA</b>	bovine serum albumin
<b>°C</b>	degree Celsius
<b>cDNA</b>	complementary deoxyribonucleic acid
<b>CDS</b>	coding sequence
<b>DMEM</b>	Dulbecco's modified Eagle's medium
<b>DMSO</b>	Dimethylsulfoxide
<b>DNA</b>	deoxyribonucleic acid
<b>dNTP</b>	deoxyribonucleoside 5'-triphosphate
<b>EGFP</b>	enhanced green fluorescence protein
<b>FBS</b>	fetal bovine serum
<b>g</b>	gram(s)
<b>GST</b>	glutathione S-transferase
<b>h</b>	hour(s)
<b>HEK</b>	human embryonic kidney
<b>Ig</b>	Immunoglobulin
<b>kb</b>	kilobase(s)
<b>kDa</b>	kilodalton(s)
<b>l</b>	liter(s)
<b>M</b>	Molarity
<b>m7GpppG</b>	
<b>Met</b>	Methionine
<b>min</b>	minute(s)
<b>mol</b>	mole(s)
<b>N-terminal</b>	amino terminal
<b>NMDA</b>	<i>N</i> -methyl- <i>D</i> -aspartate
<b>NMDAR</b>	NMDA receptor
<b>NHS</b>	<i>N</i> -Hydroxy-Succinimidyl
<b>OD</b>	optical density
<b>ORF</b>	open reading frame
<b>PCR</b>	polymerase chain reaction
<b>PDZ</b>	PSD-95/Discs-large/ZO-1

<b>PSD</b>	postsynaptic density
<b>rpm</b>	revolutions per minute
<b>s</b>	second(s)
<b>SDS</b>	sodium dodecyl sulfate
<b>TAE</b>	Tris-acetate/EDTA
<b>TEMED</b>	N,N',N,N'-Tetramethylethylenediamine
<b>U</b>	unit(s) of enzyme activity
<b>uAUG</b>	upstream start codon
<b>uORF</b>	upstream open reading frame
<b>UV</b>	ultraviolet
<b>V</b>	volt(s)
<b>v/v</b>	volume per volume
<b>w/v</b>	weight per volume



## Acknowledgements

I've had a wonderful 3 years stay in Germany doing my PhD and there are lots of reasons to give thanks for. I thank God for His guidance and provision throughout these years when I was away from home. He has been especially kind to bring me to the presence of wonderful people throughout my stay in Germany.

I thank my family for supporting my decision to do my PhD studies overseas and I am deeply grateful for their prayers and encouragement especially at the darkest time of our lives.

I'm grateful to Professor Dietmar Richter for granting me a wonderful opportunity to participate in the exciting research of his institute.

Heartfelt gratitude also goes to my supervisors Drs Stefan Kindler and Monika Rehbein for their encouragement, patience and stimulating discussions. Thanks also for making my stay in the lab so special and so memorable! Not forgetting Dr Hans-Jügen Kreienkamp as well! It was a rewarding experience and a pleasure to have learned from you.

Many thanks to the past and present members of the lab: Krishna, Birgit, Christiane, Connie, Biggi, Frederike, Inga and Janin. My appreciation also goes to the members of Dr Kreienkamp's lab: Gwen, Chongwee, Peter, Katrin and Kerstin. I'm glad to have met and worked with you all. Not forgetting the members of the Institute for Cell Biochemistry and Clinical Neurobiology too. Thanks for everything!

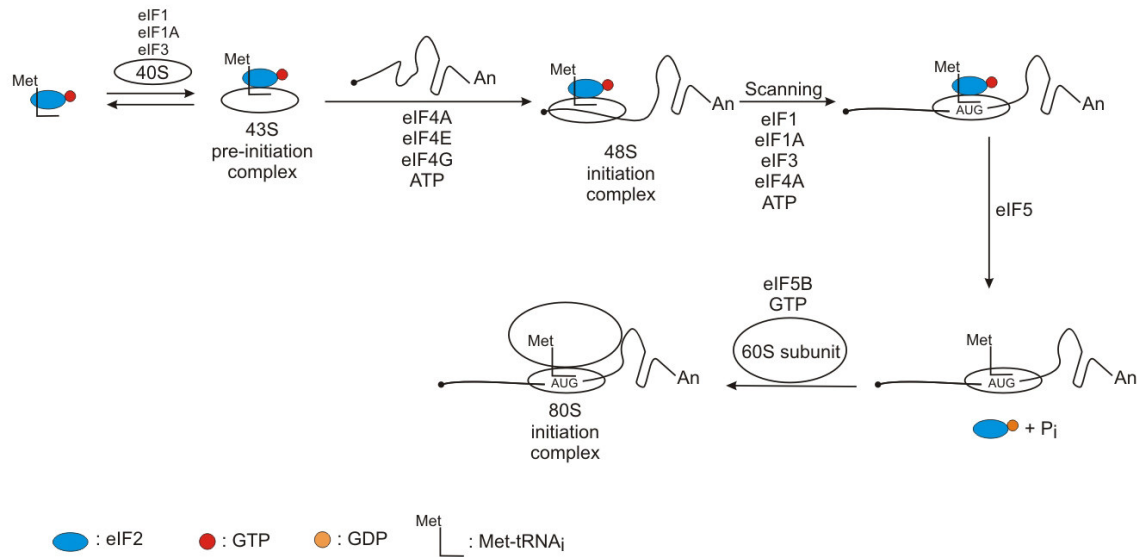
To the many friends who have helped me along the way, I can never be grateful enough. Thanks for the companionship and kindness. In particular I'd like to thank Eng Nai and Rolf who have been like a family to me away from home. Also to Lisa for her love, understanding, patience and support.

Finally, I'll like to dedicate this thesis to my mother. Without her self-sacrificing love, I would never have been able to start this journey. Mere words cannot express what my heart feels. Nothing in this world can give her a greater tribute.

## Chapter 1 Introduction

### 1.1 An Overview of the Cap-dependent Mechanism of Eukaryotic Translation Initiation

Eukaryotic translation initiation is a complex multi-step process involving at least 25 proteins (Gray and Wickens, 1998; Kapp and Lorsch, 2004; Pestova *et al.*, 2002) (Figure 1.1). Translation initiation begins with the assembly of the ternary complex consisting of eukaryotic initiation factor (eIF)2·GTP·Met-tRNA<sub>i</sub>, which facilitated by eIFs 1, 1A and 3, binds to the small (40S) ribosomal subunit, forming the 43S pre-initiation complex. This 43S complex is recruited to the 5' end of mRNAs aided by the eIF4F complex consisting of eIF4E (which binds the m<sup>7</sup>GpppG cap), eIF4A (containing the ATPase-dependent RNA helicase activity) and eIF4G (which aids the binding of the 43S complex to the mRNA by binding to eIF3) resulting in the formation of the 48S complex. eIF4F is believed to bind to the 5' end of the mRNA, unwind the local RNA structure and thereby facilitate the loading of the 43S complex onto the 5' untranslated region (5' UTR). Subsequently, the 43S complex scans linearly along the 5' UTR in a 5' → 3' direction until it recognizes an initiator codon (AUG) located in a favorable context. Codon-anticodon base pairing between the initiator codon and the initiator tRNA in the ternary complex results in the hydrolysis of GTP by eIF2 (aided by the GTPase-activating protein eIF5) and the release of Met-tRNA<sub>i</sub> from eIF2 into the peptidyl (P) site of the 40S subunit. At this point, eIFs 1, 1A, 2, 3 and 5 dissociate from the complex while eIF5B·GTP binds the complex, permitting the joining of the large (60S) ribosomal subunit to the 40S·Met-tRNA<sub>i</sub>·mRNA complex. The joining of the 60S subunit causes the hydrolysis of GTP by eIF5B and the resultant eIF5B·GDP complex dissociates from the 80S ribosome. This step is regarded to signal the end of translation initiation.



**Figure 1.1** Schematic overview of the various steps involved in eukaryotic cap-dependent translation initiation.

## 1.2 Recognizing the Initiator Codon

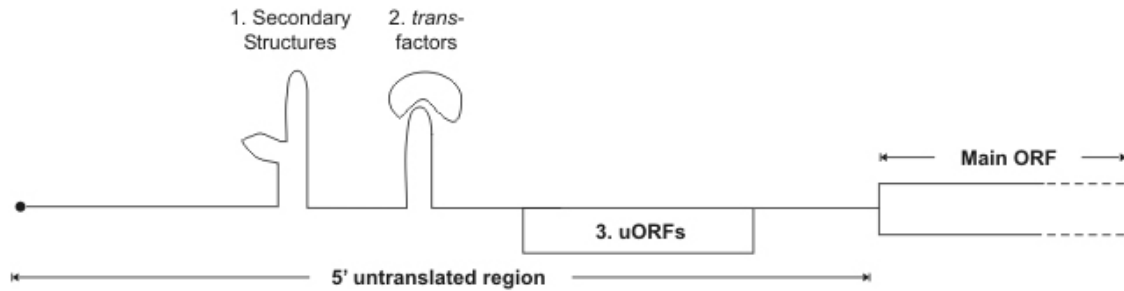
A systematic analysis of the start codons of several hundred vertebrate mRNAs has identified a consensus sequence for the eukaryotic translation start site corresponding to the sequence: GCCRCCaugG where R represents a purine residue and the position of the adenine residue of the start codon is designated as +1 (Kozak, 1987b, 1991b). The purine residue at the -3 position is most highly conserved and critical in defining the start codon. The guanine residue at the +4 position is also highly conserved and plays an important role in start codon recognition, particularly in the absence of an adenine in the -3 position (Kozak, 1997). Nucleotide substitutions at the remaining positions did not strongly affect the recognition of the start codon if the -3 and +4 rule were conformed. However, in the absence of the purine residues, the GCC motif can contribute to start codon recognition. The strength of the context surrounding the start codon can generally be classified as strong or weak based on the nucleotides present at the -3 and the +4 positions. A start codon present in a strong context for translation initiation is defined by the presence of an adenine residue at the -3 position or the presence of guanine residues at both the -3 and the +4 positions. Conversely, a weak context is defined by the absence of both the purine residue at the -3 position and the guanine residue at the +4 position (Kozak, 2002). While the context surrounding the start codon is important for its efficient recognition, the distance of the start codon

relative to the m<sup>7</sup>GpppG cap as well as the presence of secondary structures downstream of the start codon can also influence whether the start codon will be used for initiation. An AUG present in a strong context may not be used for translation initiation if it is located too near the m<sup>7</sup>GpppG cap (Kozak, 1991a) while the presence of a mild downstream secondary structure located close to the start codon can facilitate its recognition by slowing down the scanning 40S subunit and thus providing more time for start codon recognition (Kozak, 1990).

Considering the simplest case, where the start codon resides in a strong or optimal context, that is ANNaugN or GNNaugG, most if not all 43S complexes scanning along the 5' UTR will stop and initiate translation from this start codon. However, if the first start codon encountered by the scanning 43S complexes is located in a weak context, some complexes will initiate translation at this point, whereas most other 43S complexes will continue to scan and initiate translation at start codons located further downstream. The inefficient recognition of a start codon (either due to a suboptimal Kozak sequence or the local sequence context extending beyond the Kozak sequence) that permits a portion of the 43S pre-initiation complexes to continue scanning and initiate translation at a downstream start codon is known as leaky scanning (Gray and Wickens, 1998; Kozak, 1991b).

### **1.3 Regulation of Translation by the 5' Untranslated Region of mRNAs**

The preceding section describes eukaryotic translation initiation in a simplified format. In most mRNAs, a variety of features of the 5' UTR can negatively influence the 43S pre-initiation complex at the mRNA binding, scanning and AUG recognition steps (van der Velden *et al.*, 1999; Meijer and Thomas, 2002; Morris and Geballe, 2000). These features are illustrated in Figure 1.2 and are exemplified by the 5' UTRs of mRNAs encoding important regulatory molecules such as proto-oncogenes and growth factors (Davuluri *et al.*, 2000; Kozak, 1991c; Kochetov *et al.*, 1998). These 5' UTRs are typically long (more than 100 nt in length) and contain extensive secondary structures or motifs that are recognized by RNA-binding proteins as well as upstream open-reading frames (uORFs) (see Section 1.3.2).



**Figure 1.2** Some features of the 5' UTR of eukaryotic mRNAs that regulate translation.

### 1.3.1 Secondary Structures and RNA Binding Proteins

The migration of 43S complexes along the 5' UTR can be blocked by the presence of a stable stem-loop structure with  $\Delta G$  (Gibb's free energy) values greater than  $-50$  kcal/mol or by milder secondary structures if present very close to the m7GpppG cap (Kozac, 1991b). Such structures prevent the 43S complexes from reaching and initiating translation at the start codon of the main open reading frame. Indeed, stem-loop structures present in the 5' UTRs of basonuclin, NR2A and GluR2 mRNAs have been implicated in impeding the synthesis of their respective protein (Myers *et al.*, 2004; Wood *et al.*, 1996; Tang and Tseng, 1999).

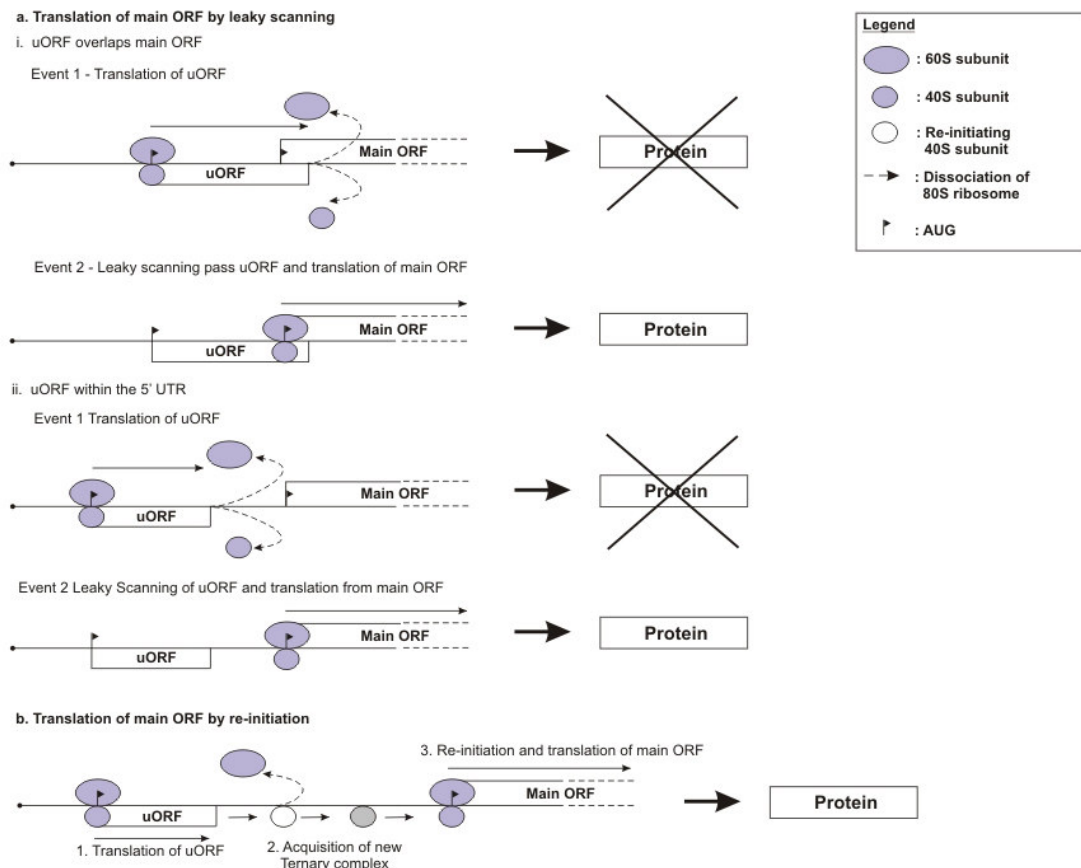
In addition to acting as physical barriers, secondary structures and sequence motifs present in the 5' UTR may also be specifically recognized by RNA-binding proteins (Gray and Hentze, 1994; Kullmann *et al.*, 2002; Meng *et al.*, 2005; Nielsen *et al.*, 1999; Paraskeva *et al.*, 1999; Timchenko *et al.*, 2002, 1999). In particular, the binding of the iron regulatory protein to the iron-responsive element present near the m7GpppG cap of the ferritin mRNA has been shown to block the recruitment of 43S pre-initiation complexes (Gray and Hentze, 1994). Shifting the location of the IRE further downstream of the m7GpppG cap can impede the scanning of 43S pre-initiation complexes along the 5' UTR (Paraskeva *et al.*, 1999).

### 1.3.2 Upstream Open Reading Frames – Leaky Scanning versus Translational Reinitiation

Unlike secondary structures, open reading frames (ORFs) located in the 5' UTR upstream of the main coding region (upstream ORFs or uORFs) can regulate translation both positively as well as negatively (Meijer and Thomas, 2002; Morris and Geballe, 2000). uORFs may be entirely contained within the 5' UTR or they may also overlap with the main ORF (Figure 1.3). Based on the scanning mechanism of initiation, some scanning 43S complexes will initiate translation upon encountering the first start codon present in a favorable context (Section 1.2). The rules governing the recognition of the start codons of uORFs (uAUGs) are identical to those used to recognize start codons of the main ORF. Upon completing the translation of an uORF, ribosomes dissociate from the mRNA and are typically unable to initiate translation from the main ORF (Figures 1.3ai and 1.3aii, Event 1). Thus, uORFs normally decrease the amount of ribosomes able to reach the start codon of the main open reading frame (Ghilardi *et al.*, 1998; Hughes and Brady, 2005; Koš *et al.*, 2002). Initiation of translation at the main open reading frame is mediated by leaky scanning past the uAUGs (Figures 1.3ai and 1.3aii, Event 2). The levels of protein synthesized are thus dependent upon the strength of the context surrounding the uAUG. Apart from filtering ribosomes away from the main open reading frame, the peptides encoded by uORFs can also inhibit translation by exerting their effects directly on ribosomes. For instance, the uORF present in the 5' UTR of the retinoic acid receptor- $\beta$ 2 mRNA encodes a peptide that inhibits synthesis of RAR $\beta$ 2 protein (Reynolds *et al.*, 1996).

In contrast to leaky scanning, reinitiation refers to the rare and inefficient mechanism in which 40S subunits initiate translation a second time following the translation of a short uORF which does not overlap with the AUG of the main ORF (Gray and Wickens, 1998; Hinnebusch, 2005). The mechanisms of reinitiation have been extensively studied for the translational control of the yeast *GCN4* mRNA (Hinnebusch, 2005) and have also been implicated in the translational control of the mammalian transcription factor *ATF4* mRNA (Lu *et al.*, 2004; Harding *et al.*, 2000; Vattam and Wek, 2004). In the simplified model proposed for the reinitiation

observed in GCN4, scanning 43S complexes initiate translation from an uORF (Figure 1.3b, Step 1) (Hinnebusch, 2005). A proportion of the 40S subunits from ribosomes completing translation of the uORF remain attached to the mRNA and are able to resume scanning along the mRNA and re-acquire a new ternary complex before reaching the start codon of the main ORF (Step 2). Binding of the new ternary complex is critical to enable these 40S subunits to recognize downstream AUGs (Section 1.1) and permits them to reinitiate translation at the main ORF (Step 3). The efficiency of reinitiation is influenced by a variety of factors including the distance between the preceding termination codon and the subsequent start codon (intercistronic distance) (Grant *et al.*, 1994; Kozak, 1987a), the length of the uORF (Kozak, 2001; Pöyry *et al.*, 2004) and the levels of eIF2 $\alpha$  phosphorylation (Grant *et al.*, 1994; Harding *et al.*, 2000; Lu *et al.*, 2004; Vattam and Wek, 2004) (Table 1.1).



**Figure 1.3** Schematic representations of the effects of uORFs on translation initiation from the main ORF.

Factor	Reason for Positive Effect on Reinitiation
Increased inter-cistronic distance	Increases the probability of ternary complex acquisition by reinitiating 40S subunits before reaching the next start codon.
Decrease in uORF size	Retention of factors important for reinitiation (e.g. eIF4F). Ribosomes completing translation of a full-length cistron cannot reinitiate translation.
Levels of eIF2 $\alpha$ phosphorylation	Decrease ternary complex levels by inhibiting recycling of eIF2-GDP to eIF2-GTP. Phosphorylated eIF2 $\alpha$ is a potent inhibitor of eIF2B (the guanine nucleotide exchange factor for eIF2). Effects on reinitiation varies with intercistronic distance.

**Table 1.1** Factors influencing translational reinitiation on eukaryotic mRNAs.

#### 1.4 Variations on a Theme: Alternative Translational Initiation based on Leaky Scanning and Reinitiation Mechanisms

Alternative translational initiation (ATI) is a term used to describe the phenomenon where AUGs within the main ORF are employed to initiate synthesis of a protein in addition to the first AUG. Multiple protein isoforms can be synthesized from a single species of mRNA via ATI events (Calkhoven *et al.*, 2000; Kozak, 1991c; Leisring *et al.*, 2004; Okazaki *et al.*, 1998; Sarrazine *et al.*, 2000; Short and Pfarr, 2002; Xiong *et al.*, 2001). In particular, 4 protein isoforms of the CCAAT/enhancer-binding *trans*-activating are synthesized from the single form of mRNA transcribed from its gene (Calkhoven *et al.*, 2000; Xiong *et al.*, 2001). Since the mRNA is transcribed from an intronless gene, alternative splicing could not be responsible for the generation of these isoforms. Indeed, it was shown that the production of the smaller isoforms results from ATI events occurring at in-frame AUGs located downstream from the first AUG of the main open reading frame. Such events are mediated by leaky scanning and/or reinitiation mechanisms.

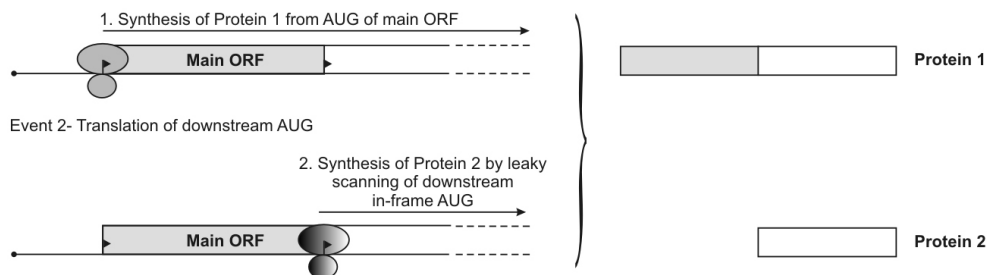
Synthesis of two or more proteins from a single mRNA can arise by leaky scanning if the first AUG is located in a sub-optimal context or if a non-conventional start codon (e.g. ACG, CUG and GUG) is used to initiate the synthesis of the longer protein (Figure 1.4a, Event 1) (Calkhoven *et al.*, 2000; Leisring *et al.*, 2004; Packham *et al.*,



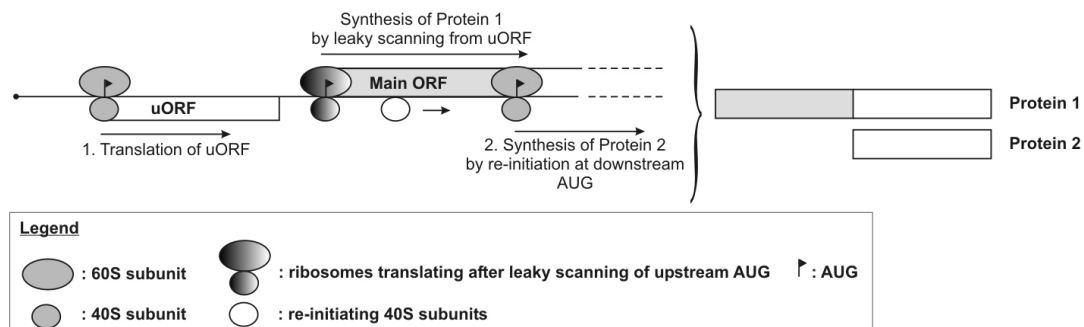
1997; Xiong *et al.*, 2001). In this case, 43S complexes scanning along the 5' UTR of these mRNAs do not efficiently recognize the upstream initiation site, permitting a portion of ribosomes to scan past this site and initiate translation at downstream start codons (Event 2). The relative amounts of proteins produced from each initiation codon depend on the strength of the context surrounding both start codons. Enhancing the strength of the context at the upstream position can negatively influence the levels of protein synthesized from downstream start codons (Calkhoven *et al.*, 2000).

(a) Synthesis of protein isoforms by leaky scanning e.g. insulin degrading enzyme (Leissring *et al.*, 2004)

Event 1- Translation of AUG of main ORF



(b) Synthesis of protein isoforms by re-initiation e.g. Fli-1 (Sarrazine *et al.*, 2000)



**Figure 1.4** Models representing alternative translational initiation mediated by leaky scanning and translation reinitiation.

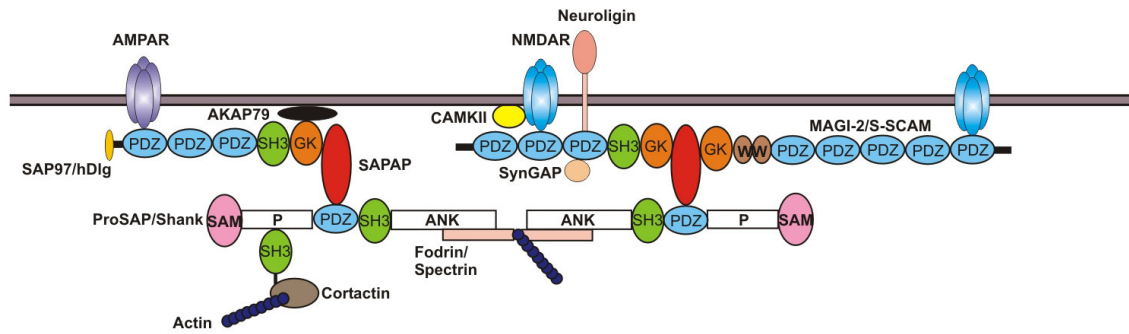
Reinitiation events achieve the synthesis of multiple proteins from a single mRNA using a slightly different mechanism as compared to leaky scanning (Figure 1.4b). The occurrence of reinitiation events necessitate the presence of an uORF and is mechanistically similar to that described in Section 1.3.2. In the case of alternative translational initiation events, the presence of the uORF acts as a reinitiation shunt (Kozak, 2002) to allow a portion of ribosomes to bypass the first start codon in the main ORF after translating the uORF. Ribosomes reinitiating at downstream start codons are thus able to synthesize shorter isoforms of the protein (Figure 1.4b, Step 2). Reinitiation thus enhances the translation from downstream start codons while

limiting the synthesis of longer proteins originating from upstream initiation sites (Sarrazine *et al.*, 2000; Calkhoven *et al.*, 2000). Translation of the longer isoform commencing from the first AUG occurs by leaky scanning of the uAUG (Step 1).

Protein isoforms generated by ATI have been shown to target to different subcellular locations (Leissring *et al.*, 2004), exhibit functional differences between each other (Calkhoven *et al.*, 2000; Timchenko *et al.*, 2002), or exhibit differences in interaction with other proteins (Yazgan and Pfarr, 2001, 2002). An analysis of the human mRNA sequences has indicated that at least 3% of human mRNAs have the potential to undergo ATI (Kochetov *et al.*, 2005). Such events have been proposed to be important in generating N-terminal protein diversity (Kochetov *et al.*, 2005; Cai *et al.*, 2005).

### **1.5 The SAP90/PSD-95-Associated Protein (SAPAP) family of proteins**

Dendritic spines are membranous protrusions from the neuronal surface in which more than 90% of excitatory synapses are located (Nimchinsky *et al.*, 2002). The excitatory synapses of mammalian central nervous system (CNS) neurons are characterized by the presence of the postsynaptic density (PSD), a prominent electron dense structure located at the cytoplasmic surface of the postsynaptic membrane. The PSD contains proteins involved in organizing the postsynaptic signal transduction machinery. Its purpose is to link regulatory molecules to their targets and to coordinate developmental and activity-dependent changes in post-synaptic structures (Figure 1.5) (Hering and Sheng, 2001; Husi *et al.*, 2000; Yamauchi, 2002). In addition, the PSD is also intimately involved in the expression of synaptic plasticity and dynamically changes in response to synaptic activity, learning and memory formation (Ehlers, 2003; Lamprecht and LeDoux, 2004). Some of these changes are believed to be mediated by proteins synthesized by local translation of certain mRNAs which are specifically targeted to neuronal dendrites (Kelleher *et al.*, 2004; Steward and Schuman, 2003).



**Figure 1.5** Schematic organization of the postsynaptic density (PSD). Members of the SAPAP family act as scaffolding proteins in the organization of signaling complexes in the PSD. Not all possible protein interactions involving SAPAPs are illustrated in this simplified diagram.

Binding Partner	References
<u>MAGUKs</u>	
PSD-95 family	Kim <i>et al.</i> , 1997; Naisbitt <i>et al.</i> , 1997; Satoh <i>et al.</i> , 1997; Takeuchi <i>et al.</i> , 1997
S-SCAM	Hirao <i>et al.</i> , 1998; Hirao <i>et al.</i> , 2000a
<u>Other scaffolding proteins</u>	
ProSAP/Shank family	Böeckers <i>et al.</i> , 1999; Naisbitt <i>et al.</i> , 1999; Yao <i>et al.</i> , 1999
<u>Enzymes</u>	
FAK/PYK2	Bongiorno-Borbone <i>et al.</i> , 2005
nNOS	Haraguchi <i>et al.</i> , 2000
<u>Cytoskeleton/Motor</u>	
Neurofilaments	Hirao <i>et al.</i> , 2000b
DLC1 and DLC2	Naisbitt <i>et al.</i> , 2000; Haraguchi <i>et al.</i> , 2000
LC8	Rodriguez-Crespo <i>et al.</i> , 2001
<u>Others</u>	
nArgBP2	Kawabe <i>et al.</i> , 1999

**Table 1.2** Known protein interaction partners of SAPAPs.

Members of the SAPAP (SAP90/PSD-95-Associated Protein) family were originally identified as proteins that interact with the guanylate kinase domain of the proteins of the SAP90/PSD-95 family (Kim *et al.*, 1997; Naisbitt *et al.*, 1997; Satoh *et al.*, 1997; Takeuchi *et al.*, 1997). The SAPAP family consists of four related proteins (SAPAP 1-4) encoded by 4 distinct genes (Takeuchi *et al.*, 1997). The expression of SAPAP1

and SAPAP2 genes are exclusively detected in the brain (Kim *et al.*, 1997; Satoh *et al.*, 1997; Takeuchi *et al.*, 1997) and SAPAPs are specifically localized to excitatory synapses of CNS glutamatergic neurons and interneurons as well as cholinergic synapses of the anatomic nervous system (Naisbitt *et al.*, 1997; Welch *et al.*, 2004). Functionally, SAPAP1 has been shown to mediate the synaptic targeting of the ProSAP/Shank family of proteins, another group of integral PSD proteins important in the development and maturation of synapses (Sala *et al.*, 2001; Roussignol *et al.*, 2005). Over-expression of the C-terminal region SAPAP1 containing the PDZ motif that binds to Shank proteins prevented their recruitment to dendritic spines (Naisbitt *et al.*, 1999; Yao *et al.*, 2003). Analogously, Shank variants lacking the PDZ domain required to bind SAPAPs were not recruited to synapses (Romorini *et al.*, 2004).

A wide variety of protein interaction partners have been identified for SAPAPs (in particular for SAPAP1 also known as GKAP) (Table 1.1). The 14 amino acid repeat region binding to the guanylate kinase domain of PSD-95 family proteins may also be involved in clustering these proteins to form a molecular scaffold (Satoh *et al.*, 1997; Kim *et al.*, 1997). Thus, like PSD-95, SAPAPs appear to be involved in the molecular organization of the PSD by acting as scaffolding proteins to link various signaling as well as structural proteins in the synapse (Figure 1.5) (Kim and Sheng, 2004).

## 1.6 Purpose of This Study

A number of studies have focused on the functions and protein interaction partners of SAPAP1/GKAP. Data from these studies have been used to infer the functions of the remaining SAPAPs and very few studies are available that directly investigate SAPAP 2 - 4. *In situ* hybridization studies revealed differential expression of SAPAP genes in different regions of the postnatal rodent brain (Kindler *et al.*, 2004; Welch *et al.*, 2004). These studies also showed that, unlike the transcripts of other SAPAP family members, SAPAP3 mRNA belongs to the exclusive group of transcripts that are localized to the dendrites of neurons. Local translation of such mRNAs has been postulated to play an important role in mediating synaptic plasticity (Kelleher *et al.*, 2004; Steward and Schuman, 2003). Because SAPAP3 is the only member of this family to exhibit dendritic localization of its mRNA, my studies involved the

characterization of this unique member of the SAPAP family. The primary focus was placed on the mechanisms regulating SAPAP3 mRNA translation.

## Chapter 2 Materials and Methods

### 2.1 Materials

#### 2.1.1 Chemicals

All chemicals unless stated otherwise were purchased from Merck, Sigma or Roth and are of analytical grade.

#### 2.1.2 Microbial Strains, Laboratory Animals and Cell Lines

	Name	Source
Bacterial strain	<i>Escherichia coli</i> XL-1Blue	Stratagene
Cell lines	Human Embryonic Kidney 293 (HEK293)	ATCC
Laboratory animal	<i>Rattus norvegicus</i> (Wistar Rat)	Animal facility at University Clinic Hamburg-Eppendorf (UKE)

**Table 2.1** Bacterial strains and mammalian cell lines used in this study.

#### 2.1.3 Plasmid DNA

##### 2.1.3.1 Basic Vectors

Plasmid	Source	Accession number (Acc.)
pEGFP-N1	BD Biosciences Clontech	U66474
pEGFP-N3	BD Biosciences Clontech	U57609
pcDNA <sup>TM</sup> 3.1/ <i>myc</i> -His A	Invitrogen	
pGEM <sup>®</sup> -T Easy	Promega	
pBluescript <sup>®</sup> II SK -	Stratagene	
pBicFire	Jan Christiansen, University of Copenhagen	
pBS-SK(-)-S3U	In-house	
pSAPAP3(+)-EYFP	In-house	

**Table 2.2** Plasmid vectors used in this study for cloning of PCR products and for construction of eukaryotic expression constructs. Sequences of the corresponding vectors are available at GenBank ([www.ncbi.nlm.nih.gov](http://www.ncbi.nlm.nih.gov)) via their accession numbers listed above as well as from the respective sources.

## 2.1.3.2 Vectors generated in this study

<u>Plasmid</u>	<u>Remarks</u>
<u>EGFP vectors</u>	
pE1B-EGFP	pEGFP-N3 vector containing SAPAP3 E1B 5' UTR sequence and first 8 codons of SAPAP3 $\alpha$ open-reading frame
<u>Luciferase vectors</u>	
pBFE	Bicistronic vector containing EMCV IRES at intercistronic region
pBFA	Bicistronic vector containing Arc IRES at intercistronic region
pBFS3	Bicistronic vector containing SAPAP3 E1B 5' UTR sequence at intercistronic region
pS1-BFE	pBicFire vector modified to contain SAPAP1 5' UTR sequence before <i>Photinus</i> luciferase CDS
pS3-BFE	pBicFire vector modified to contain SAPAP3 E1B 5' UTR sequence before <i>Photinus</i> luciferase CDS
pLuc	CMV promoter driven expression of <i>Photinus</i> luciferase
pREN	CMV promoter driven expression of <i>Renilla</i> luciferase
pS35-Luc	pLuc containing SAPAP3 E1B 5' UTR sequence inserted before <i>Photinus</i> luciferase CDS
pS353-Luc	S35-pLuc with additional SAPAP3 3' UTR sequence inserted after <i>Photinus</i> luciferase CDS
pS33-Luc	pLuc containing SAPAP3 3' UTR sequence inserted after <i>Photinus</i> luciferase CDS
pE1B <sup>+</sup> -Luc	pS33-Luc with additional SAPAP3 E1B <sup>+</sup> 5' UTR sequence inserted before <i>Photinus</i> luciferase CDS

**Table 2.3** Plasmid constructs expressing EGFP or luciferases generated in this study.

<u>Plasmid</u>	<u>Remarks</u>
<b><u>Flag-SAPAP3 vectors</u></b>	
pFS3	For expression of FLAG-tagged SAPAP3 protein
pS1-FS3	pFS3 containing SAPAP1 5' UTR sequence inserted before SAPAP3 CDS
pE1B-FS3	pFS3 containing SAPAP3 E1B 5' UTR sequence inserted before SAPAP3 CDS
pΔ150-FS3	Deletion of first 150 nt of SAPAP3 E1B 5' UTR in pE1B-FS3
pΔ205-FS3	Deletion of first 205 nt of SAPAP3 E1B 5' UTR in pE1B-FS3
pΔ(54-128)-FS3	Deletion of internal sequence between 54-128 nt of SAPAP3 E1B 5' UTR in pE1B-FS3
puORF2 <sup>AAG</sup> -E1B-FS3	Mutation of 2 <sup>nd</sup> uAUG to AAG of SAPAP3 E1B 5' UTR in pE1B-FS3
puORF3 <sup>AAG</sup> -E1B-FS3	Mutation of 3 <sup>rd</sup> uAUG to AAG of SAPAP3 E1B 5' UTR in pE1B-FS3
puORFs2+3 <sup>AAG</sup> -Δ150-FS3	Mutation of 2 <sup>nd</sup> and 3 <sup>rd</sup> uAUG to AAG of SAPAP3 E1B 5' UTR in pΔ150-FS3
<b><u>SAPAP3 vectors</u></b>	
pS3	Encodes SAPAP3 CDS and 3' UTR; For expression of untagged SAPAP3 protein
pE1B-S3	Encodes full-length E1B type SAPAP3 transcript; for expression of untagged SAPAP3 protein
pΔ150-S3	Deletion of first 150 nt of SAPAP3 E1B 5' UTR in pE1B-S3
pΔ205-S3	Deletion of first 205 nt of SAPAP3 E1B 5' UTR in pE1B-S3
puORF2 <sup>AAG</sup> -E1B-S3	Mutation of 2 <sup>nd</sup> uAUG to AAG of SAPAP3 E1B 5' UTR in pE1B-S3
puORF3 <sup>AAG</sup> -E1B-S3	Mutation of 3 <sup>rd</sup> uAUG to AAG of SAPAP3 E1B 5' UTR in pE1B-S3
puORFs2+3 <sup>AAG</sup> -Δ205-S3	Mutation of 2 <sup>nd</sup> and 3 <sup>rd</sup> uAUG to AAG of SAPAP3 E1B 5' UTR in pΔ205-S3
<b><u>Miscellaneous</u></b>	
pcDNA <sup>TM</sup> 3.1/ <i>myc-His(A)</i> – SAPAP3	For generation of <i>Bam</i> HI fragment for use as probe for Northern blots (corresponding to nucleotides 96 to 1440 of the rat SAPAP3 mRNA reference sequence, GenBank acc. number: NM_173138)

**Table 2.4** Plasmid constructs expressing SAPAP3 generated in this study.



## 2.1.4 Antibodies

Primary antibody	Working concentration		
	Western blot	Cytochemistry	Source
rbAnti-GFP	1:10000	-	Abcam
mAnti-FLAG™ M2	1:2000	1:1500	Sigma
rbAnti-SAPAP3 #5297	1:2000	-	Our laboratory
rbAnti-SAPAP1 #5280	1:66	-	Our laboratory
rbAnti-vGLUT1	-	1:5000	Synaptic Systems
rbAnti-vGAT	-	1:500	Synaptic Systems
mAnti-MAP2	-	1:2000	Sigma
rbAnti-MAP2	-	1:2000	Craig Garner, Stanford University
rbAnti-PSD95	1:2000	-	Craig Garner, Stanford University
mAnti-eIF1 $\alpha$	1:2000	-	Upstate Biotechnology
mAnti-eIF2 $\alpha$	1:1000	-	Cell Signalling Technology
mAnti-L7	1:2000	-	Abcam

Secondary antibody	Working concentration		
	Western blot	Cytochemistry	Source
HRP-dAnti-rbIgG	1:2000	-	Dianova
HRP-dAnti Mouse IgG	1:2000	-	Dianova
Alexa488-gAnti-mIgG	-	1:200	Molecular Probes
Alexa546-gAnti-mIgG	-	1:200	Molecular Probes
Alexa546-gAnti-rbIgG	-	1:200	Molecular Probes
Alexa633-gAnti-rbIgG	-	1:200	Molecular Probes

**Table 2.5** Antibodies used in this study for Western blot and immunocytochemistry. The species origin of the immunoglobulin is indicated by the abbreviation preceding IgG in the antibody name: d: donkey, g: goat, m: mouse, rb: rabbit.

## 2.1.5 Oligonucleotides

Oligonucleotides listed in the appendix were synthesized either at the analytical laboratory in Institute for Cell Biochemistry and Clinical Neurobiology (University Hospital Hamburg-Eppendorf) with a DNA/RNA synthesizer (Applied Biosystems)

or by Invitrogen. The oligonucleotides were suspended in sterile H<sub>2</sub>O and their concentration was determined (Section 2.2.1.2). Oligonucleotides were then diluted to either 1 μM for sequencing or 10 μM for polymerase chain reaction.

## **2.2 Methods**

### **2.2.1 Molecular Biology Techniques**

#### **2.2.1.1 Preparation of Total RNA**

Total RNA was prepared from cultured HEK cells or rat brains via extraction with either Trizol Reagent (Invitrogen) or RNeasy Midi Kit (Qiagen) according to the manufacturer's protocol.

#### **2.2.1.2 Quantitation of Nucleic Acids**

The amount and purity of nucleic acids were measured by spectrophotometry using a Genequant spectrophotometer (Amersham Biosciences).

#### **2.2.1.3 Synthesis of cDNA and 5' RACE cDNA**

Adult rat brain cDNA was synthesized using SUPERSCRIPT II™ reverse transcriptase (Gibco BRL, Grand Island, NY, USA). Adult rat brain 5' RACE ready cDNA synthesis and 5' RACE PCR were performed using SMART™ RACE cDNA Amplification Kit (BD Biosciences Clontech). All protocols were performed according to the manufacturer's recommendations.

#### **2.2.1.4 Polymerase Chain Reaction**

All PCR reactions were performed using either the *Pfu* enzyme (Promega) or BD Advantage™ 2 Polymerase Mix (BD Biosciences Clontech) according to the manufacturer's protocol with minor modifications. PCR amplifications were performed using a GeneAmp PCR System 2400 Thermocycler (Perkin Elmer).

<u><i>Pfu</i> DNA polymerase</u>	<u>BD Advantage™ 2 Polymerase Mix</u>
1× polymerase buffer	1× polymerase buffer
0.2 mM of each dNTP (dATP, dCTP, dGTP, dTTP)	0.2 mM of each dNTP (dATP, dCTP, dGTP, dTTP)
<sup>1</sup> 3 µl DMSO	<sup>1</sup> 3 µl DMSO
10 pmol of each primer	10 pmol of each primer
50 ng of template plasmid DNA or 200 ng of cDNA library	50 ng of template plasmid DNA or 200 ng of cDNA library
2.5 U Polymerase	1× Advantage 2 Polymerase Mix
ddH <sub>2</sub> O to a final volume of 50 µl	ddH <sub>2</sub> O to a final volume of 50 µl

<sup>1</sup>For amplification of SAPAP3 5' UTR.

	<u><i>Pfu</i> DNA polymerase</u>	<u>BD Advantage™ 2 Polymerase Mix</u>
Initial denaturation	94°C; 2 min	94°C; 2 min
Denaturation	94°C; 30 s	95°C; 30 s
Annealing	4-6°C below melting temperature (T <sub>m</sub> ) of primers used	
Extension		
Final extension	72°C; 2 min per kb of intended PCR product	68°C; 1 min per kb of intended PCR product
	72°C; 3-7 min	68°C; 3-7 min
		4°C; indefinite

Following completion of the cycling profile, an aliquot of the PCR product was analyzed by agarose gel electrophoresis.

### 2.2.1.5 Agarose Gel Electrophoresis

Aliquots of restriction endonuclease digestions or PCR reactions were analyzed using submerged horizontal non-denaturing agarose gel electrophoresis. Agarose (Invitrogen) was dissolved in 1× TAE (100 mM Tris/Acetate, 5 mM EDTA; pH8.0) to a final concentration of 1 to 2% (w/v) and 0.2 g/ml of ethidium bromide was added to the mixture. DNA samples were then mixed with 6× gel loading buffer (10 mM Tris-HCl, 0.03% (w/v) bromophenol blue, 0.03% (w/v) xylene cyanol FF, 60% (v/v) glycerol and 60 mM EDTA; pH 7.6) and loaded into the wells of the gel. Gene Ruler™ 100bp DNA Ladder (MBI Fermentas) was used as standard DNA molecular

weight marker. The gel was electrophoresed in 1× TAE buffer at a constant voltage of 100 V. Gel viewing and documentation were performed under ultraviolet light illumination from a UV transilluminator (UVT 2035, Herolab).

#### **2.2.1.6 Excision and Purification of DNA Bands**

DNA products of interest were purified using the E.Z.N.A gel extraction kit (PEQLAB Biotechnologie) according to the manufacturer's protocol. An aliquot of the DNA was analyzed by agarose gel electrophoresis and the remaining samples stored at -20°.

#### **2.2.1.7 Molecular Cloning**

Standard molecular cloning techniques were performed according to Sambrook *et al.*, 1989.

Restriction enzyme digestion of DNA samples was performed according to manufacturers' (Invitrogen, MBI Fermentas, New England Biolabs) recommendations. DNA fragments were ligated using the T4 DNA polymerase (Invitrogen). Direction cloning of PCR fragments into pGEM<sup>®</sup>-T Easy vectors was performed using the pGEM<sup>®</sup>-T Easy Vector system (Promega). DNA was then transformed into of *E. coli* (XL1-Blue strain, Stratagene) following the manufacturer's protocol.

For sequencing, plasmids were isolated from *E. coli* using the FastPlasmid Mini extraction kit (Eppendorf). Larger quantities of plasmids were obtained with either the QIAGEN EndoFree plasmid Maxi kit (Qiagen) or NucleoBond<sup>®</sup> AX plasmid Midi kit (Macherey-Nagel).

#### **2.2.1.8 Site-directed Mutagenesis**

Point mutations and deletions were introduced into plasmids using either standard PCR procedures with *Pfu* polymerase or using the QuikChange<sup>®</sup> Multi Site-Directed

Mutagenesis Kit (Stratagene) with primer(s) containing the mutated sequence. All mutations were verified by DNA sequencing of the mutated region of interest.

### **2.2.1.9 DNA Sequencing**

All DNA sequencing reactions were done in the analytical laboratory of Institute for Cell Biochemistry and Clinical Neurobiology (University Hospital Hamburg-Eppendorf) or the sequencing facility of the Institute for Human Genetics (University Hospital Hamburg-Eppendorf) according to the dideoxy methodology (Sanger *et al.*, 1977).

### **2.2.1.10 Northern Blot**

Commercially available Human Brain Multiple Tissue Northern (MTN) Blots (II and V) and Rat MTN Blots were obtained from Clontech. To generate in-house Northern blots, electrophoresis of denatured RNA (isolated as described in Section 2.2.1.1) using the glyoxal method and transfer of resolved denatured RNA to nitrocellulose membranes were performed according to Sambrook *et al.*, 1989. To synthesize <sup>32</sup>P-labeled SAPAP3 specific probes for Northern blots, a 1.3 kb *Bam*HI fragment corresponding to nucleotides 96 to 1440 of the rat SAPAP3 mRNA reference sequence (GenBank accession number: NM\_173138) was excised from pcDNA3.1(A)-myc-his-SAPAP3, which contains the complete coding region of SAPAP3 cDNA. The fragment was purified according to Section 2.2.1.6, radioactively labeled using the Prime-It<sup>®</sup> II Random Primer Labeling Kit according to the manufacturer's protocol and purified using MicroSpin<sup>™</sup> G-25 columns (Amersham Biosciences). The resultant radioactively-labeled probe was hybridized to the RNA blots using ULTRAhyb hybridization buffer (Ambion) and the blots were washed according to the manufacturer's protocol. Labeled bands were visualized using a BAS-1800II phosphoimager (FujiFilm).

## **2.2.2 Cell Biology Techniques**

### **2.2.2.1 Culture and Transient Transfection of Established Cell Lines**

Human embryonic kidney 293 cells (HEK293) were cultured in Dulbecco's modified Eagle's medium (DMEM, Cambrex) supplemented with 10% heat-inactivated fetal bovine serum (FBS, Sigma), 100 U/ml penicillin and 100 g/ml streptomycin at 37°C in a humidified atmosphere of 5% CO<sub>2</sub>. For normal maintenance of the cell line, cells were passaged every 3-5 days by rinsing the cell monolayer once with Versene buffer (137 mM NaCl, 8.8 mM Na<sub>2</sub>HPO<sub>4</sub>, 2.7 mM KCl, 0.7 mM KH<sub>2</sub>PO<sub>4</sub>, 1mM EDTA; pH 7.4) followed by incubating with 0.25% (w/v) trypsin (Invitrogen) in Versene buffer until the cell layer was dispersed. Trypsinized cells were then replated in new culture dishes with fresh culture medium with a passage ratio of 1:5.

Transient transfection of HEK293 cells was performed using either the calcium phosphate precipitation method (Sambrook *et al.*, 1989) or with Lipofectamine 2000 (Invitrogen). For transfection with calcium phosphate, 500 µl of the mixture (10 µg of plasmid DNA in 250 mM CaCl<sub>2</sub>) was mixed with 500 µl of 2× HBS buffer (280 mM NaCl, 10 mM KCl, 1.5 mM Na<sub>2</sub>PO<sub>4</sub>, 12 mM dextrose, 50 mM HEPES; pH 7.05) while continuously vortexing the reaction tube. Precipitates were then allowed to form for 15 min at RT. The precipitates were then added onto cells with 50-80% confluency. Transfection medium was replaced with fresh culture medium 6-18 h after transfection to allow for cell recovery. Transfections with Lipofectamine 2000 were performed according to the manufacturer's protocol.

### **2.2.2.2 Preparation of Primary Hippocampal and Cortical Neuron Cultures**

Preparation and transfection of primary hippocampal and cortical neurons were according to the protocols described in Blichenberg *et al.* (1999) with the following modifications: Neurons from the hippocampi of E18-E20 rat embryos were plated in Minimal Essential Medium (MEM, GIBCO, Invitrogen) with 10% (v/v) horse serum (GIBCO, Invitrogen) for 3 hours at 37°C on poly-L-lysine (Sigma) coated coverslips washed with sterile water. The plating medium was then removed and cells were grown in Neurobasal medium (NB, GIBCO, Invitrogen) supplemented with B27

(GIBCO, Invitrogen), 0.5 mM L-glutamine and 25  $\mu$ M glutamate. Four days later, half of the medium from each well was removed and fresh NB medium containing 5 $\mu$ M AraC (Cytosine- $\beta$ -D-Arabinofluranoside, Sigma) was added to remove glial cells from the culture.

Neurons were transfected on day 7 using the calcium phosphate method. Ten  $\mu$ g of plasmid DNA was mixed with 10  $\mu$ l of 2.5 mM CaCl<sub>2</sub> and topped up with water to a final volume of 100  $\mu$ l. One hundred  $\mu$ l of 2 $\times$  BBS (50 mM BES, 280 mM NaCl, 1.5mM Na<sub>2</sub>HPO<sub>4</sub>; pH 6.96) was then added drop-wise while continuously vortexing the reaction tube. Precipitates were allowed to form by incubation at RT for 20 min. One hundred  $\mu$ l of this mixture was added drop-wise into each well. The cells were incubated at 37°C in a humidified atmosphere of 5% for another four hours. Cells were washed thrice with 1 $\times$  Hanks Balanced Salt Solution (HBSS, 10mM HEPES, 2mM NaOH; GIBCO, Invitrogen) and fresh NB medium was added to the cells.

### **2.2.2.3 Stimulation of Neuronal Cultures by Spaced Stimuli Protocol**

Stimulation of cortical neurons was performed according to the spaced stimuli protocol published by Wu and co-workers (Wu *et al.*, 2001). Briefly, cortical neurons were transfected with luciferase expressing constructs following the procedure detailed in Section 2.2.2.2. One day after transfection, the NB medium was replaced with Tyrode's solution containing 1  $\mu$ M tetrodotoxin (TTX) for 1-2 h to block spontaneous neuronal activity. The solution was then replaced with hyperkalemic solution (Tyrode's solution containing 90 mM KCl) and incubated for 3 min. This solution was then removed and quickly replaced with Tyrode's solution containing 1  $\mu$ M TTX for a further incubation of 10 min. The stimulation with hyperkalemic solution and washing steps were repeated 3 more times. After the last stimulation, NB media was replaced to each well and the cells allowed to recover for 1 h. Luciferase assays were then performed as detailed in Section 2.2.4.3.

### **2.2.3 Immunofluorescence Techniques**

#### **2.2.3.1 Cell Fixation and Permeabilization**

For immunofluorescence studies, cells were cultured on coverslips in 12-well plates (Nunc). At the time of fixation, the growth medium was removed from each coverslip. The cells were then washed once with PBS and fixed with 3.7% paraformaldehyde in PBS solution for 15 min at room temperature with shaking. The fixative subsequently was decanted and excessive fixative removed by washing the cells thrice with PBS. To allow the antibodies to gain access to their intracellular targets, cells were permeabilized by incubating with 0.3% Triton-X in PBS solution for 5 min at room temperature with shaking. Cells were then rinsed thrice with PBS.

#### **2.2.3.2 Labeling with Antibodies**

Prior to incubation with primary antibodies, cells were first blocked with blocking buffer (10% (v/v) normal goat serum in PBS solution) for ½ hour at RT with shaking. Primary and secondary antibodies were diluted to their working concentrations with the blocking buffer as detailed in Section 2.1.4. For double immuno-labeling, two primary antibodies from different host species were first mixed in blocking buffer. Fifty µl of the diluted antibody mixture was then spotted on parafilm. Coverslips were inverted on the parafilm with the cell layer facing the drop of antibody and incubated for 1-3 hr at RT in a humidified dark chamber. Excess antibodies were washed off thrice with PBS for 5 min each at room temperature with shaking. Isotype-specific secondary antibodies were similarly prepared in blocking buffer. For double immuno-labeling, secondary antibodies of different isotype specificity were premixed in blocking buffer. Incubation and washing procedures are as detailed in the previous paragraph. Coverslips were mounted onto glass microscopic slides using Permaflour (Beckman Coulter). Excess mounting medium was removed by blotting with lint-free paper. The mounting medium was then allowed to solidify and the slides stored at 4°C until ready for microscopic viewing.



### **2.2.3.3 Image Acquisition**

Immunofluorescence images were recorded using either a Zeiss Axiovert 135 microscope mounted with a C4742-95-12NRB CCD camera (Hamamatsu) and the OpenLab 2.2.5 software (Improvision) or a confocal microscope (LSM 510, Zeiss, Germany). Images were processed using Adobe Photoshop 7.0 software (Adobe Systems Incorporated).

## **2.2.4 Biochemical Techniques**

### **2.2.4.1 SDS-Polyacrylamide-Gel-Electrophoresis (SDS-PAGE)**

SDS-PAGE gels containing 8-12% polyacrylamide in the separation gel and a stacking gel, cast according to the methodology established by Laemmli (Laemmli, 1970), were used for protein separation according to their molecular weight. The gel electrophoresis was carried out with the Mini-PROTEAN II System (BioRad). Protein samples were first heat denatured at 95°C for 5 min in 1× Laemmli buffer (10% (v/v) glycerin, 20 mM DTT, 1.5% (w/v) SDS, 60 mM Tris/HCl, 0.05% Coomassie G-250; pH 6.8) and then electrophoresed in SDS running buffer (25 mM Tris, 192 mM glycine, 0.1% (w/v) SDS) at a constant voltage of 100-180 V. In order to determine the molecular weight of the proteins of interest, a protein molecular weight marker (Full Range Rainbow Marker, Amersham Biosciences) was loaded alongside the samples with each run.

### **2.2.4.2 Western Blotting**

Prior to electroblotting, polyvinylidene difluoride (PVDF) membranes (Millipore) were placed in methanol for 15 sec and then rinsed with deionized H<sub>2</sub>O for 10 min. The SDS-PAGE gel, PVDF membranes and filter papers were then equilibrated in 1× CAPS transfer buffer (10 mM CAPS, 10% (v/v) methanol; pH 11.0) for 30 min. The electroblotting procedure was carried out in 1× CAPS transfer buffer using a Mini Trans-Blot module (Biorad) at 100 V for 1 hr. After blotting, the PVDF membrane was removed from the transfer apparatus and blocked in blocking solution [5% (w/v) skim milk or bovine serum albumin in TBST solution (15mM Tris-HCl, 150mM

NaCl, 0.5% (v/v) Tween 20; pH 7.4)] for 1 h at room temperature. Primary antibodies were diluted to their working concentrations in blocking solution as detailed in Section 2.1.4 and incubated with the membranes at 4°C overnight with shaking. Membranes were washed thrice for 15 min each with TBST solution. Secondary antibodies were diluted to their working concentrations in TBST solution as detailed Section 2.1.4 and incubated with the membranes for 1 h at RT. Membranes were washed thrice for 15 min each with TBST solution. Labeled bands were detected via chemiluminescence using the Lumi-Light Western Blotting substrate (Roche) according to the manufacturer's protocol.

### **2.2.4.3 Luciferase Assays**

Dual luciferase assays were performed using the Dual-Luciferase<sup>®</sup> Reporter Assay System (Promega) according to the manufacturer's recommendations. *Photinus* luciferase activities were normalized against values obtained for *Renilla* luciferase activities.

### **2.2.4.4 Translation Initiation Assays**

Translation assays were performed according to Wang *et al.*, 2002.

Capped <sup>32</sup>P-labeled programming mRNA transcripts were synthesized using the mMACHINE<sup>®</sup> kit (Ambion) according to the manufacturer's protocol.  $\alpha$ -<sup>32</sup>P-UTP was purchased from Amersham Biosciences.

*In vitro* translation reactions using rabbit reticulocyte lysates (Promega) were set up according to the manufacturer's protocol without the addition of mRNA. The reaction was preincubated at 30°C for 15 min with either guanosine-5'-[ $\gamma$ -thio]triphosphate (GTP $\gamma$ S; 1 mM) or cycloheximide (0.8 mM). Subsequently, <sup>32</sup>P-labeled programming mRNA (10<sup>5</sup> cpm) was added and incubation was continued for another 5 min at 30°C. Complexes were resolved by centrifugation through a 5 - 25% sucrose gradient in SG buffer (20 mM Tris-HCl, 100 mM KCl, 2 mM DTT, 2 mM magnesium acetate; pH 7.5) for 3 hr at 4°C at 154, 012 $\times$  g with a TH-641 rotor (Sorvall, Kendro Laboratory

Products). Starting from the top, 25 fractions were collected manually per tube. The amount of labeled mRNA from each fraction was determined by Cerenkov counting.

To monitor the migration of the 48S pre-initiation complexes and the 80S ribosome in the sucrose gradients, proteins were extracted from each fraction using trichloroacetic acid (TCA) precipitation. An equal amount of ice-cold 20% TCA was added to each fraction and incubated on ice for 30 min. The mixture was then centrifuged at 14 000× *g*, 4°C for 10 min and the resultant supernatant discarded. Each pellet was rinsed with 1.5 ml of cold acetone (prechilled to -80°C), followed by centrifugation at 14 000× *g* for 10 min, 4°C. The pellets were then air-dried briefly and resuspended in 100 µl of 2× SDS loading buffer. The samples were then boiled for 5 min and analyzed by SDS-PAGE and Western blotting (Sections 2.2.4.1 and 2.2.4.2).

#### 2.2.4.5 *In vitro* Competition Experiments

*In vitro* competition experiments were performed with reference to Paraskeva *et al.*, 1999 with modifications.

Capped programming mRNA transcripts were synthesized as described in Section 2.2.4.4 without the inclusion of radioactively labeled <sup>32</sup>P-UTP. SAPAP3 5' UTR containing competitor transcripts were synthesized using the T7 RiboMAX<sup>TM</sup> Express Large Scale RNA production systems kit (Promega) according to the manufacturer's protocol. SAPAP3 5' UTR competitor transcripts were added to the programming mRNAs (2.5 ng) on ice prior to the addition of the translation mixture. Capped *in vitro* synthesized *Renilla* mRNA was co-translated as an internal control. *In vitro* translation mixtures using rabbit reticulocyte lysates (Promega) were set up according to the manufacturer's protocol. The translation mixture was then added to the RNAs and translation was allowed to proceed for 90 min in a 37°C water bath. Two µl of the translation mixture was assayed for both *Photinus* and *Renilla* luciferase activities using the Dual-Luciferase<sup>®</sup> Reporter Assay System (Promega) according to the manufacturer's protocol. *Photinus* luciferase activities were normalized against values obtained for *Renilla* luciferase activities.

#### 2.2.4.6 Biochemical Isolation of Post-Synaptic Densities

Biochemical isolation of synaptosomes and postsynaptic densities were performed according to Carlin *et al.*, 1980 with modifications. Rat brains were homogenized in 40 to 50 ml of Solution A (4 mM HEPES, 0.32 M sucrose, 1 mM MgCl<sub>2</sub>, 0.5 mM CaCl<sub>2</sub>; pH 7.4) supplemented with Protease Inhibitor Cocktail Complete (Roche Applied Science) and phenylmethane sulfonyl fluoride (PMSF) (1 mM). The homogenate was centrifuged for 10 min at 1400× *g*, 4°C after which the supernatant was collected (S1). The remaining pellet was homogenized again in 10 ml of Solution A and centrifuged for 10 min at 710× *g*, 4°C. The ensuing supernatant (S2) was pooled with S1, mixed by homogenizing and centrifuged for 10 min at 13 800× *g* using a SS-34 rotor (Sorvall, Kendro Laboratory Products). An aliquot of the supernatant (= cytosolic extract) was collected. The pellet was homogenized in 18 ml of Solution B (4 mM HEPES, 0.32 M sucrose; pH 7.4) and layered on gradients composed of 3 ml of 1.2 M sucrose-4 mM HEPES (pH 7.4), 3 ml of 1.0 M sucrose-4 mM HEPES (pH 7.4) and 2 ml of 0.85 M sucrose-4 mM HEPES (pH 7.4). The gradients were centrifuged at 82 500× *g* for 2 hours at 4°C using the TH-641 rotor (Sorvall, Kendro Laboratory Products). The band (= synaptosomal fraction) between 1.0 and 1.2 M sucrose was removed by first aspirating off the solution above the band and removing the band with a 1 ml pipette with a plastic tip. This fraction was diluted in 15 ml of Solution B and an equal amount of 1% (v/v) Triton X-100 in 12 mM Tris-HCl, 0.32 M sucrose; pH 8.0. The mixture was stirred for 15 min at 4°C. The mixture was centrifuged at 32 800× *g* for 30 min at 4°C using the SS-34 rotor and the resultant pellet was resuspended in 1 ml of Solution B (= PSD fraction). Aliquots were snap frozen in liquid nitrogen and stored at -80°C.

#### 2.2.4.7 Production and Affinity Purification of Anti-SAPAP antibodies

Rabbits were immunised against purified GST-fusion proteins corresponding to amino acids 722 to 776 of SAPAP1 (GenBank Acc no: NP\_075235) and amino acids 694 to 747 of SAPAP3 (GenBank Acc no: NP\_775161), respectively. SAPAP3-specific antibodies were purified using NHS columns coupled with GST-SAPAP3

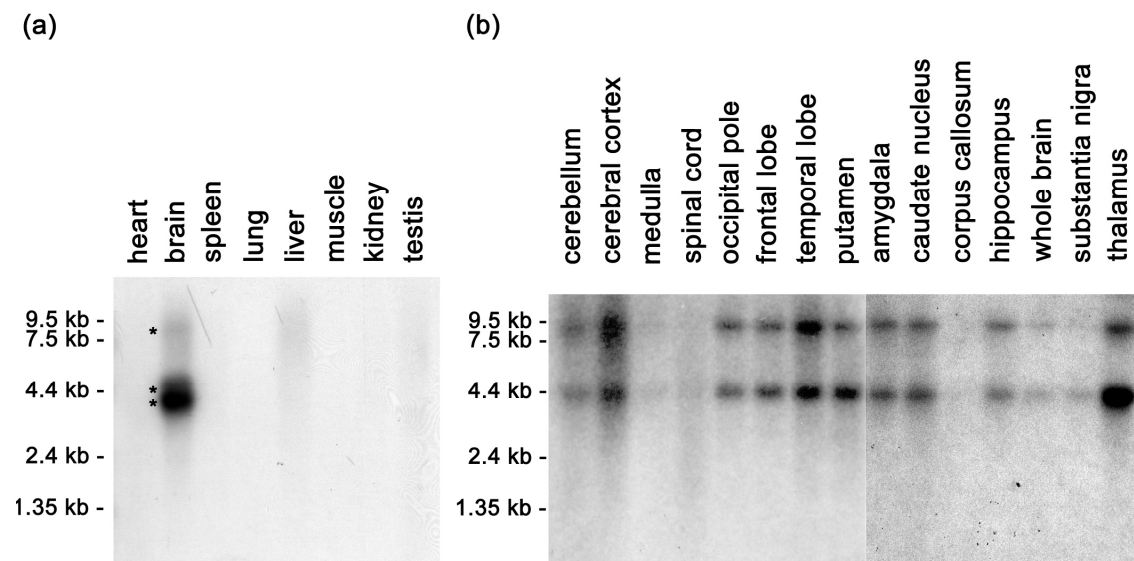
fusion protein. SAPAP1-specific antibodies were purified according to Monshausen *et al.*, 2002. Both antibodies specifically recognised their corresponding antigens.

## Chapter 3 Results

### 3.1 SAPAP3 Expression Profile

#### 3.1.1 SAPAP3 is Specifically Expressed in the Brain and is Strongly Enriched in the Post-Synaptic Density

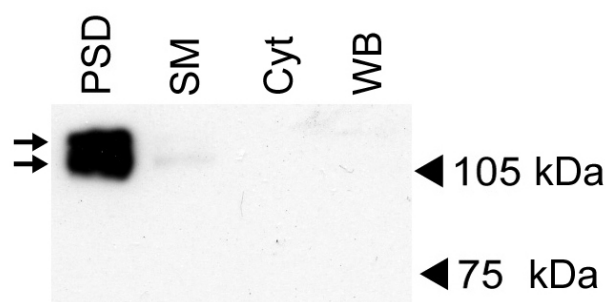
The expression of SAPAP3 transcripts in various tissues and brain regions was analyzed via Northern blotting using a SAPAP3 coding-region specific probe. In the rat, SAPAP3 mRNAs are exclusively expressed in the brain. Three different transcripts are identified: a 4 kb major, a 4.4 kb minor and a weakly visible 8 kb transcript (Figure 3.1a). Using the same probe, a 4.4 kb and an 8 kb transcript are detected in the human brain (Figure 3.1b). Both human SAPAP3 transcripts are present at similar ratios in most of the brain regions analyzed with the exception of the putamen and thalamus where the smaller transcript predominates, and the cerebral cortex where the larger transcript is more abundant.



**Figure 3.1** SAPAP3 transcripts are exclusively found in the mammalian brain and are differentially expressed across individual regions. PolyA mRNA multiple tissue Northern blots were probed with a  $^{32}\text{P}$ -labeled SAPAP3 probe (See Section 2.2.1.10 for details of probe used). (a) Tissue distribution of SAPAP3 mRNAs in the rat. The positions of the 8.0 kb, 4.4 kb and 4 kb transcripts are indicated by asterisks (\*). (b) Distribution of SAPAP3 mRNAs in different regions of the human brain. Positions of RNA molecular size markers are shown.

SAPAP3 transcript levels vary in the different human brain regions analyzed (Figure 3.1b). The highest levels of both SAPAP3 transcripts are observed in the cerebral cortex and the temporal lobe. The 4.4 kb SAPAP3 transcript is also highly abundant in the putamen and thalamus where the 8 kb transcript is less strongly detected. In contrast, SAPAP3 mRNAs are weakly expressed in the cerebellum and substantia nigra, and are undetectable in the medulla, spinal cord and corpus callosum. Moderate amounts of SAPAP3 mRNAs are present in the rest of the brain regions analyzed. The high levels of SAPAP3 transcripts found in the forebrain and not in the hindbrain points to a possible role of SAPAP3 in the higher brain functions in vertebrates. The absence of SAPAP3 transcripts in the corpus callosum (a region consisting mostly of axon tract bundles linking the two cerebral hemispheres and devoid of dendrites and neuronal cell bodies) indicates that the expression of SAPAP3 is restricted to neuronal cell types.

At the protein level, the expression of SAPAP3 was analyzed via Western blotting of different subcellular fractions from the adult rat brain. Using an affinity purified anti-SAPAP3 antibody, two isoforms of SAPAP3 migrating around 105 kDa and 120 kDa are detected (Figure 3.2). Both proteins are highly enriched in the postsynaptic density (PSD) fraction. Comparable bands are only detectable in the crude homogenate, cytosolic and synaptic membrane fractions after highly prolonged exposure.



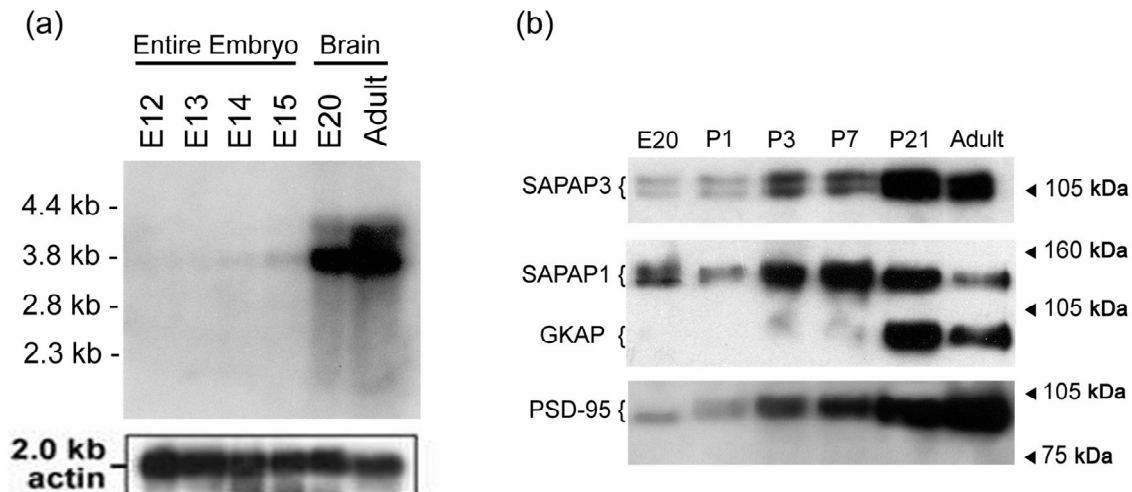
**Figure 3.2** SAPAP3 is highly enriched in the PSD fraction. Western blot analysis of subcellular fractions from the adult rat brain using affinity purified anti-SAPAP3 antibodies. Lanes were loaded as follows: WB: Crude homogenate (20  $\mu$ g), Cyt: Cytosolic fraction (25  $\mu$ g), SM: Synaptic membrane fraction (25  $\mu$ g), and PSD: postsynaptic density fraction (10  $\mu$ g). The positions of the 120 and 105 kDa SAPAP3 isoforms are indicated by arrows. Protein molecular size markers are indicated on the right.

### 3.1.2 SAPAP3 mRNAs and Proteins are Developmentally Regulated

Several PSD proteins have been shown to undergo developmental regulation (Petralia *et al.*, 2003, 2005; Sans *et al.*, 2000). In particular, the levels of SAPAP1 (also known as GKAP)-related transcripts and protein isoforms have been shown increase post-natally in the rat brain (Kawashima *et al.*, 1997; Petralia *et al.*, 2005; Sans *et al.*, 2000; Yoshii *et al.*, 2003). Therefore, I was interested to see if the expression of SAPAP3 changes during development.

Total RNA obtained from rat embryos and whole brains or PSD protein fractions obtained from whole brains at different stages were analyzed on Northern and Western blots, respectively. On Northern blots, two SAPAP3 transcripts appear relatively late in rat embryonic development (Figure. 3.3a). The 3.8 kb transcript is undetectable from E (embryonic day) 12 to E14 and becomes faintly visible in the E15 rat embryo. High levels of this transcript are present in the E20 rat brain which are further elevated in the adult brain. In comparison, the 4.2 kb transcript is first detected at low levels in the E20 rat brain and becomes more strongly expressed in the adult rat brain. The 3.8kb transcript is the major SAPAP3 mRNA present in both the E20 and adult rat brain. A slight difference in the migration of the two SAPAP3 transcripts was observed when the data from the commercial rat multiple tissue blot and the in-house made developmental blot were compared (Figures 3.1a, 3.1b and 3.3). Since the RNA size markers of the latter blot are in agreement with the sizes of the 28S (4.7 kb) and 18S rRNAs (1.9 kb) as well as the  $\beta$ -actin transcript (2.0 kb) (data not shown), the sizes of the SAPAP3 transcripts were determined based on this blot. Thus, the 4.4 kb and 4 kb transcripts detected in the multiple tissue blot are equivalent to the 4.2 kb and 3.8 kb transcripts detected in the rat developmental blot, respectively.





**Figure 3.3** SAPAP3 expression is developmentally regulated. Analyses of total RNA and PSD fractions from various developmental stages of the rat. (a) Northern blot probed with  $^{32}\text{P}$ -labeled SAPAP3 cDNA (See Section 2.2.1.10 for details of probe used). The same blot was reprobed for  $\beta$ -actin mRNA to demonstrate loading and integrity of the mRNAs. Equal amounts of total RNA were loaded from each developmental stage. (b) Developmental Western blots of PSD fractions probed with anti-SAPAP3, -SAPAP1 and -PSD95 antibodies. 2.5  $\mu\text{g}$  of protein samples were loaded per lane. Positions of the RNA and protein molecular size markers are shown for (a) and (b), respectively.

Western analysis reveals that the expression of SAPAP3 isoforms also undergoes developmental regulation (Figure 3.3b). Both proteins are faintly detected in PSD samples obtained from E20 and P (post-natal day) 1 rat brains. After a slight increase from P3 to P7, there is a dramatic increase in the levels of both isoforms at P21 before dropping slightly in the PSD of the adult rat. Both isoforms are expressed at similar ratios throughout development. Interesting, while E20 and adult brains both contain comparable amounts of SAPAP3 transcripts, a significantly larger amount of SAPAP3 isoforms are detected in adult PSDs in contrast to E20 PSDs (Figures 3.3a and 3.3b, compare lane E20 and Adult). This indicated that a post-transcriptional mechanism may be involved in regulating the levels of SAPAP3.

Western blots of the same PSD fractions were also probed with antibodies recognizing SAPAP1/GKAP and PSD-95. While PSD-95 and SAPAP1 both undergo developmental up-regulation as previously reported (Bence *et al.*, 2005; Petralia *et al.*, 2005; Sans *et al.*, 2000; Yoshii *et al.*, 2003), a significant decrease in the levels of

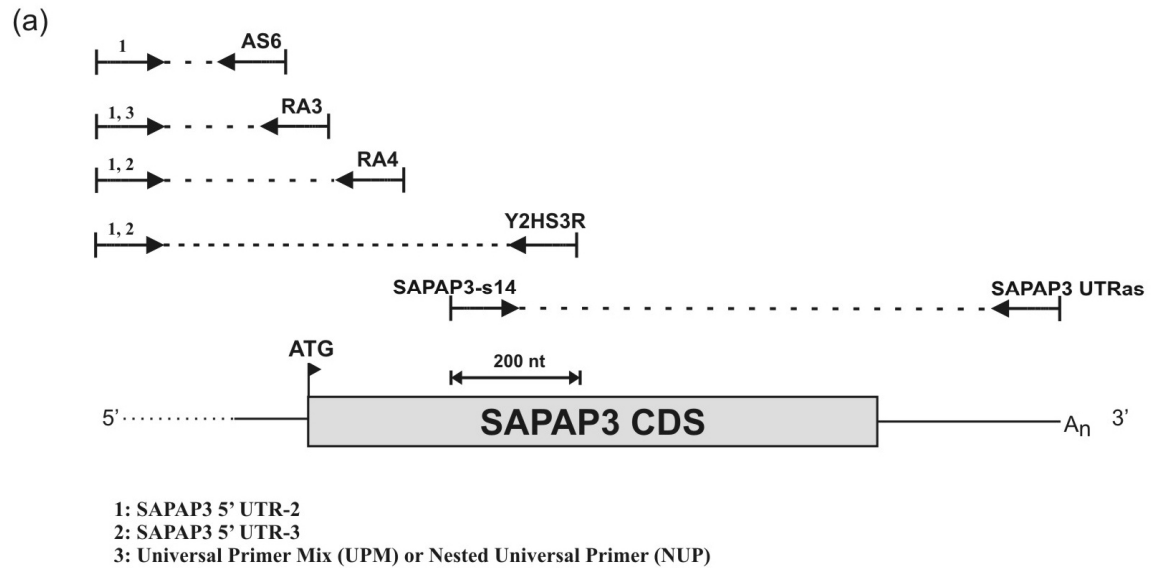
SAPAP1 in the adult PSD was also observed that has not been described. In particular, this decrease was more dramatic for SAPAP1 than for GKAP.

## 3.2 5' Untranslated Regions (UTRs) of SAPAP3 Transcripts

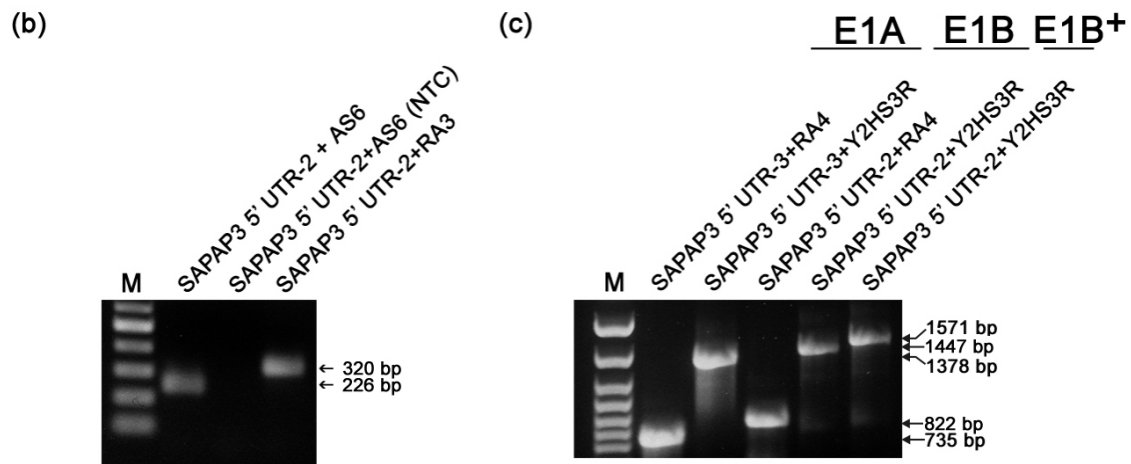
### 3.2.1 SAPAP3 mRNAs Possess Different 5' UTRs

The existing reference rat SAPAP3 mRNA entry (GenBank accession number: NM\_173138) reports a sequence of 3105 nt. This is much shorter than the transcripts observed in Northern blots (Figures 3.1a, 3.1b, 3.3a) and is partially due to an incomplete 3' UTR sequence in the database entry. However, even with the addition of the complete 3' UTR (648 nt; Kinder and Schwanke, unpublished), this sequence still fell short of the observed transcript lengths. In comparison, the reference mRNA for mouse SAPAP3 is 3845 nt long. A comparison of the two sequences indicates that sequences were missing from the 5' UTR of the existing rat SAPAP3 mRNA (104 nt versus 229 nt). Using a combination of BLAST searches and RT-PCR, three distinct SAPAP3 5' UTRs were identified (Figures 3.4 and 3.5). These sequences were named E1A, E1B and E1B<sup>+</sup> variants based on the unique exon that is included in the respective UTR.

The E1B 5' UTR variant was identified by searching rat EST entries using the first 200 nt from the rat reference mRNA. Several overlapping rat ESTs were found that contained additional upstream sequences (Table 3.1). A sense PCR primer (SAPAP3 5' UTR-2 primer) derived from the novel 5' UTR sequence was used to perform RT-PCR with several anti-sense primers that bind to the known 5' UTR (AS6) or coding region of the rat reference mRNA (RA3 and RA4) (Figure 3.4a). Using this approach, we were able to specifically amplify the expected PCR products of 226 bp, 320 bp and 822 bp (Figure 3.4b; Figure 3.4c, lane SAPAP3 5' UTR-2+RA4). These results demonstrate that the ESTs indeed represent the authentic SAPAP3 5' UTR cDNA. The E1B 5' UTR variant is similar to the 5' UTR reported in the mouse SAPAP3 reference mRNA. Using the nested universal primer (which only binds to the 5' end of full-length cDNAs synthesized via 5' RACE) and RA3 primer for 5' RACE analysis, a single PCR product identical in sequence to that amplified by SAPAP3 5'



5' UTR Type	Primers used to isolate UTR	
	Sense	Antisense
E1A	SAPAP3 5' UTR-3	RA4, Y2HS3R
E1B	SAPAP3 5' UTR-2, UPM, NUP	AS6, RA3, RA4, Y2HS3R
E1B <sup>+</sup>	SAPAP3 5' UTR-2	Y2HS3R



**Figure 3.4** PCR analysis of SAPAP3 5' UTR. (a) Schematic representation of the location of oligonucleotides used to isolate the E1A, E1B and E1B<sup>+</sup> 5' UTRs. The 200 nt overlap between the PCR products obtained for the 5' half (amplified using SAPAP3 5' UTR-2 or -3 and Y2HS3R) and the 3' half (amplified using SAPAP3-s14 and SAPAP3 UTRas) is indicated. The table below the scheme indicates the primer combinations used to amplify the three 5' UTRs identified in this study. (b) PCR products corresponding to the E1B 5' UTR variant isolated via PCR using the sense SAPAP3 5' UTR-2 primer with either AS6 or RA3 antisense primers. NTC: no template control. (c) Amplified E1A and E1B<sup>+</sup> SAPAP3 5' UTR variants and 5' half region PCR products used to confirm the existence of multiple 5' UTRs for a single SAPAP3 coding sequence (see text for details of the primer

combinations used). The sizes of the PCR products amplified are indicated to the right of each gel photo. M: 100 bp DNA ladder.

UTR-2 and RA3 was obtained. These results confirmed that the E1B sequence corresponds to the complete 5' UTR of SAPAP3. The addition of the E1B 5' UTR sequence to the existing sequence of the rat SAPAP3 mRNA gives a length of 3874 nucleotides which corresponds well in length to the 3.8 kb transcript identified in Northern blots (Figure 3.3a).

GenBank Acc no.	Definition
<b><u>Rat ESTs</u></b>	
BF409391	UI-R-CA1-blj-a-04-0-UI.s1 UI-R-CA1 Rattus norvegicus cDNA clone UI-R-CA1-blj-a-04-0-UI 3', mRNA sequence.
BF409457	UI-R-CA1-blj-d-03-0-UI.s1 UI-R-CA1 Rattus norvegicus cDNA clone I-R-CA1-blj-d-03-0-UI 3', mRNA sequence.
BF409585	UI-R-CA1-blm-b-02-0-UI.s1 UI-R-CA1 Rattus norvegicus cDNA clone I-R-CA1-blm-b-02-0-UI 3', mRNA sequence.
BF409774	UI-R-CA1-bls-f-05-0-UI.s1 UI-R-CA1 Rattus norvegicus cDNA clone I-R-CA1-bls-f-05-0-UI 3', mRNA sequence.
BF417882	UI-R-CA1-blu-d-09-0-UI.s1 UI-R-CA1 Rattus norvegicus cDNA clone UI-R-CA1-blu-d-09-0-UI 3', mRNA sequence.
<b><u>Mouse ESTs</u></b>	
CF536861	UI-M-FY0-chp-b-03-0-UI.r1 NIH_BMAP_FY0 Mus musculus cDNA clone IMAGE:30534074 5', mRNA sequence.
CA324003	UI-M-FY0-cco-m-05-0-UI.r1 NIH_BMAP_FY0 Mus musculus cDNA clone IMAGE:6822414 5', mRNA sequence.

**Table 3.1** List of rat and mouse ESTs containing novel SAPAP3 5' UTR sequences.

To determine if additional 5' splice variants exist, the genomic sequence upstream of the known mouse SAPAP3 gene (since the rat genomic sequence is not available) was used to screen for additional EST entries. Two overlapping mouse EST clones (CF536861 and CA324003) were identified containing sequences located in the immediate upstream vicinity of exon 1B in the genomic sequence. To determine if these sequences indeed represent an alternative SAPAP3 5' UTR, RT-PCR was performed with the SAPAP3 5' UTR-3 primer (derived from the EST sequences) in combination with the RA4 primer. A single PCR product of approximately 800 nt was obtained (Figure 3.4c, lane SAPAP3 5' UTR-3 + RA4). Interestingly, this 5' UTR variant isolated was different from that predicted by the mouse EST entries. In particular, it lacks most of the sequences present in both EST entries but does include the nucleotides 73-144 present in CF536861.

**SAPAP3 E1A 5' UTR**

1 *atgtgcttcg gacagtcccc tttcccttct ctaccccacc cccgccatgg*  
 51 *cacagcccct ggctcggggc ccagag*gagc cagtggctct gcgcctgctg  
 101 aagttaggat tctgcctggt ggtggggatc ctgacatcaa ggatgggacg  
 151 ccccggatgg agGTTCTTGG GGCCTGGCCC CCAACAGTAT GAAGAGCCTT  
 201 TACTGAGGCC **ATG**

**SAPAP3 E1B 5' UTR**

1 *acgcggggag cactcgctcg gggctccgca gccggcgag cccctccgcc*  
 51 *gggggctccg cagtgccggg tccgggagcc cgcaactcgct cccgcagccg*  
 101 *cagcgcccc ggcccgggcc gccggcacca tgtaaccccc accggagccc*  
 151 *gaccgggcca ggagccagtg gtctgcgcc tgctgaagtt aggattctgc*  
 201 ctggtggtgg ggatcctgac atcaaggatg ggacgccccg gatggagGTT  
 251 CCTGGGGCCT GGCCCCAAC AGTATGAAGA GCCTTTACTG AGGCC**ATG**

**SAPAP3 E1B<sup>+</sup> 5' UTR**

1 *acgcggggag cactcgctcg gggctccgca gccggcgag cccctccgcc*  
 51 *gggggctccg cagtgccggg tccgggagcc cgcaactcgct cccgcagccg*  
 101 *cagcgcccc ggcccgggcc gccggcacca tgtaaccccc accggagccc*  
 151 *gaccgggcca ggtaggcact caacaaatgt ctgtggaacg cggccatatt*  
 201 taagggcaat gaaaacgctg tagctgagcc tcatggacag atcacacaga  
 251 cacctgcagt tggaggagcc agtggctctg cgctgctga agttaggatt  
 301 ctgcctggtg gtggggatcc tgacatcaag gatgggacgc cccggatgga  
 351 gGTTCTTGGG GCCTGGCCCC CAACAGTATG AAGAGCCTTT ACTGAGGCC**A**  
 401 **TG**

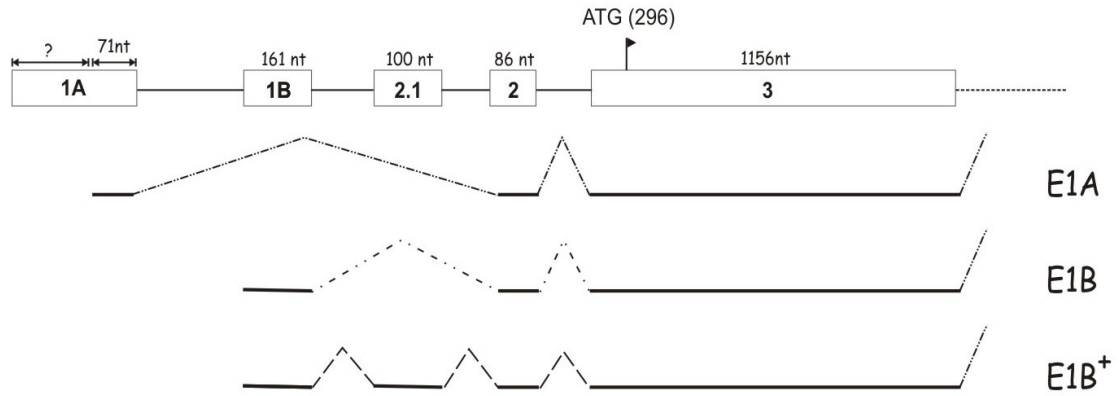
**Figure 3.5** SAPAP3 5' UTR sequences. Sequences from exons 1A, 1B, 2.1 and 2 are shown in lower case. In addition, sequences from exon 1A are italicized and in bold; sequences from exon 1B is italicized; sequences from exon 2.1 is underlined; sequences from exon 3 are capitalized. Numbers indicate the positions of the nucleotides. The start codon is indicated by **ATG**.

The presence of multiple 5' UTRs suggests that each UTR could be associated with different coding regions. To determine if this is the case, additional PCRs were

performed. Amplification of complete SAPAP3 cDNAs was not possible because of their GC-rich nature so an alternative approach was adopted. For the purpose of performing PCR, the entire SAPAP3 cDNA was divided into 2 subregions with an overlapping region of 200 nt between them (Figure 3.4a). Each region was then individually amplified by PCR. Amplification of the 2<sup>nd</sup> half of the cDNA was performed using SAPAP3-s14 and SAPAP3 UTRas primers. This produced a single band at the expected size of 2.6 kb. PCR of the 1<sup>st</sup> half of the cDNA using SAPAP3 5' UTR2 or UTR3 (for E1B and E1A UTRs, respectively) and Y2HS3R primers also resulted in the amplification of single PCR products with the expected sizes (Figure 3.4c, lanes SAPAP3 5' UTR-2 + Y2HS3R and SAPAP3 5' UTR-3 + Y2HS3R). Further, the same analysis using the SAPAP3 5' UTR-2 and Y2HS3R primer pair identified another longer 5' UTR containing additional sequences within the E1B variant (Figures 3.4c lane E1B<sup>+</sup>, 3.5 and 3.6). This 5' UTR variant was denoted as E1B<sup>+</sup>. The sequences of the overlapping region for the three 5' region PCR products was compared against that of the 3' region PCR product and found to be identical. This demonstrated that several 5' UTRs exist for a single SAPAP3 coding region.

A closer analysis of the organization of the SAPAP3 gene sequences indicates that the 5' UTR sequences are encoded by 5 exons, namely: exons 1A, 1B, 2.1, 2 and 3. The latter contains the start codon (Figure 3.6). All 5' UTR variants isolated so far invariably contain exons 2 and 3. As mentioned previously, inclusion of exon 1A and exclusion of exons 1B and 2.1 result in the generation of the E1A transcript. Similarly, fusion of exon 1B, and of exons 1B and 2.1 to exon 2 generates the E1B and E1B<sup>+</sup> transcripts, respectively. All 5' UTRs obtained are unusually long (more than 200 nt in length) and possess a high GC content. Secondary structure predictions with the MFOLD program (Mathews *et al.*, 1999; Zuker, 2003) indicate that, apart from the E1A variant, both E1B and E1B<sup>+</sup> 5' UTRs form extremely stable secondary structures, with free energies ( $\Delta G$ ) predicted to lie between -189.5 to -146.8 kcal/mol (Figure 3.6). The higher the value of  $\Delta G$  (with the minus sign) the more stable the secondary structure. In comparison, the rat SAPAP1 5' UTR (GenBank Acc no: NM\_022946), which is comparable in length (274 nt versus 295 nt for E1B type 5' UTR), is not GC rich (%GC = 50.18%) and is not predicted to form stable secondary structures ( $\Delta G$  between -85.6 to -81.4 kcal/mol). Interestingly, E1B 5' UTR is highly conserved across the human, rat and mouse genomes while SAPAP1 5' UTR is much less

conserved between rat and mouse (Figures 3.7 and 3.8). Pairwise alignment scores between rat and mouse SAPAP3 5' UTRs ranges from 95-96% while that for SAPAP1 5' UTR is only 88%. The highly conserved nature of E1B 5' UTR variant suggests that it may possess important functional properties. In particular, there is extensive evidence from the literature that long, GC-rich 5' UTR sequences contain elements that impede translation (Han *et al.*, 2003a, b; Lammich *et al.*, 2004; Tang and Tseng, 1999; van der Velden and Thomas, 1999). The cumulative evidence here strongly suggests that E1B and E1B<sup>+</sup> SAPAP3 5' UTRs may function as translational inhibitory elements. To address this question, the E1B variant was chosen because mRNAs containing this 5' UTR represent the most abundant transcripts in the adult brain (data not shown). For the remainder of the thesis, the E1B variant will be referred to as SAPAP3 5' UTR.

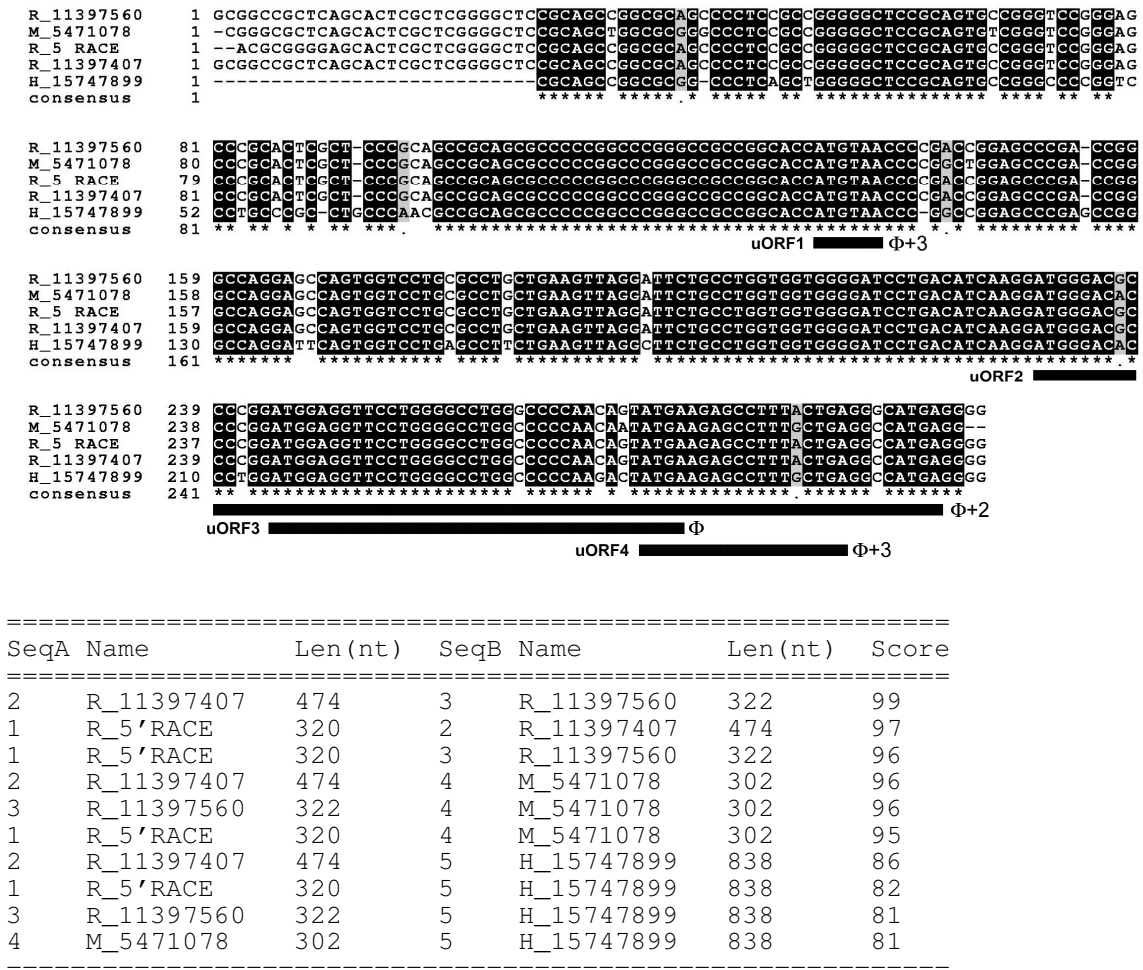


<u>Type of 5' UTR</u>	<u>Length (nt)</u>	<u>% GC</u>	<u><math>\Delta G</math> (kcal/mol) range</u>
E1A	213	62.91 %	-85.3 to -81.1
E1B	295	72.15 %	-154.5 to -146.8
E1B <sup>+</sup>	404	66.58 %	-189.5 to -180.1
<sup>†</sup> SAPAP1	277	50.18 %	-85.6 to -81.4

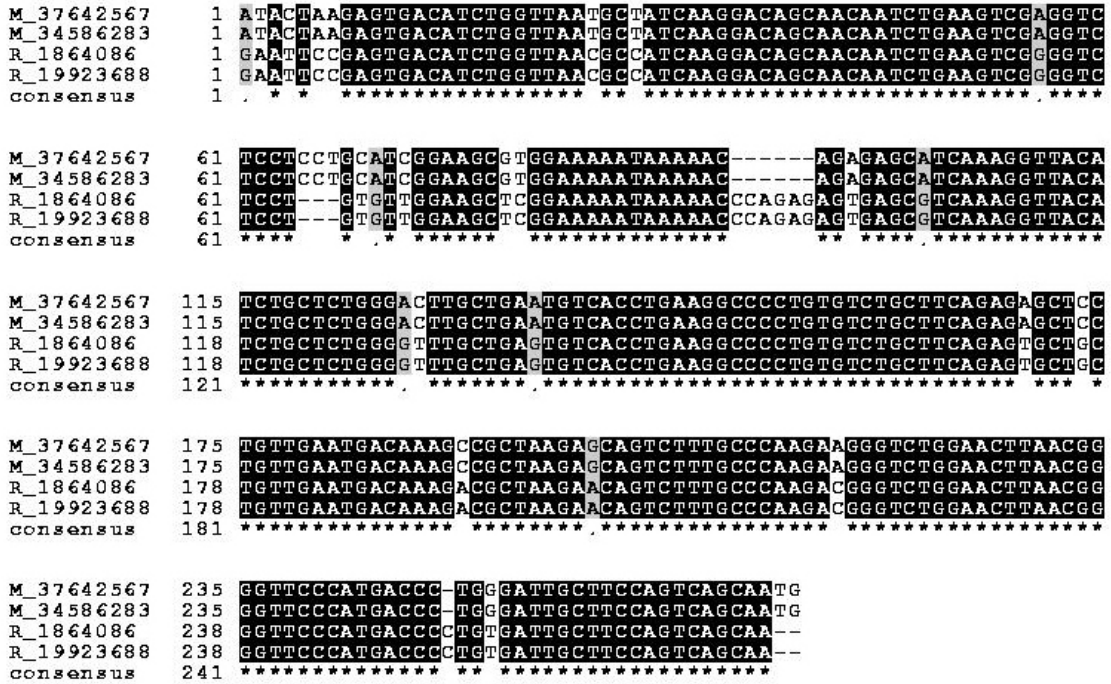
<sup>†</sup>5' UTR obtained from GenBank rat SAPAP1 mRNA entry (Acc no: NM\_022946)

**Figure 3.6** Structure of the 5' UTRs of SAPAP3 transcripts isolated in this study. The top diagram indicates the organization of part of the rat SAPAP3 gene. Exons are indicated by open boxes together with the exon numbers. The sizes of the exons are listed above their respective boxes. The start codon (ATG) in exon 3 is indicated. Below this diagram, the various alternatively spliced 5' UTRs are schematically shown. Sequence regions included in the transcripts are indicated by solid lines linked to each other by dotted lines. The table lists some physical properties of each 5' UTR variant as well as the rat SAPAP1 5' UTR as a comparison.  $\Delta G$  values were predicted using the MFOLD server.





**Figure 3.7** The E1B type SAPAP3 5' UTR is evolutionarily conserved across human, rat and mouse species. Human, rat and mouse SAPAP3 5' UTR encoding sequences were obtained from GenBank dbEST database and aligned against the rat SAPAP3 5' UTR sequence derived from the 5' RACE PCR product. Nucleotides conserved amongst all species are shown in a black background. The four conserved uORFs are indicated and underlined. The phases of the open reading frames of the uORFs are indicated at the end of their respective lines. The phase of SAPAP3 open reading frame is designated as Φ. Beneath the alignment is the CLUSTALW Scores Table indicating the pairwise alignment scores for each sequence. The GI number of the sequence is indicated. R: rat, M: mouse, H: human.



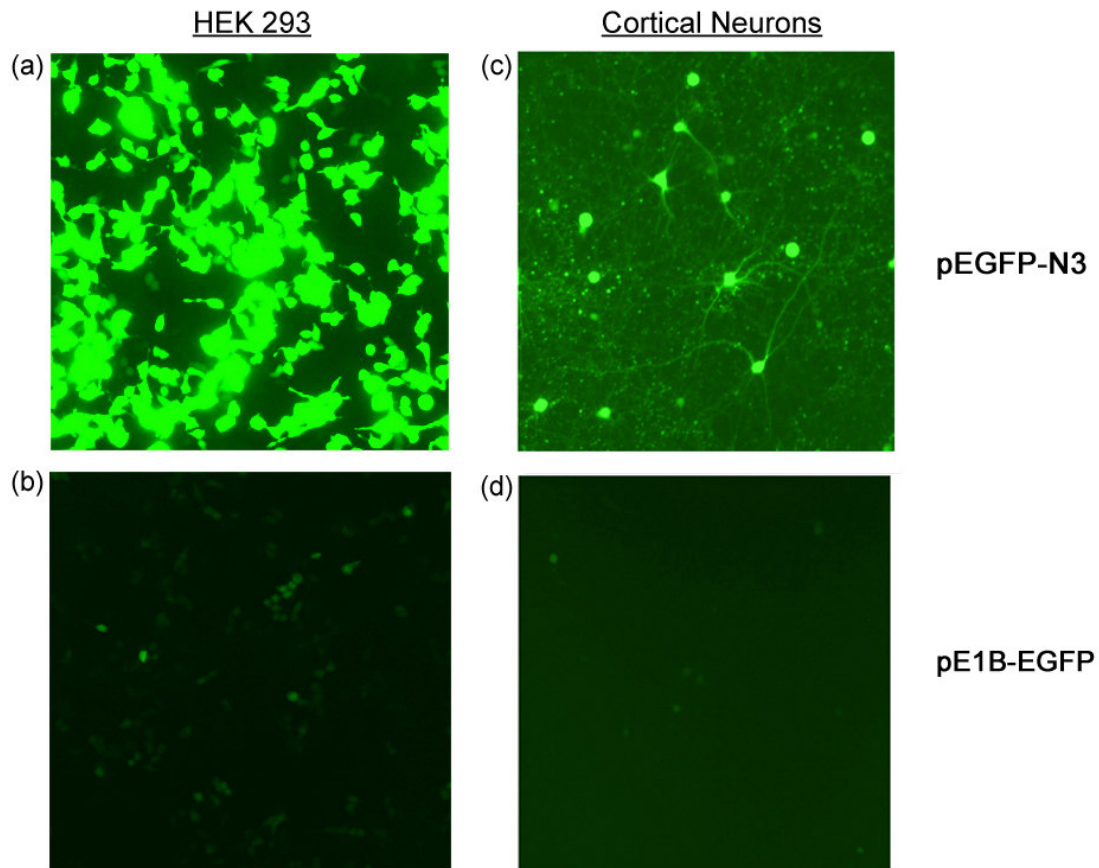
**Figure 3.8** Alignment of SAPAP1 5' UTR encoding sequences from rat and mouse. Rat and mouse SAPAP1 5' UTR sequences were obtained from GenBank dbEST database. Nucleotides conserved amongst both species are shown in a black background. Beneath the alignment is the CLUSTALW Scores Table indicating the pairwise alignment scores for each sequence. The GI number of the sequence is indicated. R: rat, M: mouse.

### 3.2.2 SAPAP3 5' UTR is a Strong Inhibitor of Translational

To test if SAPAP3 5' UTR influences translation, it was inserted upstream of the EGFP coding sequence in the pEGFP-N3 construct (pE1B-EGFP). The pE1B-EGFP construct was then used to transfect HEK293 cells. The empty pEGFP-N3 vector was separately transfected as a control. The amounts of EGFP synthesized were monitored via auto-fluorescence of this protein. Cells transfected with the control pEGFP-N3 vector exhibit strong EGFP auto-fluorescence, indicating that high levels of EGFP are produced by the cells (Figure 3.9a). In contrast, only a faint auto-fluorescence was observed when the cells were transfected with pE1B-EGFP indicating that the synthesis of EGFP is reduced upon the introduction of the UTR (Figure 3.9 b). Because SAPAP3 is specifically expressed in the brain, the assay was repeated by transfecting 7 DIV cortical neurons and assaying them for EGFP auto-fluorescence one day after transfection. Similar to the results observed for HEK293 cells, very low levels of EGFP are detected in neurons transfected with pE1B-EGFP as compared neurons transfected with pEGFP-N3 (Figures 3.9c and d).

The above assay, although fast and convenient, is unable to address several important questions. Specifically, the assay does not account for differences in transfection efficiencies in separate transfections. It also cannot discriminate if the reduced production of EGFP resulting from the inclusion of SAPAP3 5' UTR occurs at the transcriptional or translational level. More importantly, it cannot distinguish if the translational inhibition, should there be any, is a specific property possessed by SAPAP3 5' UTR or if it is merely due to the introduction of an unusually long 5' UTR upstream of the EGFP coding region. To address these questions, another strategy was devised whereby SAPAP3 or SAPAP1 5' UTR was introduced before the sequences of the SAPAP3 coding region and 3' UTR (Figure 3.10a). Three different constructs were made. The basic pFS3 construct transcribes a recombinant mRNA containing a vector-derived minimal 5' UTR optimal for translation fused to the coding region and 3' UTR of SAPAP3. This construct efficiently expresses an N-terminal FLAG-tagged SAPAP3. The pS1-FS3 and pE1B-FS3 constructs are based on the pFS3 construct but the vector-derived 5' UTR is replaced by the SAPAP1 or SAPAP3 5' UTR sequences, respectively. These three constructs were then

transfected into HEK293 cells and the levels of recombinant mRNA and SAPAP3 analyzed.

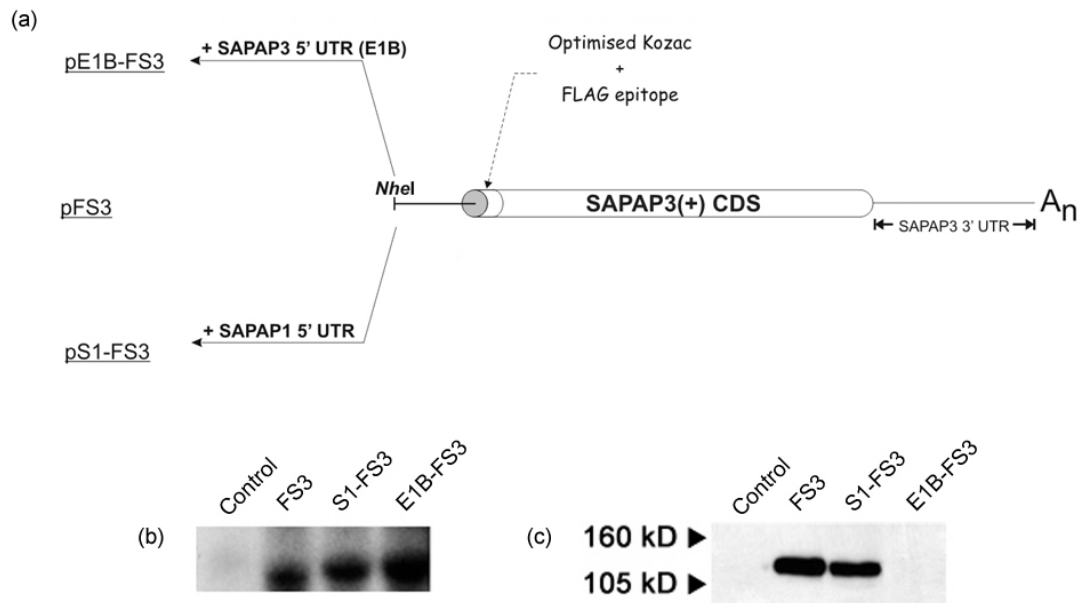


**Figure 3.9** SAPAP3 5' UTR strongly inhibits synthesis of EGFP in both HEK293 cells and cortical neurons. (a) and (c) Cells transfected with pEGFP-N3 exhibit strong fluorescence indicating that high levels of EGFP are produced. (b) and (d) Levels of EGFP are drastically reduced in cells transfected with the pE1B-EGFP construct.

Northern analysis using total RNA obtained from the transfected cells indicates that similar levels of recombinant transcripts are expressed from all three constructs (Figure 3.10b, lanes FS3, S1-FS3 and E1B-FS3). Thus, inclusion of neither SAPAP3 nor SAPAP1 5' UTR has any detrimental effect on the expression or stability of mRNA as compared to the control transcript containing a minimal 5' UTR.

Western blotting with protein extracts from pFS3 and pS1-FS3 transfected cells reveals that comparable levels of FLAG-SAPAP3 are synthesized from pFS3 and pS1-FS3 transcripts (Figure 3.10c, lane FS3 and S1-FS3). In contrast, hardly any FLAG-SAPAP3 is detected in extracts from cells transfected with the pE1B-FS3

construct (Figure 3.10c, lane E1B-FS3). Thus, 5' UTR mediated regulation of SAPAP3 expression occurs at the translational level and is a property specific to this 5' UTR.

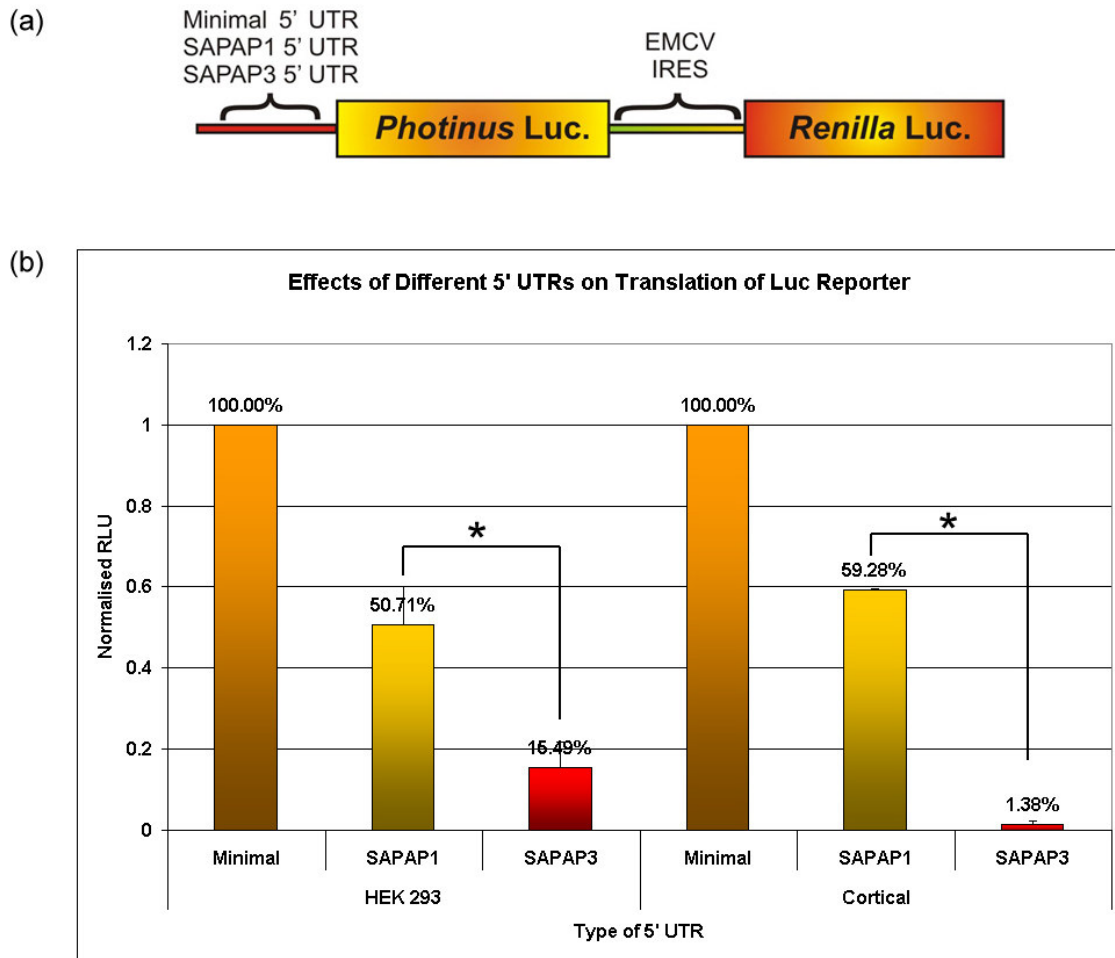


**Figure 3.10** SAPAP3 5' UTR specifically hinders translation of the FS3 open reading frame. (a) Schematic representation of the various recombinant mRNAs used. The pFS3 construct encodes a recombinant pFS3 transcript containing a vector-derived minimal 5' UTR linked to the coding region and 3' UTR of SAPAP3 and efficiently expresses recombinant FLAG-tagged SAPAP3. pS1-FS3 and pE1B-FS3 constructs are derived from pFS3. These constructs encode recombinant transcripts in which the vector derived minimal 5' UTR has been replaced with either the 5' UTR of SAPAP1 (pS1-FS3 transcript) or SAPAP3 (E1B-FS3 transcript), respectively. (b) Northern analysis of total RNA obtained from non-transfected and transfected HEK293 cells probed with a <sup>32</sup>P-labeled SAPAP3 probe. Equal amounts of RNA were loaded for each lane. Inclusion of SAPAP1 and SAPAP3 5' UTRs in pS1-FS3 and pE1B-FS3 mRNAs, respectively, does not have any influence on the amount of mRNA produced as compared to the pFS3 transcript. (c) Western analysis of SAPAP3 expression from non-transfected and transfected HEK293 cells. For each sample, equal amounts of protein were loaded. The blot was probed with anti-FLAG antibodies to detect FLAG-SAPAP3. Synthesis of FLAG-SAPAP3 from cells transfected with pE1B-FS3 is dramatically reduced compared to cells transfected with control pFS3 construct. In contrast, comparable amounts of FLAG-SAPAP3 were synthesized from cells transfected with pS1-FS3 as well as pFS3.

To quantitate the extent of translational inhibition conferred by the SAPAP3 5' UTR, pXBFE bicistronic constructs based on the pBicFire vector were generated (Figure

3.11a). The pBicFire vector has been previously described and contains the *Photinus* and *Renilla* luciferase open reading frames separated by a small 30 bp intercistronic multiple cloning site. Expression of the bicistronic mRNAs is driven by the cytomegalovirus (CMV) promoter in pcDNA3.1(+*zeo*) (Pedersen *et al.*, 2002). The internal ribosome entry site (IRES) element derived from the encephalomyocarditis virus (EMCV) was introduced into the intercistronic spacer region to generate the pBFE construct. In cells expressing the bicistronic mRNAs, synthesis of *Photinus* luciferase occurs by a cap-dependent (“scanning”) mechanism while the synthesis of *Renilla* luciferase is directed by the EMCV IRES. Levels of *Renilla* luciferase activities are used to correct for differences in transfection efficiencies. The 5' UTR of either SAPAP1 or SAPAP3 was inserted before the *Photinus* coding region to generate the pS1-BFE and pS3-BFE constructs, respectively. All three bicistronic constructs were transfected into HEK293 cells and cortical neurons.

When compared to control pBFE-transfected cells, *Photinus* luciferase activity is significantly reduced in cells transfected with pS3-BFE in both cell culture systems ( $15.49\% \pm 0.00$  in HEK293 cells and  $1.38\% \pm 0.00$  in cortical neurons) (Figure 3.11b). Under the same conditions, *Photinus* luciferase activity of pS1-BFE-transfected cells is only moderately affected ( $50.71\% \pm 0.09$  and  $59.28\% \pm 0.00$  in HEK293 cells and cortical neurons, respectively) (Figure 3.11b). Thus, the results from the quantitation experiments support the conclusions from the previous assays and confirm that SAPAP3 5' UTR functions as a translational inhibitory element.



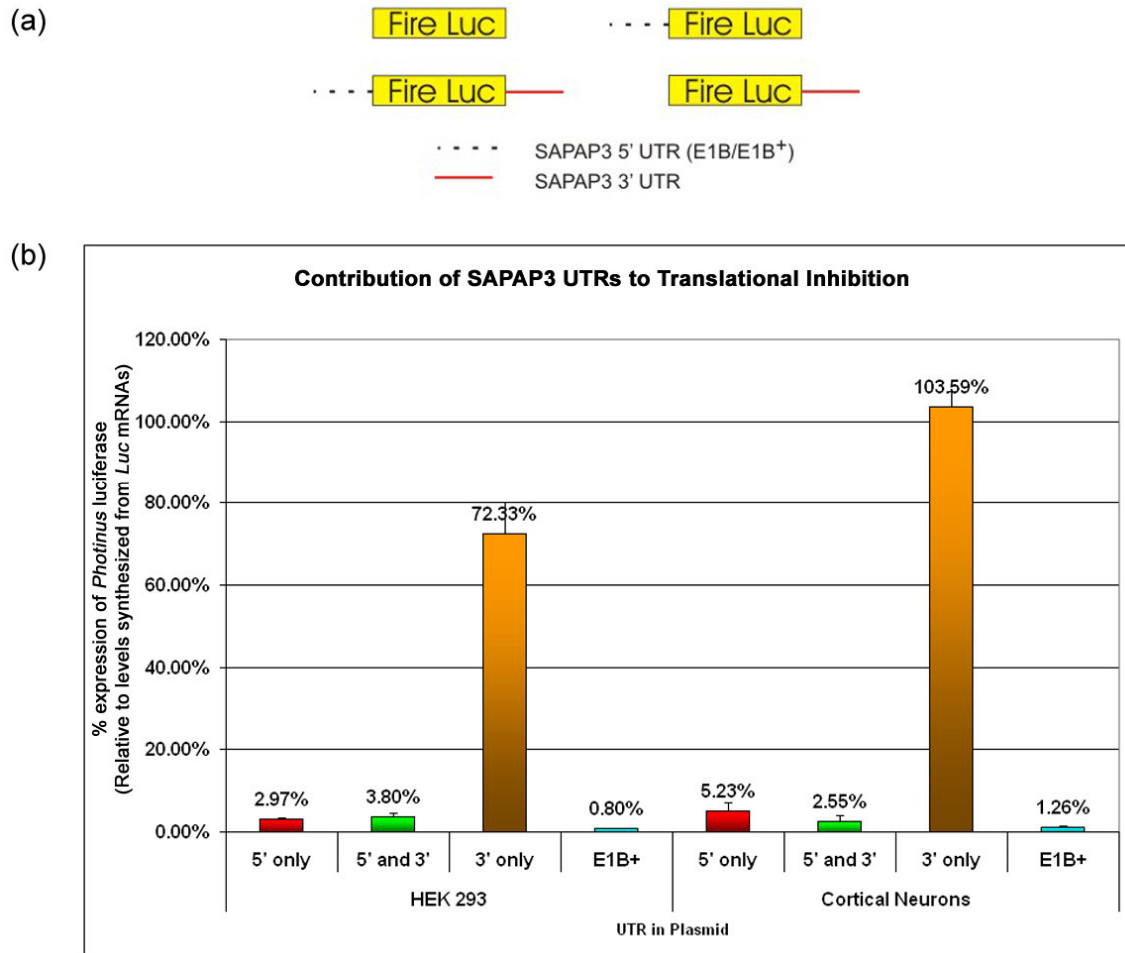
**Figure 3.11** Inclusion of SAPAP3 5' UTR sequences upstream of the *Photinus* luciferase CDS in a bicistronic mRNA dramatically reduces expression of the luciferase. Quantification of extent of translational inhibition conferred by different 5' UTRs. (a) Schematic representation of the pXBFE-encoded bicistronic mRNAs used to quantitate translational inhibition. (b) In comparison to cells transfected with the pBFE vector (minimal), pS1-BFE transfected cells synthesize slightly less luciferase (SAPAP1). However, a significant reduction of luciferase levels is observed only in cells transfected with pS3-BFE (SAPAP3). Activities of *Photinus* luciferases were normalized against *Renilla* luciferase activities to account for differences in transfection efficiencies (relative light units, RLU). The normalized values were then expressed as percentages of the RLU values for the pBFE construct (normalized RLU). \* Statistically significant ( $p < 0.05$ ).

### 3.2.3 SAPAP3 5' UTR is Sufficient to Confer Translational Inhibition

Translational regulation often occurs via an interaction between the 5' and 3' UTR elements (Kuersten and Goodwin, 2003; Mazumder *et al.*, 2001; Wilkie *et al.*, 2003). To assess if the 3' UTR of SAPAP3 mRNAs may also contribute to translational regulation, the 5' UTR alone (pS35-Luc), 3' UTR alone (pS33-Luc) or both 5' and 3' UTRs of SAPAP3 mRNAs (pS353-Luc and pE1B<sup>+</sup>-Luc) were introduced to the *Photinus* luciferase coding region of the pLuc vector (Figure 3.12a). The resulting constructs were co-transfected into either HEK293 cells or 7 DIV cortical neurons together with another plasmid expressing the *Renilla* luciferase. Levels of *Renilla* luciferase activities were used to correct for differences in transfection efficiencies.

In HEK293 cells transfected with pS33-Luc, the amount of *Photinus* luciferase synthesized is slightly lower compared to pLuc transfected control cells (Figure 3.12b, HEK293 cells, 3' only column). Most importantly, similar levels of *Photinus* luciferase were synthesized from cortical neurons transfected with either pS33-Luc or pLuc (Figure 3.12b, cortical neurons, 3' only column). Both results are essentially identical and, together, they indicate that the inclusion of the 3' UTR of SAPAP3 mRNA has no effect on the amounts of luciferase synthesized in both cell types. In contrast, very little *Photinus* luciferase activity is detected when either cell type is transfected with the pS35-Luc (Figure 3.12b, 5' only column). This result confirms that the inclusion of the 5' UTR of SAPAP3 mRNA alone is sufficient to almost completely prevent translation of the luciferase in both HEK293 and cortical neurons. Moreover, the levels of *Photinus* luciferase in cells transfected with either pS353-Luc or pS35-Luc were essentially identical, indicating that the 3' UTR does not influence translation inhibition mediated by the 5' UTR. As expected from the predicted higher  $\Delta G$  values of the E1B<sup>+</sup> 5' UTR, luciferase activity levels of either cell types transfected with pE1B<sup>+</sup>-Luc was even further reduced compared to pS353-Luc transfected cells (Figure 3.12b, E1B<sup>+</sup> column). These data confirm that the 5' UTR of SAPAP3 is the sole element responsible for mediating translational inhibition.





**Figure 3.12** The 3' UTR of SAPAP3 does not play a role in regulating translation. (a) Schematic representation of the luciferase mRNAs used to determine the contribution of SAPAP3 5' and 3' UTRs on translation of *Photinus* luciferase. (b) Inclusion of SAPAP3 3' UTR downstream of the *Photinus* luciferase coding region in pS33-Luc mRNAs (3' only) does not affect luciferase levels in both HEK293 cells and cortical neurons in comparison to the control pLuc mRNAs. Inclusion of the SAPAP3 5' UTR upstream of the luciferase coding region either alone (pS35-Luc mRNAs, 5' only) or in combination with the SAPAP3 3' UTR (pS353-Luc mRNAs, 5' and 3') results in a dramatic reduction in synthesis of luciferase as compared to both pS3-Luc and pLuc transcripts. Activities of *Photinus* luciferase were normalized against that for *Renilla* luciferase to account for differences in transfection efficiencies. The normalized values were then expressed as percentages of the normalized values obtained for the pLuc mRNAs.

### 3.2.4 SAPAP3 5' UTR does not function as an IRES

The fact that SAPAP3 5' UTR inhibits translation raises an interesting question as to how the synthesis of SAPAP3 is regulated *in vivo*. Translational control is mostly regarded to occur at the initiation step (Gingras *et al.*, 1999). Several mechanisms have been reported for eukaryotic translational initiation. While most eukaryotic mRNAs utilize conventional cap-dependent ribosome scanning mechanisms to initiate translation, a distinct group of mRNAs appear to do so via a cap-independent mechanism. Cap-independent translation of these mRNAs is mediated by IRES elements present in their 5' UTR. Although there is no observable conservation of secondary structures in the eukaryotic IRES elements identified so far, many are GC-rich and thus presumably possess complex secondary structures. IRES-dependent translation is believed to play an important role in allowing translation of specific mRNAs under circumstances when cap-dependent translation is inhibited (e.g. in cells undergoing apoptosis or in poliovirus infected cells) (Clemens *et al.*, 2000; Morrish and Rumsby, 2002; Stoneley and Willis, 2004). In particular, IRES elements have been identified for several dendritically localized mRNAs (Pinkstaff *et al.*, 2001). IRES-dependent translation of dendritically localized transcripts is hypothesized to allow specific translation of certain mRNAs under varying conditions or to enhance dendritic translation of these mRNAs since neuronal dendrites contain a lower concentration of ribosomes and initiation factors. Because SAPAP3 transcripts are dendritically localized and possess a GC-rich 5' UTR, it was of interest to determine if regulation of SAPAP3 translation could occur by an IRES-dependent mechanism.

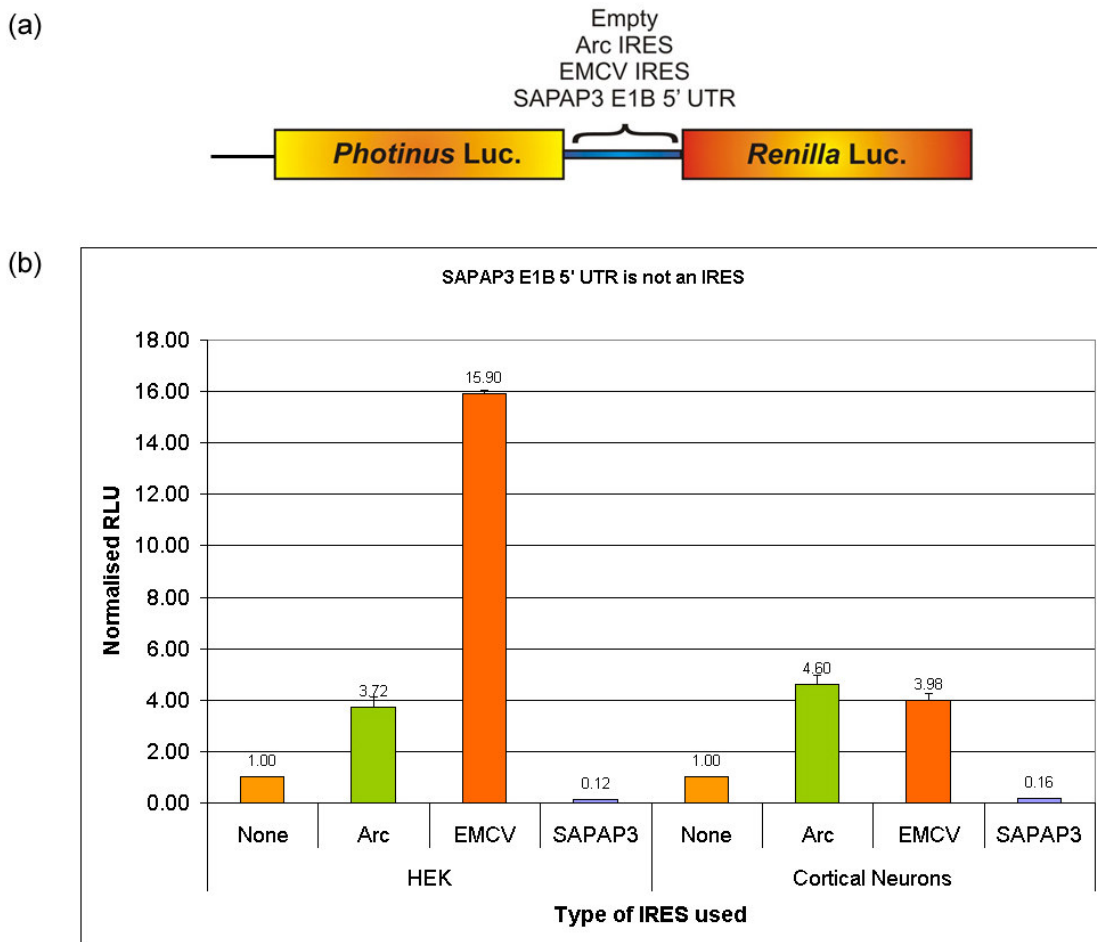
```

-----
                          Pattern = IRES
-----
Found 1 matches in 1 sequences

seq : [210,297] : TGGGGA TCCTGA CATCA A GGATG GGA CGCCC CGGAT GGAG GTTCC TGGGG CCTGG
CCCCCA AC AGTATG AAGAGCC TTTACT GAGGCC

```

**Figure 3.13** Results from the UTRScan prediction server. SAPAP3 5' UTR was predicted to contain an IRES element.



**Figure 3.14** SAPAP3 5' UTR is not an IRES. (a) Schematic representation of the bicistronic mRNAs used to test for IRES activity. (b) Results of the bicistronic mRNA assay. *Renilla* luciferase activities of each bicistronic mRNA were normalized to the *Photinus* luciferase activities. The normalized values were then expressed as ratios to the corresponding values obtained for control pBFE-transfected cells (normalized RLU). Unlike the Arc and EMCV IRESes, SAPAP3 5' UTR does not possess IRES activity.

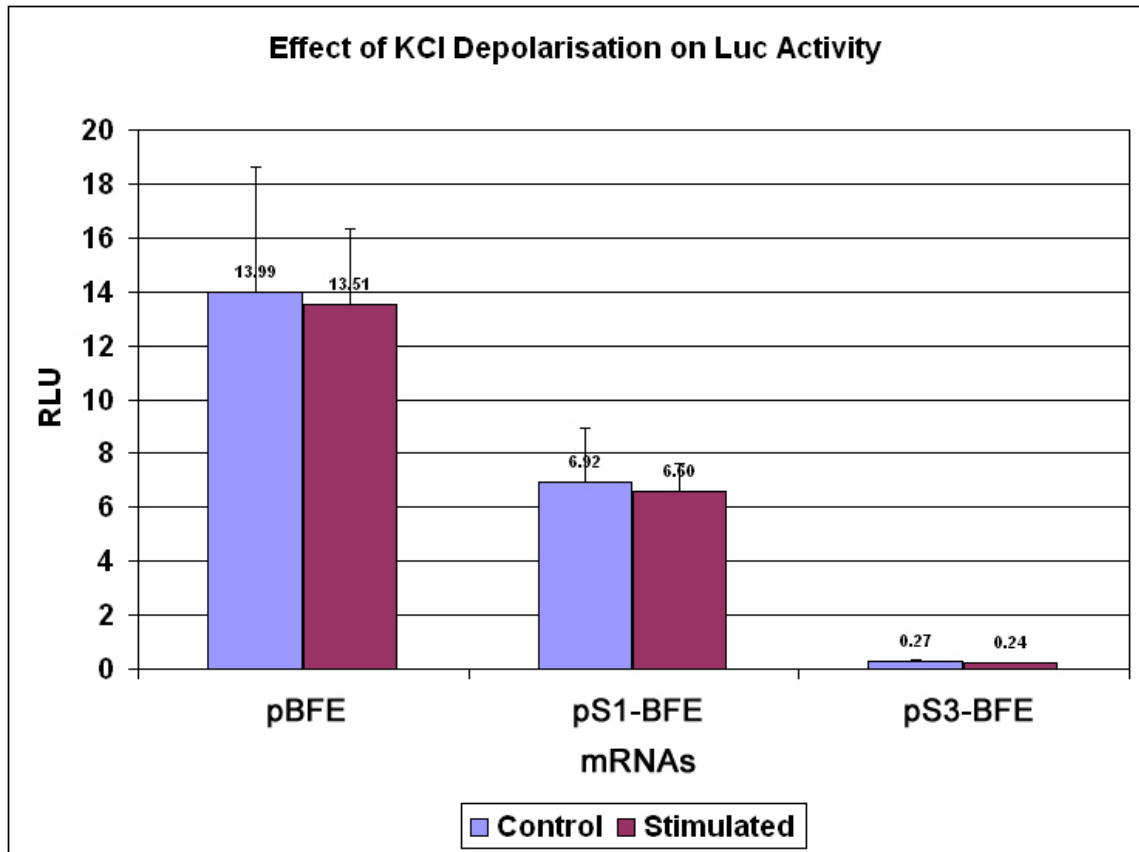
The SAPAP3 5' UTR was analyzed using the UTRScan program (Pesole and Liuni, 1999) to predict if it contains an IRES element. The program predicted that a region encoded by the common exons 2 and 3 contains a putative IRES element (Figure 3.13). A bicistronic mRNA translation assay was employed to experimentally test the SAPAP3 5' UTR for IRES activity. The SAPAP3 5' UTR sequence was introduced into the intercistronic region between the *Photinus* and *Renilla* luciferases coding sequences of the pBicFire vector to generate the pBFS3 construct (Figure 3.14a). While the translation of the *Photinus* luciferase from the resulting bicistronic mRNA is cap-dependent, the translation of the *Renilla* luciferase is now dependent on the

presence of a functional IRES element in the intercistronic region. IRES elements derived from the EMCV (pBFE) and the Arc/Arg3.1 (pBFA) mRNAs were used as positive controls. In this assay, *Photinus* luciferase levels were used to normalize against differences in transfection efficiencies.

HEK293 cells transfected with pBFE or pBFA synthesized 15.9-fold and 3.7-fold more *Renilla* luciferase compared to control pBicFire-transfected cells (Figure 3.14b). Similarly, cortical neurons transfected with constructs encoding the control IRES elements were able to synthesize approximately 4-fold more *Renilla* luciferase compared to the pBicFire-transfected cortical neurons (Figure 3.14b). In marked contrast, the levels of *Renilla* luciferase synthesized from cells transfected with pBFS3 was much lower than that produced from the control pBicFire-transfected cells (less than 0.16-fold). Thus, while internal initiation of translation is clearly mediated by EMCV and Arc IRESes in both cell types, SAPAP3 5' UTR does not function as an IRES element.

### 3.2.5 Synaptic Activity does not Modulate Translational Inhibition

Activity-dependent translational regulation of dendritically localized mRNAs has been suggested to play an important role in regulating synaptic plasticity (Steward and Schuman, 2003). Because SAPAP3 mRNAs are dendritically localized, it was of interest to examine if changes in synaptic activity could influence translation inhibition mediated by the SAPAP3 5' UTR. Since SAPAP3 is a component of the PSD, the spaced stimuli protocol (Wu *et al.*, 2001), a procedure that strongly induces the formation of dendritic spines, was used to stimulate cortical neurons transfected with pXBFE constructs. The neurons were then assayed for changes in luciferase activity compared to untreated controls. As shown in Figure 3.15, modulation of synaptic activity had no effect on luciferase activities for neurons transfected with pBFE, pS1-BFE or pS3-BFE plasmids. Thus, at least using this stimulation protocol and within the time frame tested, synaptic activity does not appear to influence SAPAP3 5' UTR-mediated translational inhibition.



**Figure 3.15** Synaptic activity has no influence on translational inhibition mediated by SAPAP3 5' UTR. Seven DIV cortical neurons were transfected with pXBFE constructs, stimulated by the spaced-stimuli protocol one day after transfection and assayed for luciferase activities. *Photinus* luciferase activities were normalized against *Renilla* luciferase activities. The normalized values (RLU) of control and stimulated samples are plotted side by side for each construct. No changes in luciferase activities are observed for control, SAPAP1 5' UTR containing and SAPAP3 5' UTR containing mRNAs.

### 3.3 Mechanisms of Translational Inhibition Mediated by SAPAP3 5' UTR

#### 3.3.1 SAPAP3 5' UTR Inhibits Formation of the 80S Ribosome

Since SAPAP3 5' UTR does not contain an IRES element, translation of SAPAP3 mRNA most likely occurs by a conventional cap-dependent scanning mechanism. According to this mechanism, the 43S pre-initiation complex consisting of the 40S ribosomal subunit, eukaryotic initiation factors (eIFs) 1, 1A, 3 and eIF2/GTP/Met-tRNA<sub>i</sub> complex first binds to the 5' cap of an mRNA. The complex then “scans” along the 5' UTR of the mRNA until it reaches an initiation codon in a favorable sequence context. A stable 48S pre-initiation complex is then formed at the start codon. This triggers GTP hydrolysis by eIF2, which is necessary for the dissociation of most initiation factors and the recruitment of the 60S ribosomal subunit to form the translationally competent 80S complex (Figure 1.1) (Gingras *et al.*, 1999; Kapp and Lorsch, 2004; Pestova *et al.*, 2001). This event is regarded to be the last step of translation initiation. Two steps in this process can be specifically inhibited by drugs (Gray and Hentze, 1994). The addition of a non-hydrolysable GTP analogue like GTP $\gamma$ S interferes with eIF2-mediated GTP hydrolysis necessary for the recruitment of the 60S ribosomal subunit to form the 80S initiation complex. This results in the accumulation of the 48S pre-initiation complex consisting of the 43S complex bound to the initiator start codon of the mRNA. Similarly, the addition of cycloheximide prevents peptide elongation by the 80S ribosome and causes it to stall at the start codon resulting in the accumulation of the 80S complexes. The stalled complexes can be analyzed using sucrose density gradient centrifugation.

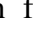
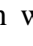
To determine which translation initiation stage is affected by the presence of SAPAP3 5' UTR, *in vitro* translation reactions were performed consisting of rabbit reticulocyte lysates (RRLs) programmed with either radioactively labeled capped control *Luc* mRNAs or radioactively labeled capped *E1B-Luc* mRNAs which contain the SAPAP3 5' UTR. The formation of 48S pre-initiation complexes or 80S initiation complexes was experimentally visualized by treating the *in vitro* translation reactions with either GTP $\gamma$ S or cycloheximide, respectively, and the stable complexes were then resolved by sucrose-gradient density centrifugation. Fractions of the gradient were collected


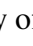
and the amount of programming mRNAs present in each fraction was analyzed by Cerenkov counting. Each fraction was also analyzed via Western blotting with antibodies against the L7 protein, a component of the 60S ribosomal subunit, to monitor the migration of 80S ribosome complexes in cycloheximide-treated reactions. Analogously, for GTP $\gamma$ S-treated reactions, antibodies against the eukaryotic initiation factors (eIF) -1 $\alpha$ 1 and -2 $\alpha$  (components of the 48S pre-initiation complex) were used to monitor the migration of the 48S pre-initiation complexes while antibodies against the L7 protein were used to monitor the migration of free 60S ribosomal subunit in the sucrose gradients.

The suitability of the RRL assay system was first examined by performing *in vitro* translation reactions using *in vitro* transcribed capped *E1B-Luc* or *Luc* mRNAs at different quantities. These assays confirm that the translational inhibition observed *in vivo* is faithfully reproducible by the *in vitro* RRL system (Table 3.2).

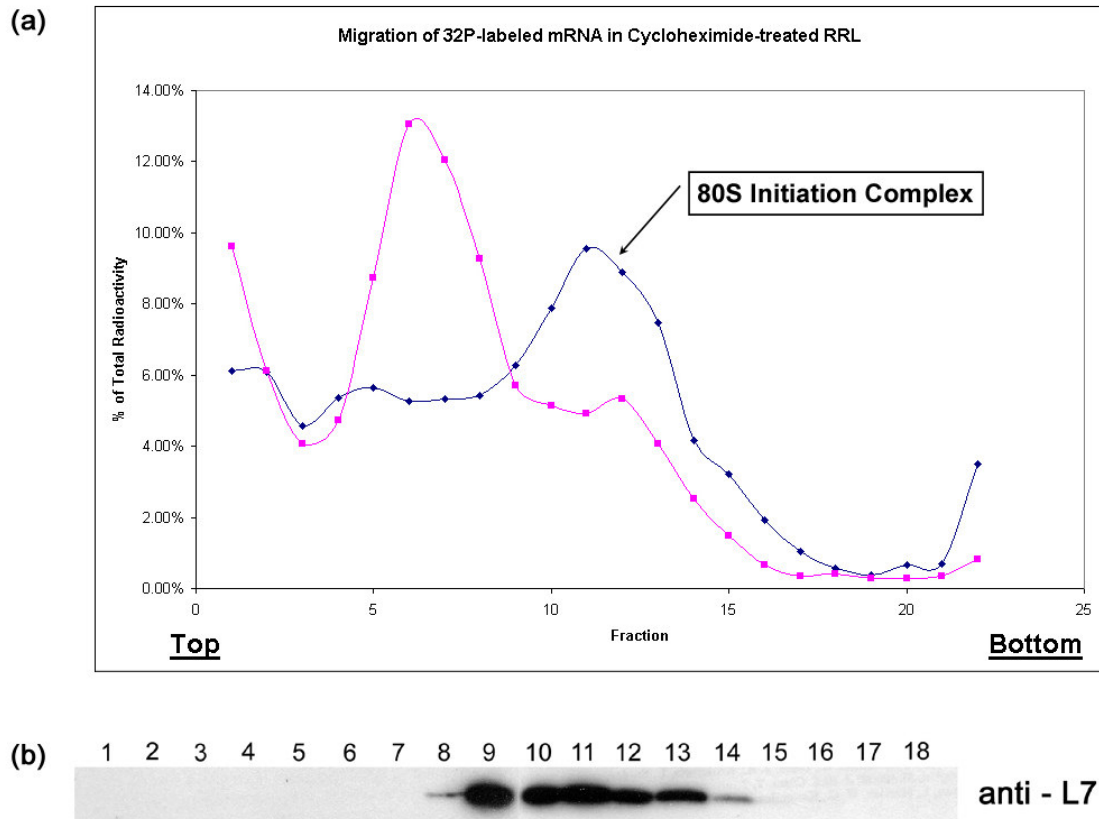
Experiment	Programming mRNA	mRNA quantity used	Raw <i>Photinus</i> luciferase values	E1B-Luc/Luc (%)
1	<i>Luc</i>	1 $\mu$ g	5346507 / 5329128	1.20%
	<i>E1B-Luc</i>	1 $\mu$ g	64280 / 64311	
2	<i>Luc</i>	1 $\mu$ g	4712167 / 4691694	1.22%
	<i>E1B-Luc</i>	1 $\mu$ g	57263 / 57148	
3	<i>Luc</i>	25 ng	564317 / 562170	3.41%
	<i>E1B-Luc</i>	25 ng	19237 / 19169	
4	<i>Luc</i>	25 ng	532731 / 530203	3.68%
	<i>E1B-Luc</i>	25 ng	19591 / 19551	

**Table 3.2** Results of *in vitro* translation reactions using RRLs programmed with different amounts of *Luc* or *E1B-Luc* mRNAs. Within each set of experiment, the amount of programming mRNA was kept constant for each reaction. Translation reactions were incubated at 30°C for 90 min and assayed for *Photinus* luciferase activities. The raw values obtained for each translation reaction are indicated. The amount of luciferase activities obtained for *E1B-Luc* mRNAs were then expressed as percentages of that obtained for *Luc* mRNAs (E1B-Luc/E1B). The inhibitory effect of the SAPAP3 5' UTR in the *in vitro* RRL system is identical to that observed *in vivo* in transfected cells (Figures 3.11b and 3.12b).



The formation of 80S complexes was first analyzed using cycloheximide-treated RRLs programmed with either radio-labeled capped control *Luc* or *E1B-Luc* mRNAs. As expected, the majority of the control *Luc* mRNAs co-migrate with the L7 subunit between fractions 9 to 14 (Figures 3.16a, , and 3.16b) indicating that the assembly of the 80S complex occurs efficiently on these mRNAs. In comparison, the majority of the *E1B-Luc* mRNA is present in lighter fractions (fractions 5-8) that do not contain the L7 subunit while only a small peak was observed between fractions 11 to 13 in which the L7 subunit was present (Figures 3.16a, , and 3.16b). This result indicates that the formation of 80S complex occurs very inefficiently for the *E1B-Luc* mRNA. However, unbound mRNAs and messenger ribonucleoprotein complexes are expected to remain at the top-most fractions of these gradients (Krichevsky and Kosik, 2001; Paraskeva *et al.*, 1999). Thus, I hypothesized that the comparatively heavier fractions containing the *E1B-Luc* mRNAs could instead represent 48S complexes in which 43S pre-initiation complexes recruited to the *E1B-Luc* mRNAs were somehow prevented from forming the 80S initiation complex by the presence of SAPAP3 5' UTR.

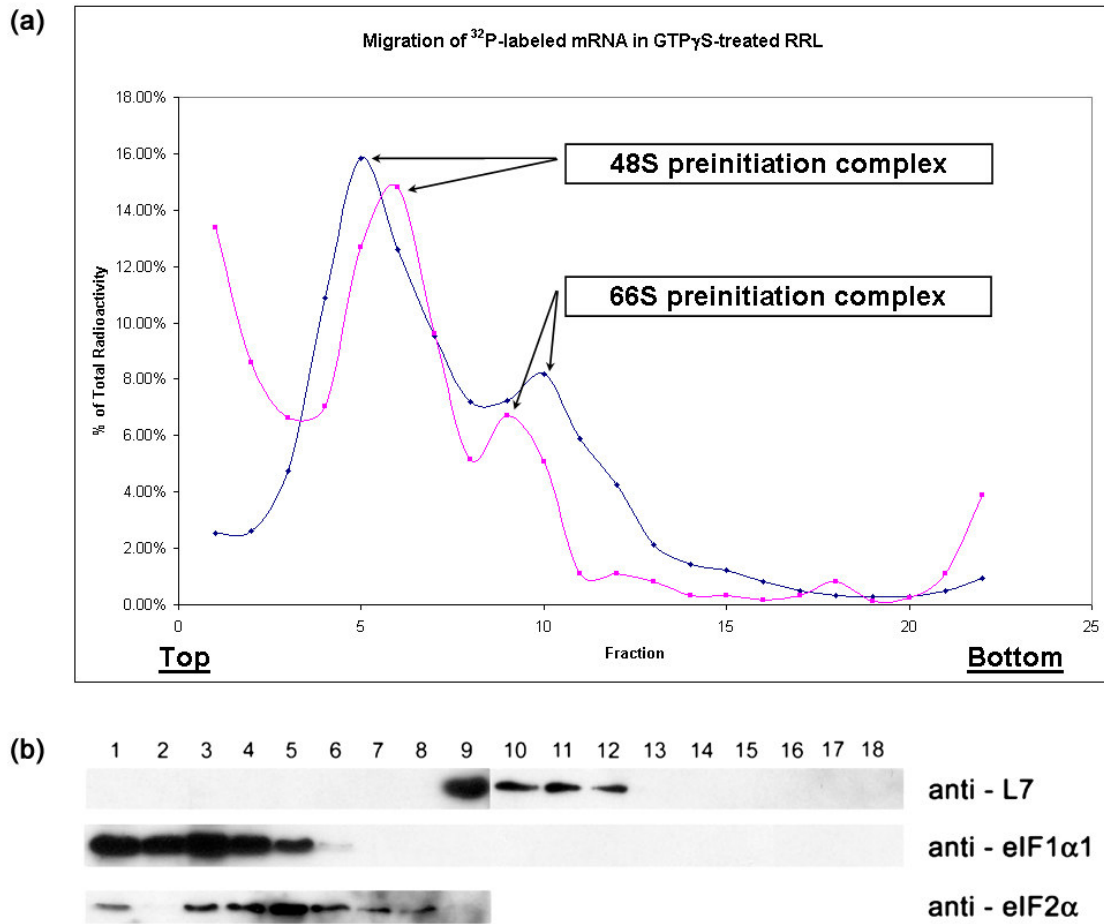
To test this hypothesis, GTP $\gamma$ S-treated RRLs programmed with either control *Luc* mRNAs or *E1B-Luc* mRNAs were set up to visualize 48S pre-initiation complexes. As mentioned previously, GTP $\gamma$ S treatment of RRLs results in the accumulation of the 48S pre-initiation complex. Analyses of the fractions obtained from RRLs programmed with the *Luc* mRNAs indicated that there is a shift in the migration of the mRNA to lighter fractions compared to that observed before with cycloheximide-treated RRLs (Figure 3.17a, ). In agreement with the effects of the treatment, the majority of the *Luc* mRNA co-migrates with eIF1 and eIF2 $\alpha$  (Figure 3.17a, , and 3.17b; fractions 4 to 6), proteins which are only present in the 48S pre-initiation complex (Kapp and Lorsch, 2004; Pestova *et al.*, 2001) but not with the L7 protein (fractions 9-12) which now serves as a marker for the migration of the 60S ribosomal subunit. An additional smaller *Luc* mRNA peak is observed between fractions 8 and 10. This peak corresponds to the previously reported 66S pre-initiation complexes which consist of mRNAs associated with two small ribosomal subunits (Paraskeva *et al.*, 1999) in contrast to 48 pre-initiation complexes which only contain one small ribosomal subunit. These results indicate that GTP $\gamma$ S treatment of the RRLs had





**Figure 3.16** Analysis of translational initiation complex assembly using cycloheximide-treated rabbit reticulocyte lysates.  $^{32}\text{P}$ -labeled capped *Luc* and *E1B-Luc* transcripts were used as programming mRNAs in the presence of cycloheximide to visualize formation of 80S complexes. (a) The graph shows the migration of the radio-labeled *Luc* (—◆—) or *E1B-Luc* (—■—) mRNAs in the sucrose gradients. (b) Western blot of different fractions obtained from the sucrose gradients probed with antibodies against the L7 protein of the large ribosomal subunit. While 80S complexes are efficiently assembled on the control *Luc* mRNAs, assembly of the complex occurs inefficiently when *E1B-Luc* mRNAs are used. Instead, a lighter complex is observed.

worked successfully. Importantly, *E1B-Luc* mRNAs are also observed to co-migrate only with eIF1 and eIF2 $\alpha$  but not with the L7 protein (Figures 3.17a, , and 3.17b; fractions 5-7). A much smaller 66S peak was also observed for *E1B-Luc* mRNA (fractions 9-12). These data confirm my hypothesis that the *E1B-Luc* mRNA-protein complexes observed in RRLs treated with either cycloheximide or GTP $\gamma$ S indeed correspond to stalled 48S pre-initiation complexes. Taken together, the results indicate that the mechanism of translation inhibition mediated by SAPAP3 5' UTR acts at the initiation stage. While the assembly of the 48S pre-initiation complexes is not affected by the presence of the SAPAP3 5' UTR, the UTR appears to limit the formation of the 80S initiation complex by inhibiting 60S ribosomal subunit joining. The small 80S peak observed in cycloheximide-treated RRLs (Figure 3.16a, , fractions 12 and 13) indicates that this inhibition, while strong, is not absolute. Thus, a limited amount of translation still occurs even in the presence of the SAPAP3 5' UTR. This finding is in agreement with the results obtained from luciferase reporter assays (Figures 3.11b and 3.12b; Table 3.2), which also indicate that translation inhibition mediated by the 5' UTR does not cause a complete shutdown of protein synthesis.

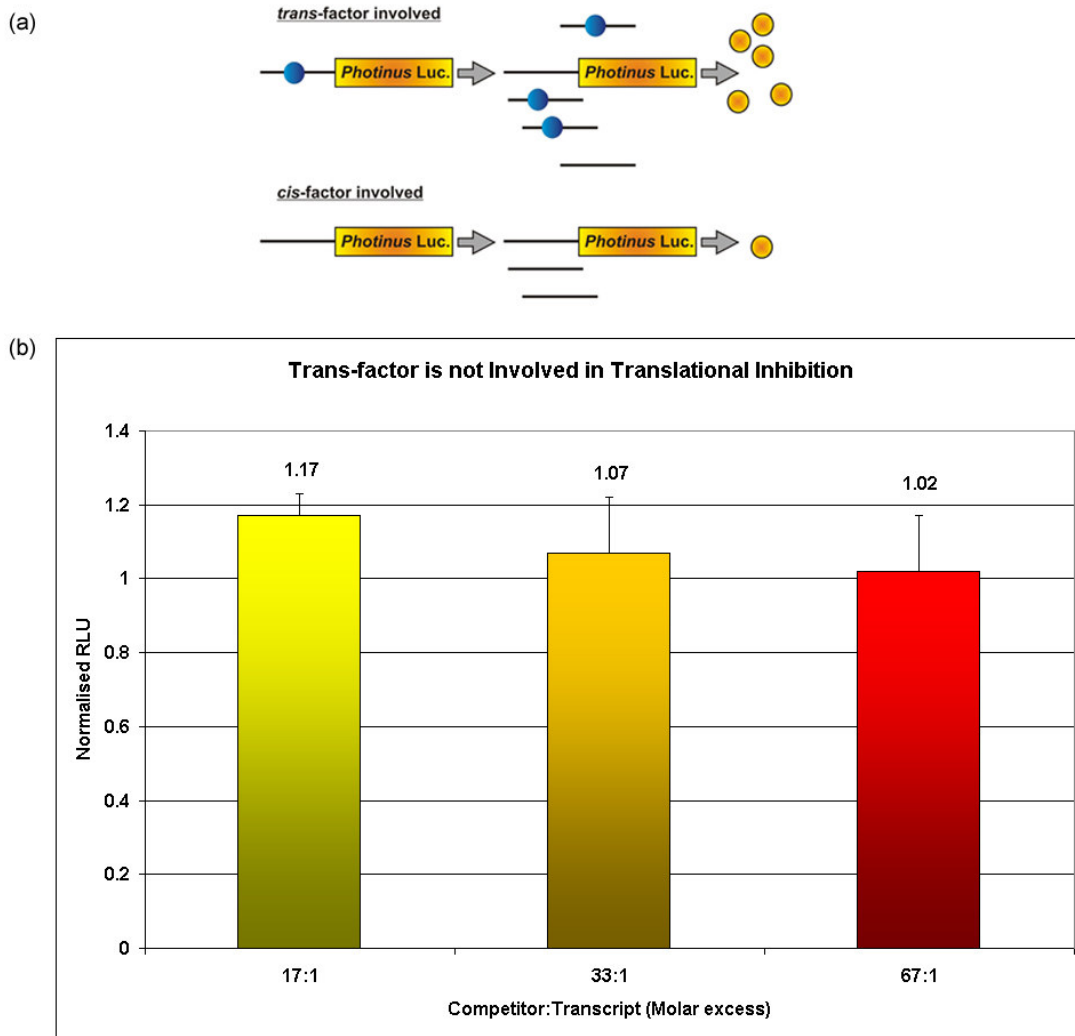


**Figure 3.17** Analysis of translational initiation complex assembly using GTP $\gamma$ S-treated rabbit reticulocyte lysates.  $^{32}\text{P}$ -labeled capped *Luc* and *E1B-Luc* transcripts were used as programming mRNAs in the presence of GTP $\gamma$ S to visualize formation of 48S pre-initiation complexes. (a) The graph shows the migration of the radio-labelled *Luc* (—◆—) or *E1B-Luc* (—■—) mRNAs in the sucrose gradients. Both mRNAs co-migrate in similar fractions. (b) Western blot analyses of different fractions obtained from the *in vitro* translation reaction programmed with *Luc* mRNAs. Antibodies against the L7 protein were used to track the migration of the 60S ribosomal subunit. Analogously, anti-eIF1 $\alpha$ 1 and anti-eIF2 $\alpha$  antibodies were used to follow the migration of the 40S ribosomal subunit. The slight shift between both mRNA migration profiles and the Western blot analyses is due to the manual collection of the fractions.

### 3.3.2 Translational Inhibition is not Mediated by *trans*-acting Factors

Stalling of translation at the stage 48S pre-initiation complex formation can be attributed to extensive secondary structure and upstream open reading frames present in the 5' UTR of mRNAs (Meijer and Thomas, 2002; van der Velden and Thomas, 1999). However, *trans*-acting factors that bind specifically to motifs or secondary structures present in the 5' UTR may also arrest translation by interfering with 60S subunit joining (Meng *et al.*, 2005; Paraskeva *et al.*, 1999). I was interested to determine if the binding of such factors to SAPAP3 5' UTR could be responsible for stalling the 48S pre-initiation complexes. To do this, I devised an *in vitro* competition assay where *EIB-Luc* mRNAs were used to program RRLs. The assays involved addition of increasing concentrations of competitor SAPAP3 5' UTR RNA alone to the translational reactions programmed with *EIB-Luc* mRNAs to titrate out putative *trans*-factors. Figure 3.18a schematically illustrates the expected results for both *cis*-element and *trans*-factor involvement. Specifically, if *trans*-factors were involved in mediating inhibition, then addition of excess competitor RNA should titrate out these factors and result in an increase in luciferase activity. Conversely, the action of a *cis*-acting element would not be affected by increasing amounts of competitor RNA and thus no changes in luciferase activities should be observed. Transcripts expressing *Renilla* luciferase were co-translated as an internal control.

Addition of different amounts of competitor RNA to the *in vitro* translation assays does not affect luciferase activities (Figure 3.18b). This result indicates that SAPAP3 5' UTR-mediated translation inhibition does not involve *trans*-acting proteins. Instead, an element acting in *cis* appears to be sufficient for mediating translational inhibition.

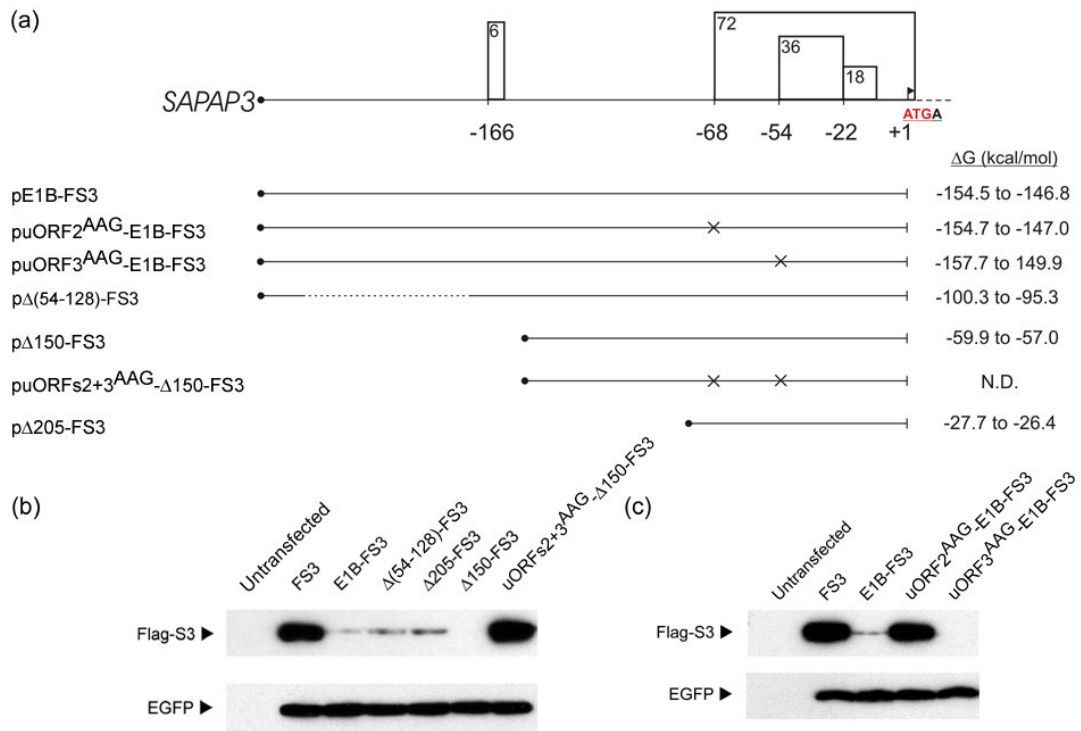


**Figure 3.18** SAPAP3 5' UTR translational inhibition is not mediated by *trans*-acting factors. (a) Diagrammatic representation of the expected results of the competition assays. An increased luciferase activity upon the addition of competitor RNAs would be expected if *trans*-acting factors are involved in translational inhibition since an excess of competitors should titrate out the factor. No changes in luciferase activity would be observed if only *cis*-acting elements are involved. (b) Results of the competition assay. *E1B-Luc* mRNAs were translated in RRLs in the presence of increasing amounts of competitor RNA. Transcripts expressing *Renilla* luciferases were co-translated as an internal control. *Photinus* luciferase activities were normalized to *Renilla* luciferase activities. The normalized values were then expressed as ratios to samples not containing competitor RNAs (normalized RLU). Increasing the amounts of SAPAP3 5' UTR competitor added to the *in vitro* translation reaction mixtures does not alter luciferase activities.

### 3.3.3 An uORF is Responsible for Mediating Translational Inhibition by SAPAP3 5' UTR

Two mechanisms can act in *cis* to prevent translation initiation: excessive secondary structure in the 5' UTR and upstream open reading frames (uORFs). Mfold predictions indicated that the SAPAP3 5' UTR indeed has the potential to form stable secondary structures (Figure 3.4 and Appendix II). Consequently, I first investigated the influence of secondary structures on translation inhibition.

The presence of a stable stem-loop structure with  $\Delta G$  greater than -50kcal/mol within the 5' UTR is thought to be inhibitory to the scanning 43S complex and thus strongly inhibits translation (Kozak, 1991b). A series of deletion constructs was generated in which the 5' UTR was sequentially truncated (Figure 3.19a). These constructs are based on the pFS3 and pE1B-FS3 constructs previously described in Section 3.2.2. p $\Delta$ 150-FS3 and p $\Delta$ 205-FS3 constructs express recombinant mRNAs containing deletions of either the first 150 or 205 nucleotides of the SAPAP3 5' UTR present in the pE1B-FS3 construct, respectively. Similarly, the p $\Delta$ (54-128)-FS3 construct expresses a recombinant mRNA containing an internal deletion of nucleotides 54 to 128 in the SAPAP3 5' UTR. This region was predicted to form a strong stem-loop structure which could impede ribosome scanning. The resultant truncated 5' UTRs were predicted to contain progressively less stable secondary structures with  $\Delta G$  ranging from -100.3 kcal/mol for the p $\Delta$ (54-128)-FS3 transcript to -26.4 kcal/mol for the p $\Delta$ 205-FS3 transcript (Figure 3.19a). If strong secondary structures were the cause of inhibition, then a systematic truncation of the 5' UTR should lead to a progressive increase in mRNA translation by virtue of the increased ease by which 43S complexes can scan the remaining 5' UTR (Han *et al.*, 2003a, b). However, this is not observed. Removal of the distal 150 (50.7%) or 205 nt (69.5%) of the 5' UTR is insufficient to improve translation efficiency to the level observed for the pFS3 mRNA (Figure 3.19b, lanes  $\Delta$ 150-FS3 and  $\Delta$ 205-FS3). The removal of the putative stem-loop structure formed by nucleotides 54 to 128 also does not improve synthesis



**Figure 3.19** Translational efficiency of the SAPAP3 ORF is influenced by an uORF. (a) Schematic representation of the SAPAP3 5' UTR modifications and characteristics of the mRNAs transcribed from the corresponding constructs. Only the relevant region of the mRNA is drawn. pE1B-FS3, pΔ(54-128)-FS3, pΔ150-FS3 and pΔ205-FS3 transcripts contain full-length and progressively shortened SAPAP3 5' UTR sequences. Locations of the four uORFs and the positions of their AUGs in the 5' UTR are illustrated as boxes and numbers beneath them, respectively. The lengths of each uORF (in nucleotides) are indicated by numbers within their respective boxes. The overlapping start and termination codons of uORF2 and SAPAP3 ORF are shown. The position of the adenine residue of the SAPAP3 start codon is designated +1. Point mutations of uAUGs to AAG are indicated by a "x" in the diagram. A dashed line in the pΔ(54-128)-FS3 mRNA refers to an internal deletion of nucleotides 54-128 of the 5' UTR. MFOLD ΔG predictions of the various deletion constructs are indicated where relevant. N.D.: Not determined. (b) Sequential deletion of SAPAP3 5' UTR does not result in increased synthesis of SAPAP3. Western blots of equal amounts of lysates obtained from the various transfected HEK293 cells were probed using an anti-FLAG antibody. Duplicate protein samples were probed with anti-EGFP antibodies to detect EGFP that was co-expressed to account for differences in transfection efficiencies. A double mutation of uAUGs 2 and 3 to AAG results in a substantial increase in the synthesis of Flag-SAPAP3 indicating a role for uORFs 2 and/or 3 in mediating translational inhibition. (c) Sequential mutation of uAUG2 and uAUG3 indicates that only uORF2 is necessary for mediating translational inhibition.

of FLAG-SAPAP3 in p $\Delta$ (54-128)-FS3 transcripts (lane  $\Delta$ (54-128)-FS3). Noteworthy, the predicted  $\Delta$ G of the 5' UTR remaining in the p $\Delta$ 205-FS3 transcript is about -27 kcal/mol and is thus unlikely to interfere with ribosomal scanning. Thus, the high GC content and the predicted stable secondary structures of the E1B 5' UTR are not the primary causes of translational inhibition.

<u>Sequence surrounding AUG</u>	<u>Name</u>	<sup>1</sup> <u>Position</u>	<sup>2</sup> <u>NetStart Score</u>
C <b><i>A</i></b> CCATGG <b><i>G</i></b>	Kozac sequence	N.A.	N.A.
CACCATGT	uAUG1	-166	0.491
AAGGATGG	uAUG2	-68	0.584
CCGGATGG	uAUG3	-54	0.577
CAGTATGA	uAUG4	-22	0.424
G <b><i>G</i></b> GCATGA	AUG <sub>+1</sub>	+1	0.754
GCATATGG	AUG <sub>+67</sub>	+67	0.641
CAGGATGT	AUG <sub>+277</sub>	+277	0.603

<sup>1</sup>The position of the adenine residue of the SAPAP3 start codon is designated +1.

<sup>2</sup>A score greater than 0.5 indicates that the ATG is a probable translation start site.

**Table 3.3** Upstream and internal in-frame start codons present in the E1B SAPAP3 mRNA. The consensus Kozac sequence is given at the top of the table. Identity with the consensus A/G at the -3 position and the G at the +4 position is indicated in italicized bold print. uAUG: upstream start codon.

I next examined if uORFs could play a role in mediating translational inhibition. Four evolutionarily conserved uORFs are present in the 5' UTR of SAPAP3 (Figure 3.7). uORF1 consists of a start codon immediately followed by a stop codon. The open reading frames of uORFs 2 – 4 are longer, potentially encoding for peptides that are 23, 11 and 4 amino acids long, respectively. While uORF3 is positioned in-frame to the SAPAP3 start codon, the remaining uORFs are contained in different reading frames. Of the four uORFs, only uORF2 overlaps with the coding region of SAPAP3 with the first 2 nucleotides of the uORF2 stop codon forming the last 2 nucleotides of



the SAPAP3 start codon (ATGA, Figures 3.7 and 3.19). The remaining uORFs all terminate before the SAPAP3 start codon. The potential of the start codons of the uORFs to be utilized as initiation codons was analyzed using the NetStart 1.0 prediction server (Pedersen and Nielsen, 1997) (Table 3.3, uAUGs 1 to 4). Two (uAUG2 and uAUG3) could potentially be recognized as translational start sites. Thus, the potential for an inhibitory role of these uAUGs was determined by generating three constructs lacking either or both uAUGs (Figure 3.19a). The puORFs2+3<sup>AAG</sup>- $\Delta$ 150-FS3 construct is based on the described p $\Delta$ 150-FS3 construct but the start codons of uORFs 2 and 3 have been replaced by the non-initiator codon AAG. puORF2<sup>AAG</sup>-E1B-FS3 and puORF3<sup>AAG</sup>-E1B-FS3 are based on the pE1B-FS3 construct containing the full-length SAPAP3 5' UTR but contains single point mutations to mutate the start codons of uORF2 or uORF3, respectively, to the non-initiator codon AAG.

Mutations of uAUGs 2 and 3 from the p $\Delta$ 150-FS3 transcripts dramatically increases synthesis of SAPAP3 to levels comparable to that observed for the pFS3 transcript (Figure 3.19b, lane uORFs2+3<sup>AAG</sup>- $\Delta$ 150-FS3). To determine their individual contribution to translational inhibition, both uAUG2 and uAUG3 were singly mutated in the context of the full-length E1B sequence. Mutation of uAUG2 alone in the puORF2<sup>AAG</sup>-E1B-FS3 transcript is sufficient to restore translation efficiency to levels observed for the pFS3 mRNA while removal of uAUG3 alone in the puORF3<sup>AAG</sup>-E1B-FS3 transcript does not improve translation capacity (Figure 3.19c, lanes uORF2<sup>AAG</sup>-E1B-FS3 and uORF3<sup>AAG</sup>-E1B-FS3). Taken together, these results show E1B-mediated inhibition of SAPAP3 synthesis is caused by the translation of a single uORF that overlaps with the SAPAP3 ORF. Moreover, data obtained with the puORF2<sup>AAG</sup>-E1B-FS3 transcript (with  $\Delta$ G equivalent to the pE1B-FS3 construct, Figure 3.19a) further support the previous finding that the predicted secondary structure of the SAPAP3 5' UTR does not significantly obstruct ribosomal scanning and translation of the native start codon of the SAPAP3 ORF.

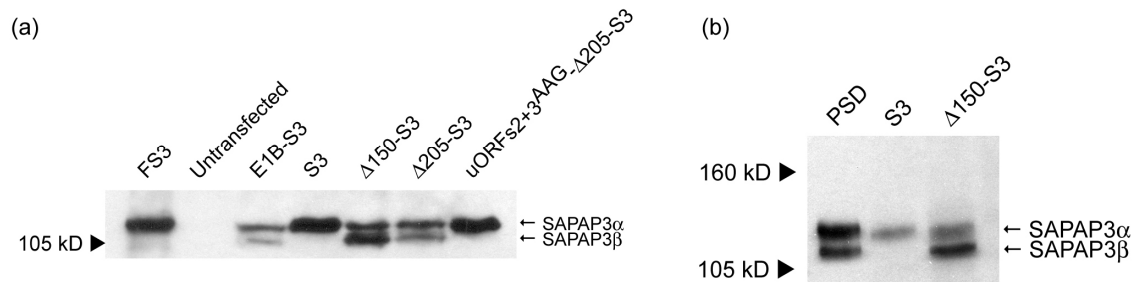
### 3.4 Biological Significance of Translational Regulation in SAPAP3

#### 3.4.1 SAPAP3 5' UTR Mediates Expression of Two SAPAP3 Isoforms from a Single Transcript

The previous experiments were performed with FLAG-tagged SAPAP3 constructs containing a modified Kozak sequence and an additional *NheI* site that was used for convenient cloning of the 5' UTR (Figure 3.10a). In order to exclude any influence that might be caused by the presence of the artificial elements in these constructs, I repeated the deletion experiments using vectors expressing “authentic” SAPAP3 transcripts without modifying the Kozak sequence. The *NheI* cloning site was also removed. The pE1B-S3 construct expresses full-length authentic E1B variant SAPAP3 transcripts. The p $\Delta$ 150-S3 and p $\Delta$ 205-S3 constructs express authentic SAPAP3 mRNAs with identical manipulations of the 5' UTR region as described for the p $\Delta$ 150-FS3 and p $\Delta$ 205-FS3, respectively (Figure 3.19a). The pS3 construct contains a similar vector-derived minimal 5' UTR found in the pFS3 construct which promotes the efficient synthesis of untagged SAPAP3. The puORFs2+3<sup>AAG</sup>- $\Delta$ 205-S3 construct is similar to p $\Delta$ 205-S3 construct but the start codons of uORFs 2 and 3 have been mutated to the non-initiator codon AAG and is analogous to the puORFs2+3<sup>AAG</sup>- $\Delta$ 150-FS3 construct. An affinity purified anti-SAPAP3 antibody was now used instead of the anti-FLAG antibody to detect untagged SAPAP3 on Western blots.

Interestingly, two protein bands are recognized by the anti-SAPAP3 antibody in Western blots of lysates obtained from cells transfected with constructs containing complete or partial SAPAP3 5' UTR sequences (Figure 3.20a, lanes E1B-S3,  $\Delta$ 150-S3,  $\Delta$ 205-S3). Remarkably, the bands are reminiscent of the SAPAP3-doublet bands observed in Western blots of PSD fractions. The larger band in these samples co-migrated with FLAG-SAPAP3 and untagged SAPAP3 indicating that these proteins are identical (Figure 3.20a, e.g. lanes FS3, E1B-S3 and S3). To confirm that the smaller protein is identical to that observed in the PSD, protein samples from PSD fractions and HEK cells transfected with pS3 or p $\Delta$ 150-S3 were co-electrophoresed in an SDS-PAGE. Lysates from p $\Delta$ 150-S3-transfected cells were used because synthesis of the smaller protein from this mRNA was strongest compared to the other transcripts (Figure 3.20a, lanes E1B-S3 and  $\Delta$ 150-S3). Western analysis again

confirmed that the protein synthesized in pS3-transfected cells indeed corresponds to the larger protein (the 120 kDa SAPAP3 isoform, henceforth named SAPAP3 $\alpha$ ) identified in the PSD fraction (Figure 3.20b, lanes S3 and PSD). Likewise, the smaller protein (henceforth named SAPAP3 $\beta$ ) observed in p $\Delta$ 150-S3-transfected cells migrates identically to the 105 kDa SAPAP3 isoform in PSD fractions (Figure 3.20b, lanes  $\Delta$ 150-S3 and PSD).



**Figure 3.20** SAPAP3 5' UTR regulates the synthesis of two SAPAP3 isoforms from the same transcript. (a) Western blots of lysates obtained from HEK293 cells transfected with constructs expressing authentic SAPAP3 mRNAs. Equal amounts of protein were loaded for each lane. Two protein bands are recognized by the anti-SAPAP3 antibody. The larger band (SAPAP3 $\alpha$ ) is identical to untagged and FLAG-tagged SAPAP3 while the smaller band (SAPAP3 $\beta$ ) represents an isoform related to SAPAP3 $\alpha$ . (b) Western blots of lysates from pS3 or p $\Delta$ 150-S3 transfected cells and PSD samples probed with anti-SAPAP3 antibodies. Equivalent amounts of each protein sample were loaded to detect the presence of SAPAP3 isoforms without overexposure of the film. Protein isoforms expressed from authentic SAPAP3 mRNAs are identical to protein isoforms identified in PSD fractions.

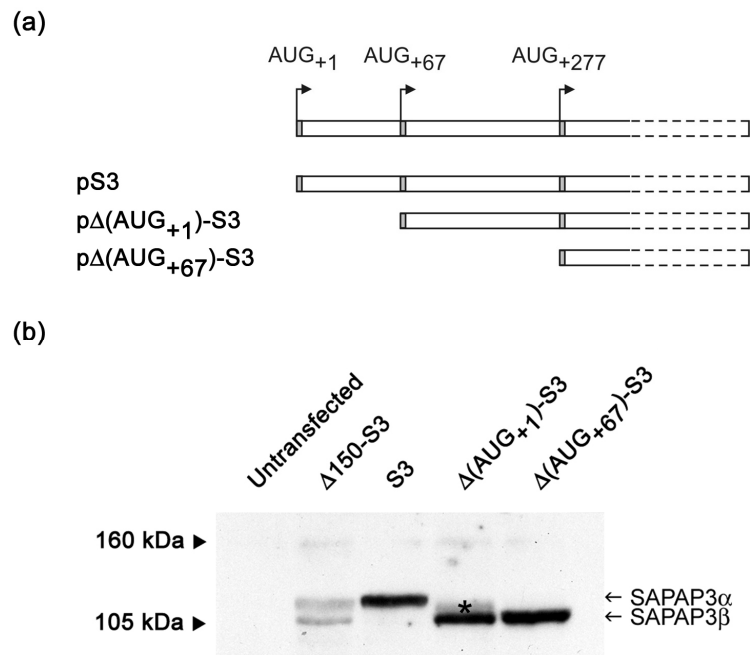
Similar to the previous findings with recombinant mRNAs, the translation inhibitory effect of the 5' UTR on the expression of SAPAP3 $\alpha$  is also observed when the native transcripts were used. The amounts of SAPAP3 $\alpha$  from cells transfected with pE1B-S3, p $\Delta$ 150-S3 and p $\Delta$ 205-S3 plasmids are much lower than that compared to the levels synthesized from pS3-transfected cells (Figure 3.20a, lane S3, E1B-S3,  $\Delta$ 150-S3 and  $\Delta$ 205-S3). Further, as observed for the p $\Delta$ 150-FS3 plasmid, mutation of the start codons of uORFs 2 and 3 from the p $\Delta$ 205-S3 construct is sufficient to restore synthesis of SAPAP3 $\alpha$  to levels comparable to that synthesized from pS3 (Figure 3.20a, lane S3 and uORFs2+3<sup>AAG</sup>- $\Delta$ 205-S3). Taken together with the data derived from the experiments performed in Section 3.3.3, the results from the expression of

native SAPAP3 transcripts confirm that the E1B-mediated inhibition of SAPAP3 $\alpha$  synthesis is caused by the translation of uORF2.

### 3.4.2 SAPAP3 $\beta$ is Synthesized from a Downstream Alternative Start Codon

The finding that both SAPAP3 $\alpha$  and SAPAP3 $\beta$  could be synthesized from the same mRNA transcript suggested that alternative translational initiation (ATI) at an internal translational start site generates the smaller isoform. Similar events have been reported for several other transcripts including the mRNAs of the transcription regulator JunD and the CCAAT/enhancer-binding *trans*-activating protein  $\beta$  (C/EBP $\beta$ ) (Okazaki *et al.*, 1998; Xiong *et al.*, 2001; Short and Pfarr, 2002). Analysis of the coding region of SAPAP3 mRNA revealed that two downstream in-frame start codons could potentially be used for the synthesis of SAPAP3 $\beta$  (Table 3.3, AUG<sub>+67</sub> and AUG<sub>+277</sub>). Netstart server predictions indicate that both start codons are suitable for translational initiation. To determine which start codon is responsible for directing the synthesis of SAPAP3 $\beta$ , two constructs (p $\Delta$ (AUG<sub>+1</sub>)-S3 and p $\Delta$ (AUG<sub>+67</sub>)-S3) were generated in which AUG<sub>+1</sub> (the start codon of SAPAP3 $\alpha$ ) or the downstream AUG<sub>+67</sub> were systematically deleted from the SAPAP3 ORF (Figure 3.21a). HEK293 cells transfected with p $\Delta$ (AUG<sub>+1</sub>)-S3 and p $\Delta$ (AUG<sub>+67</sub>)-S3 constructs continue to synthesize SAPAP3 $\beta$  (Figure 3.21b, lanes  $\Delta$ (AUG<sub>+1</sub>)-S3 and  $\Delta$ (AUG<sub>+67</sub>)-S3). Thus AUG<sub>+67</sub> is not utilized to produce SAPAP3 $\beta$ . These results indicate that the translation of SAPAP3 $\beta$  is initiated from AUG<sub>+277</sub>. Interestingly, in addition to SAPAP3 $\beta$ , a faint band intermediate in size between SAPAP3 $\alpha$  and SAPAP3 $\beta$  is detected in lysates of p $\Delta$ (AUG<sub>+1</sub>)-S3-transfected cells (Figure 3.21b, lane  $\Delta$ (AUG<sub>+1</sub>)-S3, marked by an asterisk). This band apparently reflects the product of translation initiated at AUG<sub>+67</sub> (since it is not detected in p $\Delta$ (AUG<sub>+67</sub>)-S3 transfected cells) which appears to be poorly recognized by the translational machinery even in the absence of AUG<sub>+1</sub>. However, SAPAP3 $\beta$  remains strongly expressed from this transcript, indicating that most ribosomes are able to bypass AUG<sub>+67</sub> and initiate translation efficiently at AUG<sub>+277</sub>. SAPAP3 $\beta$  has also been observed in PSD preparations from mouse brains (Welch *et al.*, 2004). Importantly, the Kozak sequence surrounding AUG<sub>+277</sub> and

AUG<sub>+277</sub> itself are conserved across human, dog, rat and mouse (Figure 3.22). This indicates that ATI is also likely to be responsible for generating SAPAP3 $\beta$  in the mouse brain.



**Figure 3.21** Alternative translational initiation from AUG<sub>+277</sub> leads to the synthesis of SAPAP3 $\beta$ . (a) Scheme of constructs used to determine the start codon responsible for initiating translation of SAPAP3 $\beta$ . The coding region of SAPAP3 mRNA is shown as a box. Positions of the AUG<sub>+1</sub>, AUG<sub>+67</sub> and AUG<sub>+277</sub> are indicated by shaded regions in the scheme. (b) Sequential deletion of AUG<sub>+1</sub> and AUG<sub>+67</sub> reveal that translation of SAPAP3 $\beta$  starts from AUG<sub>+277</sub>. The position of the band representing the minor translation product initiated from AUG<sub>+67</sub> is indicated by an asterisk.

Synthesis of SAPAP3 $\beta$  also appears to be regulated by the E1B 5' UTR. This isoform is not synthesized when uAUGs 2 and 3 were mutated (Figure 3.20a, lane uORFs2+3<sup>AAg</sup>- $\Delta$ 205-S3) indicating that uORFs 2 and/or 3 are important in up-regulating translation of SAPAP3 $\beta$ . Conversely, synthesis of SAPAP3 $\beta$  increases significantly when the distal 150 nucleotides of the 5' UTR are removed, indicating that this region limits SAPAP3 $\beta$  synthesis (lane  $\Delta$ 150-S3). Thus, two mechanisms are utilized for the synthesis of each SAPAP3 isoform. Leaky scanning of 43S complexes past all four uORFs in the SAPAP3 5' UTR and the subsequent initiation of translation at AUG<sub>+1</sub> accounts for the synthesis of SAPAP3 $\alpha$ . In contrast, synthesis of SAPAP3 $\beta$  requires the prior translation of uORF2, which generates reinitiating 40S subunits that bypass AUG<sub>+1</sub> to recommence translation at AUG<sub>+277</sub>.

```

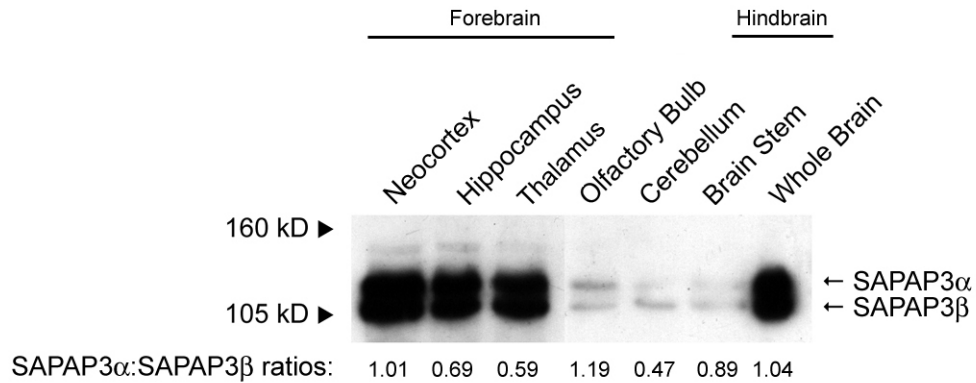
R_27465606 1 AGCAGTACCTTCCCCAGGATGTACCCGGGCCAGGGCCCTTCGACACCTGTGAAGACTGT
R_46389543 1 AGCAGTACCTTCCCCAGGATGTACCCGGGCCAGGGCCCTTCGACACCTGTGAAGACTGT
M_45686366 1 AGCAGTACCTTCCCCAGGATGTACCCGGGCCAGGGCCCTTCGACACCTGTGAAGACTGT
M_38348479 1 AGCAGTACCTTCCCCAGGATGTACCCGGGCCAGGGCCCTTCGACACCTGTGAAGACTGT
D_73977202 1 AGCAGCACCTTCCCCAGGATGTACCCGGGCCAGGGCCCTTCGACACCTGTGAAGACTGT
H_15747899 1 AGCAGCACCTTCCCCAGGATGTACCCGGGCCAGGGCCCTTCGACACCTGTGAAGACTGT
consensus 1 *****

```

**Figure 3.22** The sequences surrounding AUG<sub>+277</sub> are evolutionarily conserved in human, dog, mouse and rat SAPAP3 genes. Partial alignment of SAPAP3 cDNA sequences from human, dog, rat and mouse. Nucleotides conserved amongst all species are shown in a black background. AUG<sub>+277</sub> is indicated by a red line underneath the alignment. R: rat, M: mouse, D: dog, H: human.

### 3.4.3 Expression of SAPAP3 Isoforms in Different Regions of the Adult Rat Brain

I was interested to see if different regions of the brain may exhibit differences in levels of either SAPAP3 isoforms. PSD fractions from six different adult rat brain regions (neocortex, hippocampus, thalamus, olfactory bulb, cerebellum and brain stem) were analyzed on Western blots using a SAPAP3-specific antibody. Concentrations of both SAPAP3 isoforms are highest in the forebrain regions (neocortex, hippocampus and thalamus, Figure 3.23), consistent with high SAPAP3 mRNA levels in these regions detected in Northern blots and by *in situ* hybridizations. The highest levels of SAPAP3 are detected in the neocortex while lower but comparable levels of SAPAP3 were present in the hippocampus and thalamus. Only very low levels of SAPAP3 isoforms were detected in the hindbrain regions (cerebellum and brain stem) and the olfactory bulb (Figure 3.23). In addition, differences in SAPAP3 $\alpha$ :SAPAP3 $\beta$  ratios were observed in distinct brain areas. Quantitation of SAPAP3 $\alpha$ :SAPAP3 $\beta$  ratios for each region reveals that PSDs from the neocortex and olfactory bulb express approximately equal amounts of both isoforms. In contrast, SAPAP3 $\beta$  predominates in the other four investigated brain regions (Figure 3.23). The variations in the relative ratios of SAPAP3 isoforms expressed in the various brain regions examined may suggest that some additional forms of translational regulation occur at the E1B 5' UTR of SAPAP3. Alternatively, these differences could also be attributed to the synthesis of SAPAP3 isoforms from the other 5' UTR variants as well as from the other transcripts detected in Northern blots.



**Figure 3.23** SAPAP3 isoforms are present at different concentrations in various parts of the adult rat brain. Western blot analysis of PSD fractions (2.5  $\mu$ g per lane) from various brain regions were probed with an affinity purified anti-SAPAP3 antibody. The blot shown here corresponds to the longest exposure and is intended to show the relative difference in levels of SAPAP3 isoforms between the forebrain regions and the other brain regions analyzed. The levels of each SAPAP3 isoform in each brain regions were measured by densitometric scanning of the Western blots. Quantitation of the SAPAP3 $\alpha$ :SAPAP3 $\beta$  ratios for the forebrain regions was performed with a lower exposure that still permitted the analysis of the band intensities over a linear range. The ratios shown represent the average values obtained from two independent Western blotting experiments.

### 3.4.4 Morphological Changes in Neurons Over-expressing SAPAP3

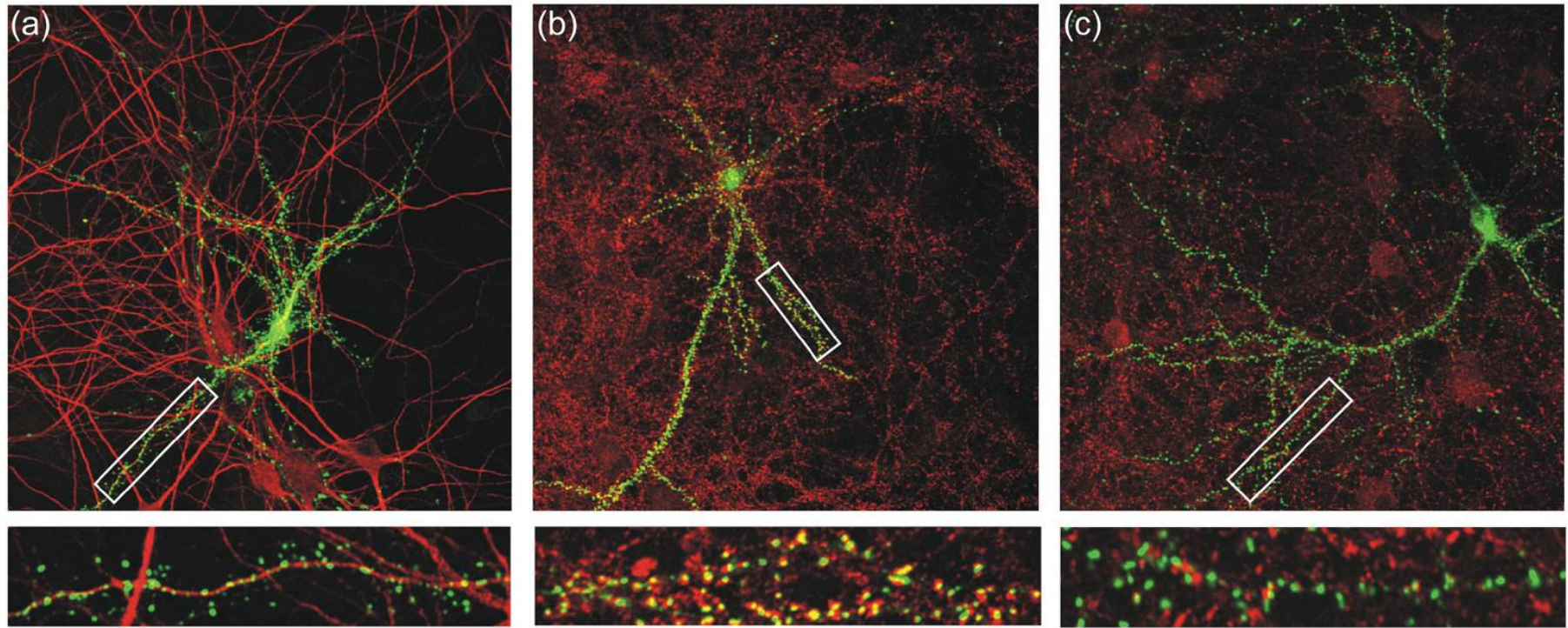
The varying levels of either SAPAP3 isoforms in distinct brain regions suggest that the ratio of SAPAP3 $\alpha$  versus SAPAP3 $\beta$  could be important in neuronal function. Since the hippocampus is one of the brain regions examined in which SAPAP3 $\alpha$  is present at lower levels compared to SAPAP3 $\beta$ , I decided to over-express this isoform in hippocampal neurons and examine what effects could be observed when the endogenous SAPAP3 ratios are perturbed.

Hippocampal neurons were transfected with the pFS3 construct at 8 DIV and fixed and stained with anti-FLAG and anti-MAP2 antibodies at 15 DIV for immunofluorescence microscopy. In 15 DIV neurons, FLAG-SAPAP3 $\alpha$  is distributed in a punctuate-like pattern along the dendritic shafts indicating its localization in dendritic spines (Figure 3.24a). To determine if the protein is indeed localized at synapses, double immuno-labeling was performed using anti-FLAG antibodies in

combination with antibodies against either vesicular GABA transporter (VGAT) or vesicular glutamate transporter 1 (VGLUT1 or BNPI), markers for inhibitory and excitatory, synapses respectively.

FLAG-SAPAP3 $\alpha$  exhibits strong co-localization with VGLUT1 (Figure 3.24b) while no co-clustering is observed for FLAG-SAPAP3 $\alpha$  and VGAT (Figure 3.24c). This indicates that over-expressed FLAG-SAPAP3 $\alpha$  is also targeted to excitatory synapses and is absent from inhibitory synapses as has been reported for endogenous SAPAP3 (Welch *et al.*, 2004). No gross changes in dendritic arborization are observed between transfected and non-transfected neurons. In addition, no significant differences in the density of excitatory synapses were detected as indicated by the number of VGLUT puncta along the dendritic shafts of transfected versus untransfected neurons. On the whole, no gross differences in morphology of neurons are observed in neurons over-expressing FLAG-SAPAP3 $\alpha$  as compared to untransfected neurons.





**Figure 3.24** Over-expression of SAPAP3 $\alpha$  does not result in gross morphological changes in neurons. 8 DIV hippocampal neurons were transfected with pFS3 construct. Neurons were fixed at 15 DIV and stained for FLAG-SAPAP3 $\alpha$  and co-stained for the following endogenous markers: (a) MAP2, (b) VGLUT1 and (c) VGAT. Flag-SAPAP3 $\alpha$  is localized in a punctuate-like pattern along dendrites and co-localizes strongly with the excitatory synaptic marker VGLUT. No co-localization is observed with the inhibitory synaptic marker VGAT.

## Chapter 4 Discussion

The functions and protein interaction partners of SAPAP1/GKAP have been extensively studied (Haraguchi *et al.*, 2000; Hirao *et al.*, 2000; Kawabe *et al.*, 1999; Kawashima *et al.*, 1997; Kim *et al.*, 1997; Kindler *et al.*, 2004; Naisbitt *et al.*, 1997, 1999, 2000; Takeuchi *et al.*, 1997, Romorini *et al.*, 2004; Satoh *et al.*, 1997; Welch *et al.*, 2004; Wu *et al.*, 2000; Yao *et al.*, 2003). Despite this, very little information is available for the remaining three members of the SAPAP family. In this study, I have taken several approaches to characterize SAPAP3, a unique member of the SAPAP family whose transcripts are dendritically localized in neurons.

SAPAP3 is specifically expressed in the mammalian brain and appears to be present only in neuronal cell types as evidenced by the lack of SAPAP3 transcripts in the corpus callosum. SAPAP3 mRNAs are abundant in the majority of the forebrain regions analyzed (Figure 3.1b) but are only present at low amounts in the cerebellum and substantia nigra. Most regions of the human brain contain comparable levels of the 8 kb and 4.4 kb SAPAP3 transcripts. Variations in the ratios of the two transcripts are observed in the putamen and thalamus where the shorter form predominates. The significance of this variation is currently unknown. SAPAP3 transcripts are noticeably absent in the medulla and spinal cord. SAPAP3 mRNA levels from different brain regions correspond well to the protein levels detected in their corresponding PSD preparations, particularly with regard to the forebrain regions analyzed (Figure 3.23). These data agree with *in situ* hybridization results which also indicate high levels of SAPAP3 transcripts in the neocortex and thalamus and low levels of SAPAP3 in the substantia nigra and medulla (Kindler *et al.*, 2004; Welch *et al.*, 2004). Discrepancies between results from Northern blotting and *in situ* hybridizations were observed in the cerebellum and spinal cord. In these regions, high levels of SAPAP3 transcripts detected in tissue sections using *in situ* hybridizations did not correlate with the relatively weak bands observed by Northern blotting. These discrepancies are possibly due to the different sensitivities of the analytical techniques used. In comparison to Northern blots which analyze RNA levels from entire brain regions, *in situ* hybridizations offer a higher level of resolution by permitting visualization of cell type-specific transcript levels. A similar reasoning could account for the discrepancy observed between transcript levels detected via Northern blots and *in situ*

hybridizations versus protein levels analyzed by Western blots in the olfactory bulb and thalamus. Alternatively, the discrepancies observed could simply reflect species-specific differences in the expression pattern of different SAPAP3 transcripts in these areas of the rat brain (analyzed by *in situ* hybridizations and Western blots) against the corresponding human brain regions (analyzed by Northern blots).

At least three different SAPAP3 transcripts were detected in the rat, namely, a 3.8 kb, a 4.2 kb and an 8 kb transcript. Based on the calculated sizes of the full-length transcripts from the known SAPAP3 cDNA sequence and 5' UTR sequences isolated in this study, the sizes of the E1B and E1B<sup>+</sup> variant SAPAP3 transcripts (3874 and 3978 nt long, respectively) correlate well with the major 3.8 kb transcript observed in the rat. Thus, a minimum of five different SAPAP3 transcripts were identified in this study: three based on alternatively spliced variants of the 5' UTR (E1A, E1B and E1B<sup>+</sup>) and two other larger transcripts (4.2 and 8 kb transcripts) of which exact sequence information is currently not available. A previous study identified another alternatively spliced region within the coding sequence of SAPAP3 (Kindler *et al.*, 2004). Taken together, multiple SAPAP3 transcripts are generated by extensive alternative splicing. This phenomenon has also been reported for SAPAP1/GKAP mRNAs (Kawashima *et al.*, 1997; Kim *et al.*, 1997; Naisbitt *et al.*, 1997).

SAPAP3 is expressed relatively late in rat embryonic development. SAPAP3 mRNAs are undetectable in early embryonic stages. Significant levels of the 3.8 kb rat transcript are first observed at E20 while strong expression of the 4.2 kb transcript only occurs in the adult brain. At the protein level, both SAPAP3 isoforms are already detectable in rat PSDs at E20. However, their amounts only reached a maximum much later during development at a time coinciding with the height of spinogenesis during the third post-natal week (Nimchinsky *et al.*, 2002) (Figure 3.3b, lane P21). The onset of increase in the amounts of SAPAP3 and GKAP detected in the PSD fractions appears to lag behind that of SAPAP1. SAPAP1 is abundant in PSDs obtained from neonatal rats. In particular, the highest levels of SAPAP1 are observed at P7 which corresponds to the completion of cortical neurogenesis and neuronal migration (Haberny *et al.*, 2002). These results are also consistent with *in vitro* data indicating that SAPAP1, together with PSD95, is already present at excitatory synapses of cultured hippocampal neurons early in development (Rao *et al.*, 1998;

Gerrow *et al.*, 2006). In comparison, low amounts of SAPAP3 are present in PSDs from these stages and GKAP is virtually undetectable. By P21, however, SAPAP1 levels begin to decline which is accompanied by a dramatic increase in the amounts of both SAPAP3 and GKAP. While the quantities of all three proteins appear to decrease in the PSDs of the adult brain, significantly higher amounts of SAPAP3 and GKAP persisted whereas the amounts of SAPAP1 had returned to levels comparable to those present in neonatal rats. Despite the observed fluctuations in the levels of SAPAPs in the PSD, the amount of PSD95 steadily increases in the developing rat brain as has been previously reported (Bence *et al.*, 2005; Sans *et al.*, 2000; Petralia *et al.*, 2005). These results suggest that SAPAP1 is the predominant form of this protein family present in young developing synapses and becomes progressively replaced by SAPAP3 and GKAP as synapses mature.

The developmental switch from SAPAP1 to GKAP expression in rat PSDs has been previously described (Petralia *et al.*, 2005; Yoshii *et al.*, 2003). These and other studies examining developmental changes in the levels of PSD proteins in various regions of the brain also revealed that the appearance of the NR2B and NR2A subunits of the NMDA receptor (NMDAR) complex appears to parallel the trend observed for SAPAP1 and GKAP. Specifically, NR2B is already present in the early postnatal rat brain while NR2A only becomes detectable after the first post-natal week (Hsieh *et al.*, 2002; Petralia *et al.*, 2005; Shi *et al.*, 1997). In addition, there is some evidence to suggest that SAP102 and PSD-95 (which also undergo an analogous complementary developmental switch) may exhibit different binding properties to individual isoforms of the NR2 receptor subunit, with SAP102 preferentially binding to NR2B and PSD-95 to NR2A (Sans *et al.*, 2000). These observations have led to the hypothesis that the maturation of synapses is accompanied by a change in the association of the NMDAR with different scaffolding complexes (van Zundert *et al.*, 2004). Specifically, it has been proposed that the neonate NR2B-rich NMDAR complexes bound to SAP102 are anchored to synapses via interaction with SAPAP1. In response to synaptic activity, PSD-95 (which preferentially binds the NR2A subunit) and GKAP are synthesized and localized to synapses, gradually replacing the NMDAR-SAP102 complexes from synapses. Thus, in this model, the developmental switch to the GKAP isoform plays a role in stabilization of mature synapses. Analogously, the late expression of both SAPAP3 isoforms and their abundance in the

adult PSDs may indicate their role in the stabilization or maturation of synapses. In support of this hypothesis, an increase in the levels of Shank proteins, known binding partners of SAPAPs and important in the development and maturation of dendritic spines, has also been observed to occur at the third post-natal week (Böckers *et al.*, 1999;; Naisbitt *et al.*, 1999; Lim *et al.*, 1999; Roussignol *et al.*, 2005; Sala *et al.*, 2001).

The three unique 5' UTRs identified in this study are all associated with the same SAPAP3 coding sequencing. While the average 5' UTR of most mRNAs ranges between 20 to 100 nt in length (Davuluri *et al.*, 2000; Kozak, 1987b, 1991d), the isolated SAPAP3 UTRs are exceptionally long, ranging in size from 213 nt to 404 nt, and contain several uORFs. Moreover, the E1B and the E1B<sup>+</sup> 5' UTR variants are predicted to form stable secondary structures. Remarkably, the E1B 5' UTR sequence is highly conserved across the human, mouse and rat sequences (Figure 3.7). Unusually long 5' UTRs containing uORFs and extensive secondary structures, which inhibit translation, are characteristic of eukaryotic mRNAs encoding important regulatory proteins such as proto-oncogenes, growth factors and their corresponding receptors (Davuluri *et al.*, 2000; Kochetov *et al.*, 1998; Kozak, 1991c) whose expression has to be stringently regulated. Therefore, a tight regulation of SAPAP3 levels via a 5' UTR dependent mechanism suggests an important role of these proteins in the formation and/or function of synapses in the brain as implied by the previous developmental data.

Indeed, the inclusion of the E1B and E1B<sup>+</sup> 5' UTRs sequences in constructs encoding SAPAP3 or heterologous proteins results in a marked reduction in the amounts of recombinant protein expression (Figures 3.9, 3.10c, 3.11b, 3.12b, 3.19b and 3.20a; Table 3.2). This inhibitory effect of the 5' UTRs on protein yield occurs at the translational level as indicated by the reduction of protein/mRNA expression ratios for the respective constructs (Figure 3.10b, 3.10c). In addition, the 3' UTR of SAPAP3 is not necessary for inhibiting translation (Figure 3.12b). Further, while a number of studies have indicated that a variety of RNA-binding proteins recognizing sequences present in 5' UTRs can inhibit translation of certain mRNAs (Gray and Hentze, 1994; Kullmann *et al.*, 2002; Meng *et al.*, 2005; Nielsen *et al.*, 1999; Paraskeva *et al.*, 1999; Timchenko *et al.*, 2002, 1999), competition assays in this

study have confirmed that *trans*-factors are not required for translational inhibition mediated by the SAPAP3 5' UTR (Figure 3.18b). Progressive truncations of the 5' UTR in SAPAP3-expressing mRNAs (Figures 3.19b and 3.20a) have no effect on protein yield. This rules out the involvement of stable secondary structures as the major cause of the inhibition, which has been implicated for the translational inhibition of mRNAs encoding NR2A and GluR2, subunits of NMDA and AMPA receptors, respectively (Liu *et al.*, 2003; Myers *et al.*, 2004; Wood *et al.*, 1996). Instead, the translation of uORF2 present in the SAPAP3 5' UTR is responsible for inhibiting the synthesis of SAPAP3 $\alpha$  since the removal of the AUG from this uORF is sufficient to strongly elevate translation of SAPAP3 $\alpha$  in both pFS3-related (Figures 3.19b and 3.19c) and authentic mRNAs (Figure 3.20a). Such an uORF-dependent mechanism of translational inhibition has also been reported for a variety of other mRNAs encoding important regulatory proteins like Axin2 (Hughes and Brady, 2005), thrombopoietin (Ghilardi *et al.*, 1998) and estrogen receptor  $\alpha$  (Koř *et al.*, 2002).

Surprisingly, SAPAP3 5' UTR is also responsible for enabling the synthesis of two different SAPAP3 isoforms from a single mRNA coding sequence (Figures 3.20a and 3.20b). Whereas only SAPAP3 $\alpha$  is produced from SAPAP3 mRNAs lacking the E1B 5' UTR variant, inclusion of the complete or portions of the 3' region of the 5' UTR results in the generation of a second smaller protein (SAPAP3 $\beta$ ) that co-migrates on SDS-PAGE gels with the 105 kDa SAPAP3 isoform detected in PSD fractions (Figure 3.20b). Sequence analysis of the SAPAP3 coding region revealed that two downstream in-frame start codons (AUG<sub>+67</sub> and AUG<sub>+277</sub>) could be utilized as alternative initiation sites in place of the SAPAP3 $\alpha$  start codon, AUG<sub>+1</sub>. Therefore, an alternative translational initiation (ATI) event occurring at either of these downstream start codons could be responsible for synthesizing SAPAP3 $\beta$ . Such a mechanism has been shown to be responsible for the synthesis of multiple protein isoforms for several other mRNAs (Byrd *et al.*, 2002; Calkhoven *et al.*, 2000; Okazaki *et al.*, 1998; Sarrazine *et al.*, 2000; Short and Pfarr, 2002; Xiong *et al.*, 2001). Indeed, systematic removal of AUG<sub>+1</sub> and AUG<sub>+67</sub> sequences confirmed that synthesis of SAPAP3 $\beta$  is initiated from AUG<sub>+277</sub> (Figure 3.21). Interestingly, SAPAP3 transcript variants containing ORFs initiating only from AUG<sub>+277</sub> were not found in dbEST nor were they isolated via RT-PCR despite the use of two different 5' UTR primers in

combination with two different anti-sense oligonucleotides (RA4 and Y2HS3R) which prime at locations downstream from AUG<sub>+277</sub>. Moreover, exon 2, which contains the regulatory uORF2, is present in all 5' UTR variants isolated thus far (Figure 3.6). This suggests that endogenous SAPAP3 $\beta$  is unlikely to be produced from another transcript that does not simultaneously encode SAPAP3 $\alpha$ . Thus, ATI is likely to mediate the generation of both SAPAP3 isoforms from other SAPAP3 mRNAs. SAPAP3 $\alpha$  and SAPAP3 $\beta$  were also observed in PSD preparations obtained from the mouse (Welch *et al.*, 2004). Further, AUG<sub>+277</sub> and its surrounding sequences are highly conserved between the human, dog, mouse and rat SAPAP3 coding sequences. Taken together, these data suggest that ATI events are responsible for the synthesis for both SAPAP3 isoforms and that this phenomenon is evolutionarily conserved.

How could two related proteins be translated from the same transcript? A combination of leaky scanning and translation reinitiation mechanisms most likely accounts for this phenomenon. Inefficient recognition of a start codon (either due to a suboptimal Kozak sequence or local sequence context extending beyond the Kozak sequence) permits a portion of the 43S pre-initiation complexes to continue scanning and initiating at a downstream start codon in a process known as leaky scanning (Gray and Wickens, 1998; Kozak, 1991b). In addition to leaky scanning, the presence of small uORFs may also allow 40S subunits to reinitiate at a subsequent start codon after translation of the small uORF (Gray and Wickens, 1998; Hinnebusch, 2005; Wang and Rothnagel, 2004). The length of the uORF and distance between the uORF and the subsequent start codon are important considerations for reinitiation to occur. In general, a distance of more than 80 nucleotides separating short uORFs and a downstream start codon appears to support reinitiation by giving the 40S subunits sufficient time to re-acquire ternary complexes (Kozak, 1987a; Kozak, 2001; Wang and Rothnagel, 2005). The data from this study support the notion that SAPAP3 $\alpha$  is synthesized as a result of leaky scanning of the four uORFs present in the SAPAP3 E1B 5' UTR variant. The AUGs of uORF1, uORF3 and uORF4 are all surrounded by suboptimal Kozak sequences (Table 3.3). uORFs1 and 4 contain the important purine residue at the -3 position but lack the other important guanine residue at the +4 position. Similarly, while the +4 position of uORF3 contains the important guanine

residue, it lacks a purine at the -3 position. These considerations suggest that scanning 43S complexes are likely to bypass the start codons of uORFs 1, 3 and 4. This idea is confirmed by 5' UTR deletion and uAUG point mutation experiments which demonstrate that uORFs 1, 3 and 4 do not contribute significantly to the inhibition of synthesis of SAPAP3 $\alpha$ . In contrast, the start codon of uORF2 is present in a favorable Kozak sequence, indicating that 43S complexes should be able to efficiently recognize this start codon. Indeed, point mutations removing the start codon of uORF2 in puORF2<sup>AAG</sup>-E1B-FS3 as well as puORFs2+3<sup>AAG</sup>- $\Delta$ 205-S3 mRNAs are required for a dramatic increase in SAPAP3 $\alpha$  protein synthesis (Figures 3.19c and 3.20a) confirming that most 43S complexes are able to recognize and initiate translation at uORF2. However, due to the overlap of uORF2 with the start codon for SAPAP3 $\alpha$ , the reinitiation mechanism cannot account for the residual synthesis of SAPAP3 $\alpha$  from mRNAs retaining uORF2. Rather, some 43S complexes appear to bypass uORF2 and initiate translation at AUG<sub>+1</sub>. These results are in agreement with existing data showing that initiation at the main ORF can still occur by the leaky scanning mechanism for transcripts containing multiple inhibitory uORFs (Hughes and Brady, 2005; Wang and Rothnagel, 2004).

In contrast, the synthesis of SAPAP3 $\beta$  cannot be attributed to leaky scanning of the uORFs and AUG<sub>+1</sub>. This is shown by results obtained from the translation of the pS3 transcript containing AUG<sub>+1</sub> and AUG<sub>+277</sub> which yields high amounts of SAPAP3 $\alpha$  but no SAPAP3 $\beta$ . These data indicate that, in the absence of uORF2, the vast majority of ribosomes are recruited to initiate translation at AUG<sub>+1</sub> and synthesize SAPAP3 $\alpha$ . Thus, 43S complexes are apparently unable to bypass AUG<sub>+1</sub> to initiate translation at AUG<sub>+277</sub>, excluding the use of leaky scanning to initiate translation at this start codon. Instead, SAPAP3 $\beta$  synthesis occurs in the presence of uORF2 which strongly suggests the involvement of the reinitiation mechanism in its translation. Compelling evidence for this comes from the observation that SAPAP3 $\beta$  is efficiently synthesized from the uORF2 containing pE1B-S3, p $\Delta$ 150-S3 and  $\Delta$ 205-S3 mRNAs and that mutation of the uORF2 start codon abolishes the synthesis of SAPAP3 $\beta$  in the puORFs2+3<sup>AAG</sup>- $\Delta$ 205-S3 transcript. Therefore, synthesis of SAPAP3 $\beta$  is strongly dependent on the recognition of AUG<sub>+277</sub> by reinitiating 40S subunits having completed the translation of uORF2 and consequently skipped AUG<sub>+1</sub>. Therefore,



uORF2 acts as an reinitiation shunt (Kozak, 2002) to limit ribosomal initiation at AUG<sub>+1</sub>, permitting a proportion of 40S subunits to bypass AUG<sub>+1</sub> and reinitiate at AUG<sub>+277</sub> in order to synthesize SAPAP3 $\beta$ . Thus, two translational mechanisms are utilized in parallel to synthesize two SAPAP3 isoforms.

Remarkably, 40S subunits that resume scanning after translating uORF2 are evidently unable to recognize AUG<sub>+67</sub>. Although this may indicate that the distance between AUG<sub>+1</sub> and AUG<sub>+67</sub> does not permit sufficient time for the 40S subunits to re-acquire eIF2·GTP·Met-tRNA<sub>i</sub><sup>Met</sup> ternary complexes necessary for translation reinitiation at AUG<sub>+67</sub> (Kozak, 1987a), data from the translation of p $\Delta$ (AUG<sub>+1</sub>)-S3 mRNAs support a different explanation. The removal of AUG<sub>+1</sub> in these mRNAs results in AUG<sub>+67</sub> being repositioned as the first AUG encountered by the scanning 43S pre-initiation complex. Despite this, initiation at AUG<sub>+67</sub> appears to occur very inefficiently as evidenced by the detection of only low levels of product corresponding to translation from this start codon (Figure 3.21). Interestingly, this indicates that almost all ribosomes that resume scanning following translation of uORF2 reinitiate at AUG<sub>+277</sub> to synthesize SAPAP3 $\beta$ . Since both AUG<sub>+1</sub> and AUG<sub>+67</sub> are flanked by relatively optimal Kozak sequences (Table 3.3), the poor recognition of AUG<sub>+67</sub> probably arises as a result of the effect of local secondary structure and context (Kozak, 1991b; Hinnebusch, 2005). The efficient synthesis of SAPAP3 $\beta$  and not the translation product of AUG<sub>+67</sub> in p $\Delta$ (AUG<sub>+1</sub>)-S3 transcripts reinforces the idea that reinitiation is necessary to generate reinitiating 40S subunits to bypass AUG<sub>+1</sub> but not AUG<sub>+67</sub> in order to initiate translation of SAPAP3 $\beta$  from AUG<sub>+277</sub>.

The use of uORFs to regulate translation from downstream initiation sites has been described for a number of other proteins (Calkhoven *et al.*, 2000; Hinnebusch, 2005; Lu *et al.*, 2004; Okazaki *et al.*, 1998; Sarrazine *et al.*, 2000; Short and Pfarr, 2002; Vatten and Wek, 2004; Xiong *et al.*, 2001). In particular, the mechanism used in regulating translation of SAPAP3 isoforms closely parallels that identified for the proto-oncogene product Fli-1 (Sarrazine *et al.*, 2000). In Friend erythroleukemia cell lines, alternative translation initiation events regulated by two conserved uORFs in the Fli-1 5' UTR are responsible for the generation of two Fli-1 isoforms from a single mRNA. Translation initiation at AUG<sub>+1</sub> of the Fli-1 mRNA leads to the production of

the 51 kDa isoform while synthesis of the 48 kDa isoform begins at AUG<sub>+100</sub>. Similar to the results obtained for SAPAP3, disruption of the two conserved uORFs in the Fli-1 mRNA results in an increased synthesis of the larger isoform accompanied by reduced levels of the smaller protein. Likewise, production of the 48 kDa Fli-1 isoform was also reasoned to be dependent on 40S subunits that resume scanning of the 5' UTR and reinitiating at AUG<sub>+100</sub> after translation of the uORF peptide.

Contrary to the stimulatory effects of uORF2 on SAPAP3 $\beta$  synthesis, the distal 5' portion of the 5' UTR appears to inhibit its synthesis. This is suggested by the observation that removing the first 150 nucleotides of the E1B sequence (corresponding to the E1B exon) significantly improves the yield of SAPAP3 $\beta$  (Figure 3.20a, lane  $\Delta$ 150-S3). Since uORF2 is encoded within exon 2, removal of exon 1 is not likely to abrogate the reinitiation mechanism necessary to synthesize SAPAP3 $\beta$ . Instead, exon 1 may contain elements that reduce the efficiency of translation at AUG<sub>+277</sub>. Interestingly, the composition of the exon 1B sequence (82% GC-rich,  $\Delta$ G between -90.1 to -85.6 kcal/mol) differs significantly from exon 1A sequence (67% GC-rich,  $\Delta$ G between -19.5 to -18.8 kcal/mol). At least based on their  $\Delta$ G values, the E1B 5' UTR represents a higher translational barrier than the E1A 5' UTR. This suggests that replacement of exon 1B with exon 1A in naturally occurring SAPAP3 transcripts variants may reproduce the positive effect on SAPAP3 $\beta$  synthesis observed in p $\Delta$ 150-S3 mRNAs. Indeed, the removal of inhibitory *cis*-acting elements by alternatively splicing within the 5' UTR has been shown to generate variant transcripts that are more efficiently translated (Frankton *et al.*, 2004; Hughes and Brady, 2005; Myers *et al.*, 2004; Wang *et al.*, 2005). Thus, for SAPAP3, the 5' UTR variant present in SAPAP3 transcripts may well be involved in determining the relative amounts of  $\alpha$  and  $\beta$  isoforms produced.

The alternative use of translational start sites results in the synthesis of two SAPAP3 isoforms that differ from each other by the addition of 92 amino acids at the N-terminus of SAPAP3 $\alpha$  against SAPAP3 $\beta$ . Alternative translation initiation has been suggested as a mechanism used by cells to generate protein diversity (Cai *et al.*, 2006; Kochetov *et al.*, 2005) in addition to alternative splicing. Protein isoforms generated by such events were predicted to differ in their functions or subcellular localization.

Experimentally, distinct isoforms of the CCAAT/enhancer-binding *trans*-activating protein- $\beta$  (C/EBP $\beta$ ) have been shown to differ in their transcriptional regulatory functions and their ability to induce cellular transformation (Calkhoven *et al.*, 2000; Xiong *et al.*, 2001 and references therein). In addition, an N-terminally extended insulin degrading enzyme (IDE) generated by ATI from an upstream in-frame start codon has been shown to target to mitochondria while the shorter isoform is predominantly cytosolic (Leissring *et al.*, 2004).

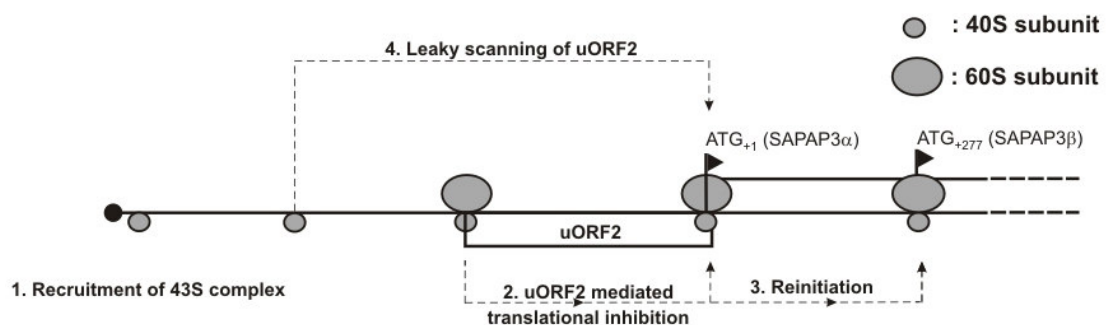
In the case of SAPAP3, the functional significance of the N-terminus diversity is less obvious. Synaptic targeting of SAPAP1 has been shown to be mediated by its N-terminal 343 residues (Yao *et al.*, 2003). Since both SAPAP isoforms are still efficiently targeted to PSD fractions (Figure 3.2), the first 92 amino acids of SAPAP3 $\alpha$  appear to be dispensable for synaptic localization. Neurofilaments have been reported to bind to the N-terminus of SAPAP1 (Hirao *et al.*, 2000). It would be interesting to examine if such an interaction also occurs for SAPAP3 and if it could be influenced by differences in the N-terminus of the two isoforms. A search of this unique region of SAPAP3 $\alpha$  against protein databases did not reveal any known protein motifs or domains although putative phosphorylation sites for several protein kinases were identified (data not shown). Nonetheless, it remains possible that a yet uncharacterized protein interaction partner exists which specifically binds to the N-terminal extended region of SAPAP3 $\alpha$ .

Analysis of PSD fractions obtained from different brain regions showed that the levels of either SAPAP3 isoform vary in individual regions (Figure 3.23). Although similar ratios of both isoforms are present in the neocortex and olfactory bulb, other regions of the brain analyzed appear to contain higher levels of SAPAP3 $\beta$ . In particular, relatively more SAPAP3 $\beta$  are present in hippocampal PSD fractions. Variations in the ratios of SAPAP3 isoforms in PSD fractions from different brain regions suggested that each isoform could perform functionally different roles in individual areas of the brain. To examine this, I over-expressed SAPAP3 $\alpha$  in culture hippocampal neurons to disturb endogenous SAPAP3 ratios. Elevated levels of SAPAP3 $\alpha$  did not result in significant morphological changes as has been reported for other PSD proteins (Calabrese and Halpain, 2005; El-Husseini *et al.*, 2000; Sala *et al.*, 2001; Quitsch *et*

*al.*, 2005) and recombinant SAPAP3 $\alpha$  remains properly targeted to excitatory synapses (Figure 3.24). However, in view of the association of SAPAPs with NMDAR complexes, a more subtle effect resulting from SAPAP3 $\alpha$  overexpression that is not identifiable by microscopic methods cannot be ruled out. Potentiation of NMDAR channel activity is observed in *Xenopus* oocytes expressing GKAP, NMDARs and PSD95 but not in the absence of GKAP (Yamada *et al.*, 1999). In addition, elevated levels of SAPAP1 found in nucleus accumbens of schizophrenic patients have been suggested to be responsible for abnormal glutamatergic neurotransmission in schizophrenia (Kajimoto *et al.*, 2003). It would be interesting to see if perturbations of endogenous SAPAP3 levels or isoform ratios could also be responsible for similar types of abnormalities.

Based on the data that has been accumulated in this study, I propose the following model to explain the translation regulatory mechanism involved in the simultaneous synthesis of two SAPAP3 isoforms from the E1B 5' UTR variant mRNAs (Figure 4.1):

The 43S ternary complex is first recruited to SAPAP3 mRNAs via a cap-dependent translational mechanism (Step 1). A portion of these complexes initiate translation at uORF2 which leads to the inhibition of translation from ATG<sub>+1</sub> (Step 2). Reinitiating ribosomes that have completed translation of uORF2 are able to resume scanning, reacquire ternary complexes and initiate translation again at ATG<sub>+277</sub> thus producing SAPAP3 $\beta$  (Step 3). The synthesis of SAPAP3 $\alpha$  most likely occurs by other ribosomes that have bypassed uORF2 by leaky scanning and subsequently initiate translation at ATG<sub>+1</sub> (Step 4).



**Figure 4.1** A proposed model for the regulation of translation mediated by SAPAP3 5' UTRs. See text for details of each step. For clarity, uORFs 1, 3 and 4 have been omitted in the scheme.

In summary, I have taken multiple approaches to characterize the mechanisms regulating translational regulation of SAPAP3. The major finding of this study is the identification of one 5' UTR variant of SAPAP3 mRNAs that directs the synthesis and regulates the ratios of two different SAPAP3 isoforms via alternative translational initiation. This is mediated by the presence of a single uORF. Such a mechanism has not yet been described for any other PSD protein.

SAPAP3 is one of the four members of the family of synapse-associated protein 90/postsynaptic density-95-associated proteins which act as adaptor proteins in the assembly of the postsynaptic density (PSD) in neuronal excitatory synapses. Of the four members, only transcripts belonging to SAPAP3 are dendritically localized. Using a combination of database searches and RT-PCR, I have isolated three different SAPAP3 5' untranslated region (UTR) sequences. One of these variants (E1B variant) is evolutionarily conserved, long, highly GC-rich and is predicted to form stable secondary structures. These features strongly suggest its involvement in regulating translation of its mRNA. Inclusion of the E1B variant 5' UTR sequence in constructs encoding SAPAP3 or heterologous proteins leads to a drastic reduction in recombinant protein expression. Northern analysis revealed that mRNA levels are not affected by the inclusion of the 5' UTR indicating that protein expression is inhibited at the translational level. *In vitro* competition assays ruled out the involvement of *trans*-acting proteins in this process. Sequential deletions of the 5' UTR segments indicated that secondary structures are not responsible for translational inhibition while mutation of the start codon of only one of the four upstream open reading frames (uORF2) is sufficient to elevate protein synthesis to comparable levels as observed in the absence of the complete 5' UTR. Remarkably, the E1B 5' UTR sequence leads to the synthesis of two SAPAP3 isoforms when positioned directly in front of the native SAPAP3 coding region. Synthesis of the shorter SAPAP3 $\beta$  isoform is achieved via alternative translational initiation from a downstream in-frame start codon (AUG<sub>+277</sub>). Initiation from AUG<sub>+277</sub> is enhanced by the presence of uORF2 indicating that uORF2 functions as a reinitiation shunt to direct ribosomes away from the AUG of SAPAP3 $\alpha$ . SAPAP3 $\alpha$  differs from SAPAP3 $\beta$  by an additional 92 amino acids at its N-terminus. The ratios of SAPAP3 isoforms vary in distinct brain regions examined suggesting functional differences between both isoforms. Over-expression of SAPAP3 $\alpha$  in hippocampal neurons indicated strong enrichment of SAPAP3 $\alpha$  at excitatory synapses. While no gross morphological disturbances are observed in these neurons, changes in glutamatergic transmission resulting from perturbations of endogenous SAPAP3 isoform ratios may exist which were not examined so far. The synthesis of two SAPAP3 isoforms via alternative translational initiation distinguishes SAPAP3 from the other PSD proteins and reveals an additional mechanism for generating protein diversity in the PSD.

- Bence, M., Arbuckle, M.I., Dickson, K.S., and Grant, S.G. (2005). Analyses of murine postsynaptic density-95 identify novel isoforms and potential translational control elements. *Brain Res Mol Brain Res* 133, 143-152.
- Blichenberg, A., Schwanke, B., Rehbein, M., Garner, C.C., Richter, D., and Kindler, S. (1999). Identification of a cis-acting dendritic targeting element in MAP2 mRNAs. *J Neurosci* 19, 8818-8829.
- Boeckers, T.M., Winter, C., Smalla, K.H., Kreutz, M.R., Bockmann, J., Seidenbecher, C., Garner, C.C., and Gundelfinger, E.D. (1999). Proline-rich synapse-associated proteins ProSAP1 and ProSAP2 interact with synaptic proteins of the SAPAP/GKAP family. *Biochem Biophys Res Commun* 264, 247-252.
- Bongiorno-Borbone, L., Kadare, G., Benfenati, F., and Girault, J.A. (2005). FAK and PYK2 interact with SAP90/PSD-95-Associated Protein-3. *Biochem Biophys Res Commun* 337, 641-646.
- Byrd, M.P., Zamora, M., and Lloyd, R.E. (2002). Generation of multiple isoforms of eukaryotic translation initiation factor 4GI by use of alternate translation initiation codons. *Mol Cell Biol* 22, 4499-4511.
- Cai, J., Huang, Y., Li, F., and Li, Y. (2006). Alteration of protein subcellular location and domain formation by alternative translational initiation. *Proteins* 62, 793-799.
- Calabrese, B., and Halpain, S. (2005). Essential role for the PKC target MARCKS in maintaining dendritic spine morphology. *Neuron* 48, 77-90.
- Calkhoven, C.F., Muller, C., and Leutz, A. (2000). Translational control of C/EBPalpha and C/EBPbeta isoform expression. *Genes Dev* 14, 1920-1932.
- Carlin, R.K., Grab, D.J., Cohen, R.S., and Siekevitz, P. (1980). Isolation and characterization of postsynaptic densities from various brain regions: enrichment of different types of postsynaptic densities. *J Cell Biol* 86, 831-845.
- Clemens, M.J., Bushell, M., Jeffrey, I.W., Pain, V.M., and Morley, S.J. (2000). Translation initiation factor modifications and the regulation of protein synthesis in apoptotic cells. *Cell Death Differ* 7, 603-615.
- Davuluri, R.V., Suzuki, Y., Sugano, S., and Zhang, M.Q. (2000). CART classification of human 5' UTR sequences. *Genome Res* 10, 1807-1816.
- Ehlers, M.D. (2003). Activity level controls postsynaptic composition and signaling via the ubiquitin-proteasome system. *Nat Neurosci* 6, 231-242.
- El-Husseini, A.E., Schnell, E., Chetkovich, D.M., Nicoll, R.A., and Bredt, D.S. (2000). PSD-95 involvement in maturation of excitatory synapses. *Science* 290, 1364-1368.

- Frankton, S., Harvey, C.B., Gleason, L.M., Fadel, A., and Williams, G.R. (2004). Multiple messenger ribonucleic acid variants regulate cell-specific expression of human thyroid hormone receptor beta1. *Mol Endocrinol* 18, 1631-1642.
- Gerrow, K., Romorini, S., Nabi, S.M., Colicos, M.A., Sala, C., and El-Husseini, A. (2006). A preformed complex of postsynaptic proteins is involved in excitatory synapse development. *Neuron* 49, 547-562.
- Ghilardi, N., Wiestner, A., and Skoda, R.C. (1998). Thrombopoietin production is inhibited by a translational mechanism. *Blood* 92, 4023-4030.
- Gingras, A.C., Raught, B., and Sonenberg, N. (1999). eIF4 initiation factors: effectors of mRNA recruitment to ribosomes and regulators of translation. *Annu Rev Biochem* 68, 913-963.
- Grant, C.M., Miller, P.F., and Hinnebusch, A.G. (1994). Requirements for intercistronic distance and level of eukaryotic initiation factor 2 activity in reinitiation on GCN4 mRNA vary with the downstream cistron. *Mol Cell Biol* 14, 2616-2628.
- Gray, N.K., and Hentze, M.W. (1994). Iron regulatory protein prevents binding of the 43S translation pre-initiation complex to ferritin and eALAS mRNAs. *EMBO J* 13, 3882-3891.
- Gray, N.K., and Wickens, M. (1998). Control of translation initiation in animals. *Annu Rev Cell Dev Biol* 14, 399-458.
- Haberny, K.A., Paule, M.G., Scallet, A.C., Sistare, F.D., Lester, D.S., Hanig, J.P., and Slikker, W., Jr. (2002). Ontogeny of the N-methyl-D-aspartate (NMDA) receptor system and susceptibility to neurotoxicity. *Toxicol Sci* 68, 9-17.
- Han, B., Dong, Z., Liu, Y., Chen, Q., Hashimoto, K., and Zhang, J.T. (2003a). Regulation of constitutive expression of mouse PTEN by the 5'-untranslated region. *Oncogene* 22, 5325-5337.
- Han, B., Dong, Z., and Zhang, J.T. (2003b). Tight control of platelet-derived growth factor B/c-sis expression by interplay between the 5'-untranslated region sequence and the major upstream promoter. *J Biol Chem* 278, 46983-46993.
- Haraguchi, K., Satoh, K., Yanai, H., Hamada, F., Kawabuchi, M., and Akiyama, T. (2000). The hDLG-associated protein DAP interacts with dynein light chain and neuronal nitric oxide synthase. *Genes Cells* 5, 905-911.
- Harding, H.P., Novoa, I., Zhang, Y., Zeng, H., Wek, R., Schapira, M., and Ron, D. (2000). Regulated translation initiation controls stress-induced gene expression in mammalian cells. *Mol Cell* 6, 1099-1108.
- Hering, H., and Sheng, M. (2001). Dendritic spines: structure, dynamics and regulation. *Nat Rev Neurosci* 2, 880-888.



- Hinnebusch, A.G. (2005). Translational regulation of GCN4 and the general amino acid control of yeast. *Annu Rev Microbiol* 59, 407-450.
- Hirao, K., Hata, Y., Deguchi, M., Yao, I., Ogura, M., Rokukawa, C., Kawabe, H., Mizoguchi, A., and Takai, Y. (2000b). Association of synapse-associated protein 90/ postsynaptic density-95-associated protein (SAPAP) with neurofilaments. *Genes Cells* 5, 203-210.
- Hirao, K., Hata, Y., Ide, N., Takeuchi, M., Irie, M., Yao, I., Deguchi, M., Toyoda, A., Sudhof, T.C., and Takai, Y. (1998). A novel multiple PDZ domain-containing molecule interacting with N-methyl-D-aspartate receptors and neuronal cell adhesion proteins. *J Biol Chem* 273, 21105-21110.
- Hirao, K., Hata, Y., Yao, I., Deguchi, M., Kawabe, H., Mizoguchi, A., and Takai, Y. (2000a). Three isoforms of synaptic scaffolding molecule and their characterization. Multimerization between the isoforms and their interaction with N-methyl-D-aspartate receptors and SAP90/PSD-95-associated protein. *J Biol Chem* 275, 2966-2972.
- Hsieh, C.Y., Chen, Y., Leslie, F.M., and Metherate, R. (2002). Postnatal development of NR2A and NR2B mRNA expression in rat auditory cortex and thalamus. *J Assoc Res Otolaryngol* 3, 479-487.
- Hughes, T.A., and Brady, H.J. (2005). Expression of axin2 is regulated by the alternative 5'-untranslated regions of its mRNA. *J Biol Chem* 280, 8581-8588.
- Husi, H., Ward, M.A., Choudhary, J.S., Blackstock, W.P., and Grant, S.G. (2000). Proteomic analysis of NMDA receptor-adhesion protein signaling complexes. *Nat Neurosci* 3, 661-669.
- Kajimoto, Y., Shirakawa, O., Lin, X.H., Hashimoto, T., Kitamura, N., Murakami, N., Takumi, T., and Maeda, K. (2003). Synapse-associated protein 90/postsynaptic density-95-associated protein (SAPAP) is expressed differentially in phencyclidine-treated rats and is increased in the nucleus accumbens of patients with schizophrenia. *Neuropsychopharmacology* 28, 1831-1839.
- Kapp, L.D., and Lorsch, J.R. (2004). The molecular mechanics of eukaryotic translation. *Annu Rev Biochem* 73, 657-704.
- Kawabe, H., Hata, Y., Takeuchi, M., Ide, N., Mizoguchi, A., and Takai, Y. (1999). nArgBP2, a novel neural member of ponsin/ArgBP2/vinexin family that interacts with synapse-associated protein 90/postsynaptic density-95-associated protein (SAPAP). *J Biol Chem* 274, 30914-30918.
- Kawashima, N., Takamiya, K., Sun, J., Kitabatake, A., and Sobue, K. (1997). Differential expression of isoforms of PSD-95 binding protein (GKAP/SAPAP1) during rat brain development. *FEBS Lett* 418, 301-304.

- Kelleher, R.J., 3rd, Govindarajan, A., and Tonegawa, S. (2004). Translational regulatory mechanisms in persistent forms of synaptic plasticity. *Neuron* 44, 59-73.
- Kim, E., Naisbitt, S., Hsueh, Y.P., Rao, A., Rothschild, A., Craig, A.M., and Sheng, M. (1997). GKAP, a novel synaptic protein that interacts with the guanylate kinase-like domain of the PSD-95/SAP90 family of channel clustering molecules. *J Cell Biol* 136, 669-678.
- Kim, E., and Sheng, M. (2004). PDZ domain proteins of synapses. *Nat Rev Neurosci* 5, 771-781.
- Kindler, S., Rehbein, M., Classen, B., Richter, D., and Bockers, T.M. (2004). Distinct spatiotemporal expression of SAPAP transcripts in the developing rat brain: a novel dendritically localized mRNA. *Brain Res Mol Brain Res* 126, 14-21.
- Kochetov, A.V., Ischenko, I.V., Vorobiev, D.G., Kel, A.E., Babenko, V.N., Kisselev, L.L., and Kolchanov, N.A. (1998). Eukaryotic mRNAs encoding abundant and scarce proteins are statistically dissimilar in many structural features. *FEBS Lett* 440, 351-355.
- Kochetov, A.V., Sarai, A., Rogozin, I.B., Shumny, V.K., and Kolchanov, N.A. (2005). The role of alternative translation start sites in the generation of human protein diversity. *Mol Genet Genomics* 273, 491-496.
- Koš, M., Denger, S., Reid, G., and Gannon, F. (2002). Upstream open reading frames regulate the translation of the multiple mRNA variants of the estrogen receptor alpha. *J Biol Chem* 277, 37131-37138.
- Kozak, M. (1987a). Effects of intercistronic length on the efficiency of reinitiation by eucaryotic ribosomes. *Mol Cell Biol* 7, 3438-3445.
- Kozak, M. (1987b). An analysis of 5'-noncoding sequences from 699 vertebrate messenger RNAs. *Nucleic Acids Res* 15, 8125-8148.
- Kozak, M. (1990). Downstream secondary structure facilitates recognition of initiator codons by eukaryotic ribosomes. *Proc Natl Acad Sci U S A* 87, 8301-8305.
- Kozak, M. (1991a). A short leader sequence impairs the fidelity of initiation by eukaryotic ribosomes. *Gene Expr* 1, 111-115.
- Kozak, M. (1991b). Structural features in eukaryotic mRNAs that modulate the initiation of translation. *J Biol Chem* 266, 19867-19870.
- Kozak, M. (1991c). An analysis of vertebrate mRNA sequences: intimations of translational control. *J Cell Biol* 115, 887-903.
- Kozak, M. (1997). Recognition of AUG and alternative initiator codons is augmented by G in position +4 but is not generally affected by the nucleotides in positions +5 and +6. *EMBO J* 16, 2482-2492.

- Kozak, M. (2001). Constraints on reinitiation of translation in mammals. *Nucleic Acids Res* 29, 5226-5232.
- Kozak, M. (2002). Pushing the limits of the scanning mechanism for initiation of translation. *Gene* 299, 1-34.
- Krichevsky, A.M., and Kosik, K.S. (2001). Neuronal RNA granules: a link between RNA localization and stimulation-dependent translation. *Neuron* 32, 683-696.
- Kuersten, S., and Goodwin, E.B. (2003). The power of the 3' UTR: translational control and development. *Nat Rev Genet* 4, 626-637.
- Kullmann, M., Gopfert, U., Siewe, B., and Hengst, L. (2002). ELAV/Hu proteins inhibit p27 translation via an IRES element in the p27 5'UTR. *Genes Dev* 16, 3087-3099.
- Laemmli, U.K. (1970). Cleavage of structural proteins during the assembly of the head of bacteriophage T4. *Nature* 227, 680-685.
- Lammich, S., Schobel, S., Zimmer, A.K., Lichtenthaler, S.F., and Haass, C. (2004). Expression of the Alzheimer protease BACE1 is suppressed via its 5'-untranslated region. *EMBO Rep* 5, 620-625.
- Lamprecht, R., and LeDoux, J. (2004). Structural plasticity and memory. *Nat Rev Neurosci* 5, 45-54.
- Leissring, M.A., Farris, W., Wu, X., Christodoulou, D.C., Haigis, M.C., Guarente, L., and Selkoe, D.J. (2004). Alternative translation initiation generates a novel isoform of insulin-degrading enzyme targeted to mitochondria. *Biochem J* 383, 439-446.
- Lim, S., Naisbitt, S., Yoon, J., Hwang, J.I., Suh, P.G., Sheng, M., and Kim, E. (1999). Characterization of the Shank family of synaptic proteins. Multiple genes, alternative splicing, and differential expression in brain and development. *J Biol Chem* 274, 29510-29518.
- Liu, A., Zhuang, Z., Hoffman, P.W., and Bai, G. (2003). Functional analysis of the rat N-methyl-D-aspartate receptor 2A promoter: multiple transcription starts points, positive regulation by Sp factors, and translational regulation. *J Biol Chem* 278, 26423-26434.
- Lu, P.D., Harding, H.P., and Ron, D. (2004). Translation reinitiation at alternative open reading frames regulates gene expression in an integrated stress response. *J Cell Biol* 167, 27-33.
- Mathews, D.H., Sabina, J., Zuker, M., and Turner, D.H. (1999). Expanded sequence dependence of thermodynamic parameters improves prediction of RNA secondary structure. *J Mol Biol* 288, 911-940.

- Mazumder, B., Seshadri, V., Imataka, H., Sonenberg, N., and Fox, P.L. (2001). Translational silencing of ceruloplasmin requires the essential elements of mRNA circularization: poly(A) tail, poly(A)-binding protein, and eukaryotic translation initiation factor 4G. *Mol Cell Biol* 21, 6440-6449.
- Meijer, H.A., and Thomas, A.A. (2002). Control of eukaryotic protein synthesis by upstream open reading frames in the 5'-untranslated region of an mRNA. *Biochem J* 367, 1-11.
- Meng, Z., King, P.H., Nabors, L.B., Jackson, N.L., Chen, C.Y., Emanuel, P.D., and Blume, S.W. (2005). The ELAV RNA-stability factor HuR binds the 5'-untranslated region of the human IGF-IR transcript and differentially represses cap-dependent and IRES-mediated translation. *Nucleic Acids Res* 33, 2962-2979.
- Monshausen, M., Rehbein, M., Richter, D., and Kindler, S. (2002). The RNA-binding protein Staufen from rat brain interacts with protein phosphatase-1. *J Neurochem* 81, 557-564.
- Morris, D.R., and Geballe, A.P. (2000). Upstream open reading frames as regulators of mRNA translation. *Mol Cell Biol* 20, 8635-8642.
- Morrish, B.C., and Rumsby, M.G. (2002). The 5' untranslated region of protein kinase C $\delta$  directs translation by an internal ribosome entry segment that is most active in densely growing cells and during apoptosis. *Mol Cell Biol* 22, 6089-6099.
- Myers, S.J., Huang, Y., Genetta, T., and Dingledine, R. (2004). Inhibition of glutamate receptor 2 translation by a polymorphic repeat sequence in the 5'-untranslated leaders. *J Neurosci* 24, 3489-3499.
- Naisbitt, S., Kim, E., Tu, J.C., Xiao, B., Sala, C., Valtschanoff, J., Weinberg, R.J., Worley, P.F., and Sheng, M. (1999). Shank, a novel family of postsynaptic density proteins that binds to the NMDA receptor/PSD-95/GKAP complex and cortactin. *Neuron* 23, 569-582.
- Naisbitt, S., Kim, E., Weinberg, R.J., Rao, A., Yang, F.C., Craig, A.M., and Sheng, M. (1997). Characterization of guanylate kinase-associated protein, a postsynaptic density protein at excitatory synapses that interacts directly with postsynaptic density-95/synapse-associated protein 90. *J Neurosci* 17, 5687-5696.
- Naisbitt, S., Valtschanoff, J., Allison, D.W., Sala, C., Kim, E., Craig, A.M., Weinberg, R.J., and Sheng, M. (2000). Interaction of the postsynaptic density-95/guanylate kinase domain-associated protein complex with a light chain of myosin-V and dynein. *J Neurosci* 20, 4524-4534.
- Nielsen, J., Christiansen, J., Lykke-Andersen, J., Johnsen, A.H., Wewer, U.M., and Nielsen, F.C. (1999). A family of insulin-like growth factor II mRNA-binding proteins represses translation in late development. *Mol Cell Biol* 19, 1262-1270.

- Nimchinsky, E.A., Sabatini, B.L., and Svoboda, K. (2002). Structure and function of dendritic spines. *Annu Rev Physiol* 64, 313-353.
- Okazaki, S., Ito, T., Ui, M., Watanabe, T., Yoshimatsu, K., and Iba, H. (1998). Two proteins translated by alternative usage of initiation codons in mRNA encoding a JunD transcriptional regulator. *Biochem Biophys Res Commun* 250, 347-353.
- Packham, G., Brimmell, M., and Cleveland, J.L. (1997). Mammalian cells express two differently localized Bag-1 isoforms generated by alternative translation initiation. *Biochem J* 328 ( Pt 3), 807-813.
- Paraskeva, E., Gray, N.K., Schlager, B., Wehr, K., and Hentze, M.W. (1999). Ribosomal pausing and scanning arrest as mechanisms of translational regulation from cap-distal iron-responsive elements. *Mol Cell Biol* 19, 807-816.
- Pedersen, A.G., and Nielsen, H. (1997). Neural network prediction of translation initiation sites in eukaryotes: perspectives for EST and genome analysis. *Proc Int Conf Intell Syst Mol Biol* 5, 226-233.
- Pedersen, S.K., Christiansen, J., Hansen, T.O., Larsen, M.R., and Nielsen, F.C. (2002). Human insulin-like growth factor II leader 2 mediates internal initiation of translation. *Biochem J* 363, 37-44.
- Pereira, C.M., Sattlegger, E., Jiang, H.Y., Longo, B.M., Jaqueta, C.B., Hinnebusch, A.G., Wek, R.C., Mello, L.E., and Castilho, B.A. (2005). IMPACT, a protein preferentially expressed in the mouse brain, binds GCN1 and inhibits GCN2 activation. *J Biol Chem* 280, 28316-28323.
- Pesole, G., and Liuni, S. (1999). Internet resources for the functional analysis of 5' and 3' untranslated regions of eukaryotic mRNAs. *Trends Genet* 15, 378.
- Pestova, T.V., Kolupaeva, V.G., Lomakin, I.B., Pilipenko, E.V., Shatsky, I.N., Agol, V.I., and Hellen, C.U. (2001). Molecular mechanisms of translation initiation in eukaryotes. *Proc Natl Acad Sci U S A* 98, 7029-7036.
- Petralia, R.S., Sans, N., Wang, Y.X., and Wenthold, R.J. (2005). Ontogeny of postsynaptic density proteins at glutamatergic synapses. *Mol Cell Neurosci* 29, 436-452.
- Pinkstaff, J.K., Chappell, S.A., Mauro, V.P., Edelman, G.M., and Krushel, L.A. (2001). Internal initiation of translation of five dendritically localized neuronal mRNAs. *Proc Natl Acad Sci U S A* 98, 2770-2775.
- Pöyry, T.A., Kaminski, A., and Jackson, R.J. (2004). What determines whether mammalian ribosomes resume scanning after translation of a short upstream open reading frame? *Genes Dev* 18, 62-75.

- Quitsch, A., Berhorster, K., Liew, C.W., Richter, D., and Kreienkamp, H.J. (2005). Postsynaptic shank antagonizes dendrite branching induced by the leucine-rich repeat protein Densin-180. *J Neurosci* 25, 479-487.
- Rao, A., Kim, E., Sheng, M., and Craig, A.M. (1998). Heterogeneity in the molecular composition of excitatory postsynaptic sites during development of hippocampal neurons in culture. *J Neurosci* 18, 1217-1229.
- Reynolds, K., Zimmer, A.M., and Zimmer, A. (1996). Regulation of RAR $\beta$ 2 mRNA expression: evidence for an inhibitory peptide encoded in the 5'-untranslated region. *J Cell Biol* 134, 827-835.
- Rodriguez-Crespo, I., Yelamos, B., Roncal, F., Albar, J.P., Ortiz de Montellano, P.R., and Gavilanes, F. (2001). Identification of novel cellular proteins that bind to the LC8 dynein light chain using a pepscan technique. *FEBS Lett* 503, 135-141.
- Romorini, S., Piccoli, G., Jiang, M., Grossano, P., Tonna, N., Passafaro, M., Zhang, M., and Sala, C. (2004). A functional role of postsynaptic density-95-guanylate kinase-associated protein complex in regulating Shank assembly and stability to synapses. *J Neurosci* 24, 9391-9404.
- Roussignol, G., Ango, F., Romorini, S., Tu, J.C., Sala, C., Worley, P.F., Bockaert, J., and Fagni, L. (2005). Shank expression is sufficient to induce functional dendritic spine synapses in aspiny neurons. *J Neurosci* 25, 3560-3570.
- Sala, C., Piech, V., Wilson, N.R., Passafaro, M., Liu, G., and Sheng, M. (2001). Regulation of dendritic spine morphology and synaptic function by Shank and Homer. *Neuron* 31, 115-130.
- Sambrook, J., Maniatis, T. and Fritsch, E.F. (1989). *Molecular Cloning: A laboratory Manual*. (Cold Spring Harbor, New York).
- Sanger, F., Nicklen, S., and Coulson, A.R. (1977). DNA sequencing with chain-terminating inhibitors. *Proc Natl Acad Sci U S A* 74, 5463-5467.
- Sans, N., Petralia, R.S., Wang, Y.X., Blahos, J., 2nd, Hell, J.W., and Wenthold, R.J. (2000). A developmental change in NMDA receptor-associated proteins at hippocampal synapses. *J Neurosci* 20, 1260-1271.
- Sarrazin, S., Starck, J., Gonnet, C., Doubeikovski, A., Melet, F., and Morle, F. (2000). Negative and translation termination-dependent positive control of FLI-1 protein synthesis by conserved overlapping 5' upstream open reading frames in Fli-1 mRNA. *Mol Cell Biol* 20, 2959-2969.
- Satoh, K., Yanai, H., Senda, T., Kohu, K., Nakamura, T., Okumura, N., Matsumine, A., Kobayashi, S., Toyoshima, K., and Akiyama, T. (1997). DAP-1, a novel protein that interacts with the guanylate kinase-like domains of hDLG and PSD-95. *Genes Cells* 2, 415-424.

- Shi, J., Aamodt, S.M., and Constantine-Paton, M. (1997). Temporal correlations between functional and molecular changes in NMDA receptors and GABA neurotransmission in the superior colliculus. *J Neurosci* 17, 6264-6276.
- Short, J.D., and Pfarr, C.M. (2002). Translational regulation of the JunD messenger RNA. *J Biol Chem* 277, 32697-32705.
- Steward, O., and Schuman, E.M. (2003). Compartmentalized synthesis and degradation of proteins in neurons. *Neuron* 40, 347-359.
- Stoneley, M., and Willis, A.E. (2004). Cellular internal ribosome entry segments: structures, trans-acting factors and regulation of gene expression. *Oncogene* 23, 3200-3207.
- Takeuchi, M., Hata, Y., Hirao, K., Toyoda, A., Irie, M., and Takai, Y. (1997). SAPAPs. A family of PSD-95/SAP90-associated proteins localized at postsynaptic density. *J Biol Chem* 272, 11943-11951.
- Tang, W., and Tseng, H. (1999). A GC-rich sequence within the 5' untranslated region of human basonuclin mRNA inhibits its translation. *Gene* 237, 35-44.
- Timchenko, L.T., Iakova, P., Welm, A.L., Cai, Z.J., and Timchenko, N.A. (2002). Calreticulin interacts with C/EBPalpha and C/EBPbeta mRNAs and represses translation of C/EBP proteins. *Mol Cell Biol* 22, 7242-7257.
- Timchenko, N.A., Welm, A.L., Lu, X., and Timchenko, L.T. (1999). CUG repeat binding protein (CUGBP1) interacts with the 5' region of C/EBPbeta mRNA and regulates translation of C/EBPbeta isoforms. *Nucleic Acids Res* 27, 4517-4525.
- van der Velden, A.W., and Thomas, A.A. (1999). The role of the 5' untranslated region of an mRNA in translation regulation during development. *Int J Biochem Cell Biol* 31, 87-106.
- van Zundert, B., Yoshii, A., and Constantine-Paton, M. (2004). Receptor compartmentalization and trafficking at glutamate synapses: a developmental proposal. *Trends Neurosci* 27, 428-437.
- Vattem, K.M., and Wek, R.C. (2004). Reinitiation involving upstream ORFs regulates ATF4 mRNA translation in mammalian cells. *Proc Natl Acad Sci U S A* 101, 11269-11274.
- Wang, G., Guo, X., and Floros, J. (2005). Differences in the translation efficiency and mRNA stability mediated by 5'-UTR splice variants of human SP-A1 and SP-A2 genes. *Am J Physiol Lung Cell Mol Physiol* 289, L497-508.
- Wang, H., Iacoangeli, A., Popp, S., Muslimov, I.A., Imataka, H., Sonenberg, N., Lomakin, I.B., and Tiedge, H. (2002). Dendritic BC1 RNA: functional role in regulation of translation initiation. *J Neurosci* 22, 10232-10241.

- Wang, X.Q., and Rothnagel, J.A. (2004). 5'-untranslated regions with multiple upstream AUG codons can support low-level translation via leaky scanning and reinitiation. *Nucleic Acids Res* 32, 1382-1391.
- Welch, J.M., Wang, D., and Feng, G. (2004). Differential mRNA expression and protein localization of the SAP90/PSD-95-associated proteins (SAPAPs) in the nervous system of the mouse. *J Comp Neurol* 472, 24-39.
- Wilkie, G.S., Dickson, K.S., and Gray, N.K. (2003). Regulation of mRNA translation by 5'- and 3'-UTR-binding factors. *Trends Biochem Sci* 28, 182-188.
- Wood, M.W., VanDongen, H.M., and VanDongen, A.M. (1996). The 5'-untranslated region of the N-methyl-D-aspartate receptor NR2A subunit controls efficiency of translation. *J Biol Chem* 271, 8115-8120.
- Wu, G.Y., Deisseroth, K., and Tsien, R.W. (2001). Spaced stimuli stabilize MAPK pathway activation and its effects on dendritic morphology. *Nat Neurosci* 4, 151-158.
- Wu, H., Reissner, C., Kuhlendahl, S., Coblenz, B., Reuver, S., Kindler, S., Gundelfinger, E.D., and Garner, C.C. (2000). Intramolecular interactions regulate SAP97 binding to GKAP. *EMBO J* 19, 5740-5751.
- Xiong, W., Hsieh, C.C., Kurtz, A.J., Rabek, J.P., and Papaconstantinou, J. (2001). Regulation of CCAAT/enhancer-binding protein-beta isoform synthesis by alternative translational initiation at multiple AUG start sites. *Nucleic Acids Res* 29, 3087-3098.
- Yamada, Y., Chochi, Y., Ko, J.A., Sobue, K., and Inui, M. (1999). Activation of channel activity of the NMDA receptor-PSD-95 complex by guanylate kinase-associated protein (GKAP). *FEBS Lett* 458, 295-298.
- Yamauchi, T. (2002). Molecular constituents and phosphorylation-dependent regulation of the post-synaptic density. *Mass Spectrom Rev* 21, 266-286.
- Yao, I., Hata, Y., Hirao, K., Deguchi, M., Ide, N., Takeuchi, M., and Takai, Y. (1999). Synamon, a novel neuronal protein interacting with synapse-associated protein 90/postsynaptic density-95-associated protein. *J Biol Chem* 274, 27463-27466.
- Yao, I., Iida, J., Nishimura, W., and Hata, Y. (2003). Synaptic localization of SAPAP1, a synaptic membrane-associated protein. *Genes Cells* 8, 121-129.
- Yazgan, O., and Pfarr, C.M. (2001). Differential binding of the Menin tumor suppressor protein to JunD isoforms. *Cancer Res* 61, 916-920.
- Yazgan, O., and Pfarr, C.M. (2002). Regulation of two JunD isoforms by Jun N-terminal kinases. *J Biol Chem* 277, 29710-29718.



- Yoshii, A., Sheng, M.H., and Constantine-Paton, M. (2003). Eye opening induces a rapid dendritic localization of PSD-95 in central visual neurons. *Proc Natl Acad Sci U S A* *100*, 1334-1339.
- Zuker, M. (2003). Mfold web server for nucleic acid folding and hybridization prediction. *Nucleic Acids Res* *31*, 3406-3415.

**Appendix 1: List of Primers Used**1.1 Isolation of E1A, E1B and E1B<sup>+</sup> UTRs

Name	Sequence 5' – 3'	<sup>1</sup> Location
SAPAP3 AS6 RACE	CTTGATGTCAGGATCCCCACCACCAGGC	35-8
SAPAP3 5RA3	CTCGGTCGCCATGGTAACCCCTC	129-107
SAPAP3 5RA4:	ACAGAGTGAACCAGGTGCCGGATG	631-608
SAPAP3 5'-3 UTR	GTGCTTCGGACAGTCCCCTTTC	N.A
SAPAP3 5'-4 UTR	CGAAGACCCAGGAACCAGCAC	N.A
Y2HSAPAP3R	TTTTCTTTTTCGGCCGCCTCCCATCCTTGCCACCCGTG	1255-1235
SAPAP3-s14	AAAGCGGCCGCCAGAAGGCCGCTGCCTTGCC	1040-1021
SAPAP3 UTRas	CCGTCTAGATGCAGTTCTGCGTTTTATTTTTCC	N.A

<sup>1</sup>Locations with reference to the rat SAPAP mRNA (Genbank number: NM\_173138.1). N.A. refers to 5' and 3' UTR primers that bind to sequences not present in the reference mRNA.

1.2 Sequencing

Name	Sequence 5' – 3'	<sup>1</sup> Location
SAPAP3A	ATACCAGCGAGGTCCAGCAG	527-546
SAPAP3B	ACCGGGACTTGAGCTTCAAG	985-1004
SAPAP3C	ATCCCCGGAGTTCCATCCCT	1435-1454
SAPAP3D	CACCCTCGAGTTGGCACCGG	1877-1896

<sup>1</sup>Locations with reference to the rat SAPAP mRNA (Genbank number: NM\_173138.1). N.A. refers to 5' and 3' UTR primers that bind to sequences not present in the reference mRNA.

1.3 5'- & 3'-RACE PCR primers**10X Universal Primer A Mix (UPM)**

Long (0.4 mM):

CTAATACGACTCACTATAGGGCAAGCAGTGGTATCAACGCAGAGT–

Short (2 mM):

CTAATACGACTCACTATAGGGC

• **Nested Universal Primer A (NUP) AAGCAGTGGTATCAACGCAGAGT**

1.4 Construction of luciferase-related plasmids

Name	Sequence 5' – 3'
EMCVF-EcoRI	GAATACAAGCTTGGGCTGCAG
EMCVR-XhoI	CCGCTCGAGTCCATGGTTGTGGCAAGCT
pS3BF-MutF	ATGACTTCGAAAGTTTATGATCC
pS3BF-MutR	GGCCTCAGTAAAGGCTCTTC
3UTRS3FireF	CCCGCCGGGCCGCCAAG
3UTRS3FireR	GCTCTAGATGCAGTTCTGCGTTTTATTTTTCC

1.5 Generation of FS3 and S3-related plasmids

Name	Sequence 5' – 3'
Flag-SAPAP3F	GATTACAAGGATGACGACGATAAGAGGGGTTACCATGGCGACCG
Flag-SAPAP3R	CATGGTGCCAGTAAAGGGCTAGCGGATC
XbaI SAPAP3-5' D1-205	CTAGTCTAGAGTGGTGGGGATCCTGACATC
XbaI S3DSL45-150F	CTAGTCTAGAGACCGGGCCAGGAGCCAGTG

1.6 Primers for deletion of uORFs and main open reading frame AUGsa. Deletion of uAUG2+3

uAUG1R: CGTCCCATCCTTGATGTCAGGATC

uAUG2F: CCCC GGATGGAGGTTCTCTGG

b. Deletion of uAUG 2 or 3 (in combination with (a)).

del1AUGR: CGTCCCTTCCTTGATGTCAGGATC

del1AUGF: CCCC GGAAGGAGGTTCTCTGG

c. Deletion of uAUG1

d1uAUGR: TTA CTTGGTGCCGGCGGCCCG

duAUG1F: CCCC GACCGGAGCCCCGACCG

## d. Deletion of iAUGs 1 and 2 (iAUG-pS3 constructs)

S3var1F: CCAGCCCCGCTTTGCTGACCAAC

S3var2F: TACCTTCCCCAGGATGTACCCG

S3var2R: GCTAGCGGATCTGACGGTTCAC

1.7 Addition primers for cloning of SAPAP1 and 3 5' UTRs

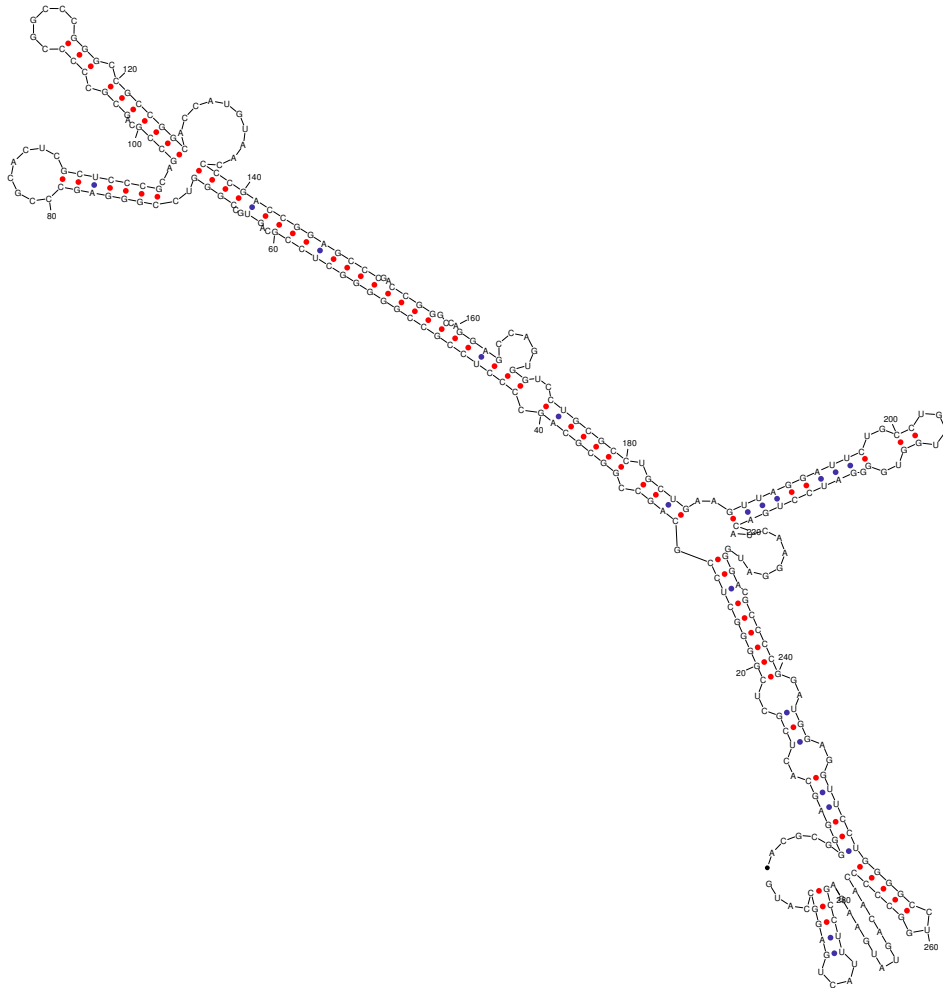
Name	Sequence 5' – 3'
SAPAP3 5'-1 UTR	GCACTCGCTCGGGGCTCCGC
SAPAP3 5'-3 UTR	GTGCTTCGGACAGTCCCCTTTC
SAPAP3 5'-3 UTR-R	GAAAGGGGACTGTCCGAAGCAC
SAPAP3 5'-4 UTR	CGAAGACCCAGGAACCAGCAC
SAPAP3-5' UTR5	TTCCTGGGTCCTCGGTGCAC
SAPAP3-5' F2	CTAGTCTAGACGCGGGGAGCACTCGCTC
SAPAP3-5'F2E	GAATTCGCGGCCGCTCAGCACTCGCTC
SAPAP3-5'F(XbaI)	CTAGTCTAGAGCGCGGCCGCTCAGCACTCGCTC
SAPAP3-5'F NheI	GCTAGCGCGGCCGCTCAGCACTCGCTC
SAPAP3-5'R NheI	GCTAGCCTCTTCATACTGTTGGGGGC
SAPAP1 5'-UTRF	GCTAGCCGAATTCCGAGTGACATCTG
SAPAP1 5' UTRR	GCTAGCTGCTGACTGGAAGCAATC

1.8 Primers for generation of pcDNA3.1(A)-mycHis-SAPAP3

SAPAP3F (EcoRI): GGAATTC ACTGAGGCCATGAGGGGTTACC

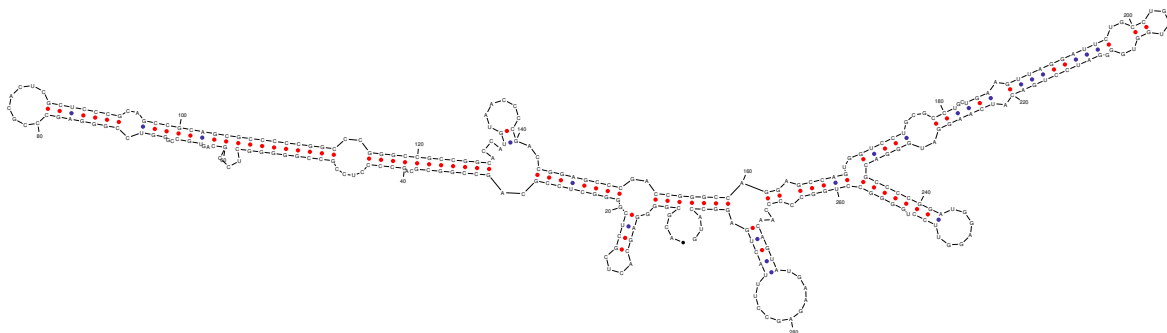
SAPAP3R (NotI-): ATAGTTTACGGCCGCACCAGCCTGGTCTGGGCCTC

plt22ps by D. Stewart and M. Zuker  
© 2004 Washington University



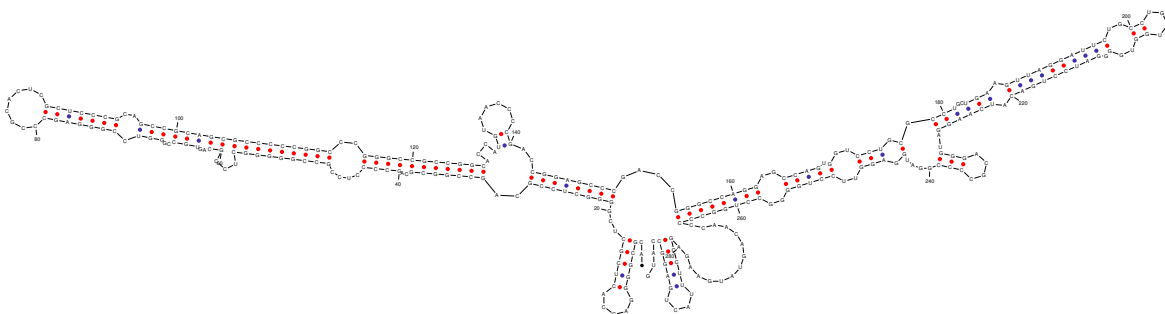
dG = -141.92 [initially -147.0] 04Sep12-02-13-04

plt22ps by D. Stewart and M. Zuker  
© 2004 Washington University



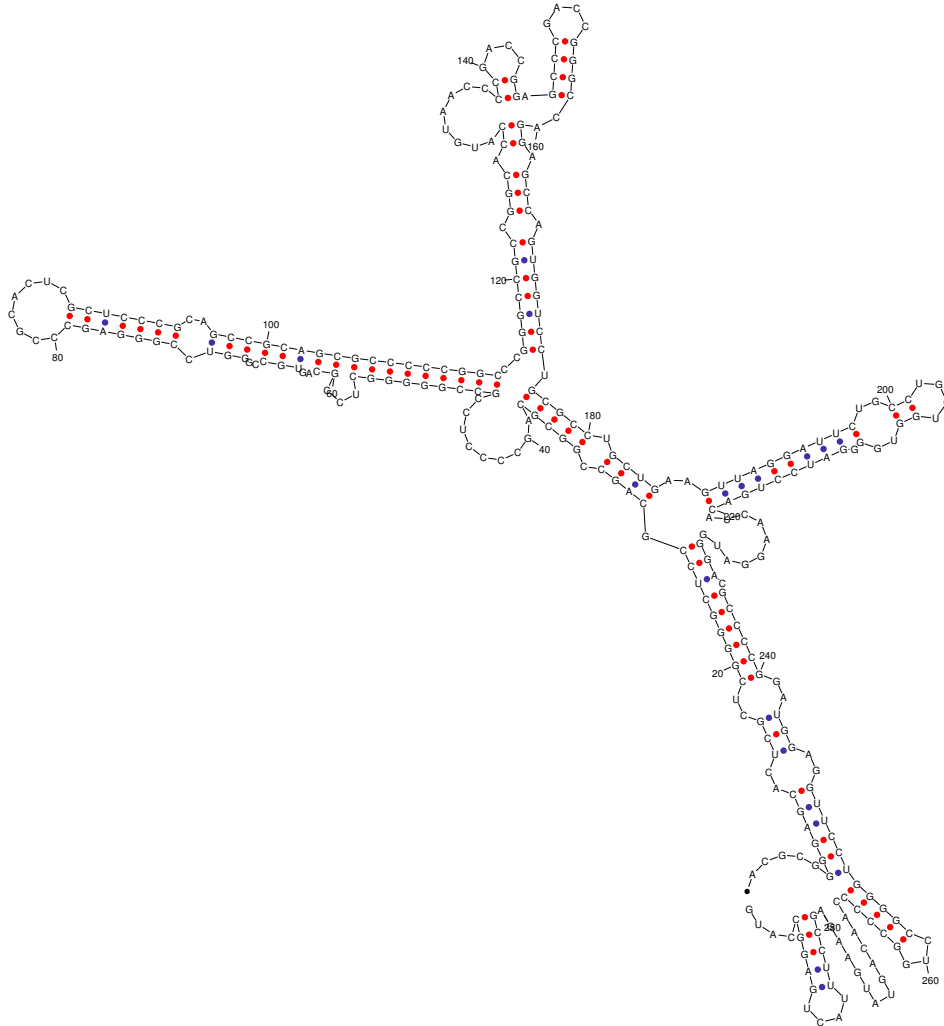
dG = -144.57 [initially -154.5] 04Sep12-02-13-04

plt22ps by D. Stewart and M. Zuker  
© 2004 Washington University



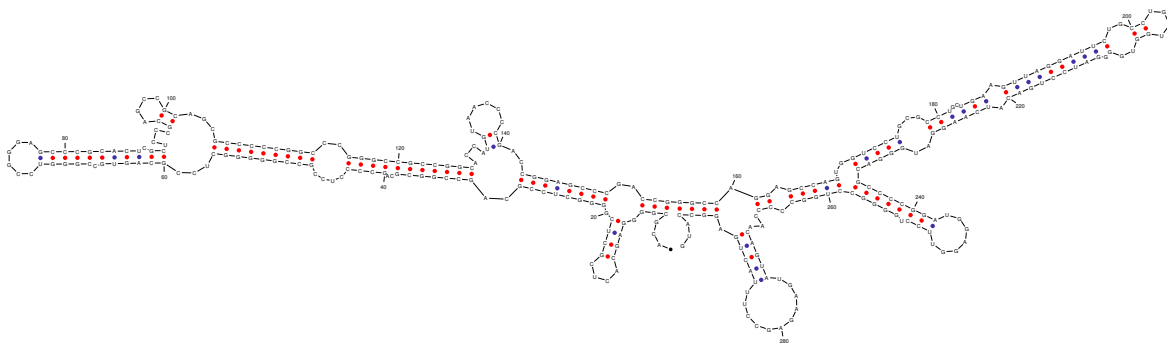
dG = -148.85 [initially -154.1] 04Sep12-02-13-04

plt22ps by D. Stewart and M. Zuker  
© 2004 Washington University



dG = -146.16 [initially -153.7] 04Sep12-02-13-04

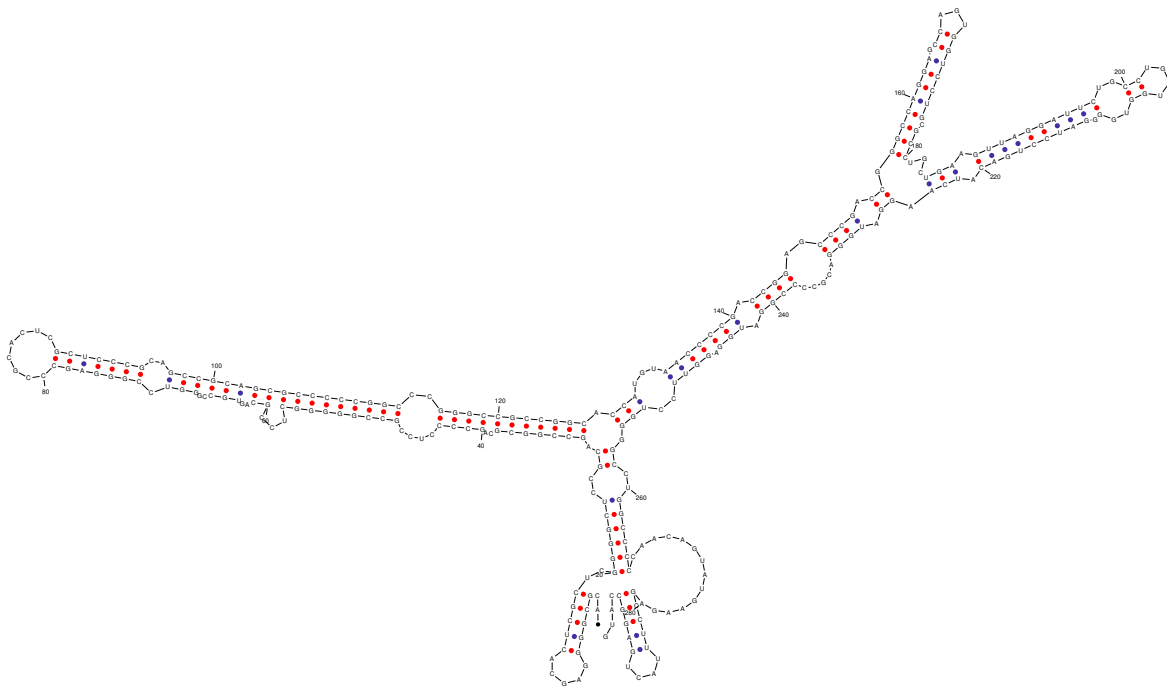
plt22ps by D. Stewart and M. Zuker  
© 2004 Washington University



dG = -140.31 [initially -153.6] 04Sep12-02-13-04

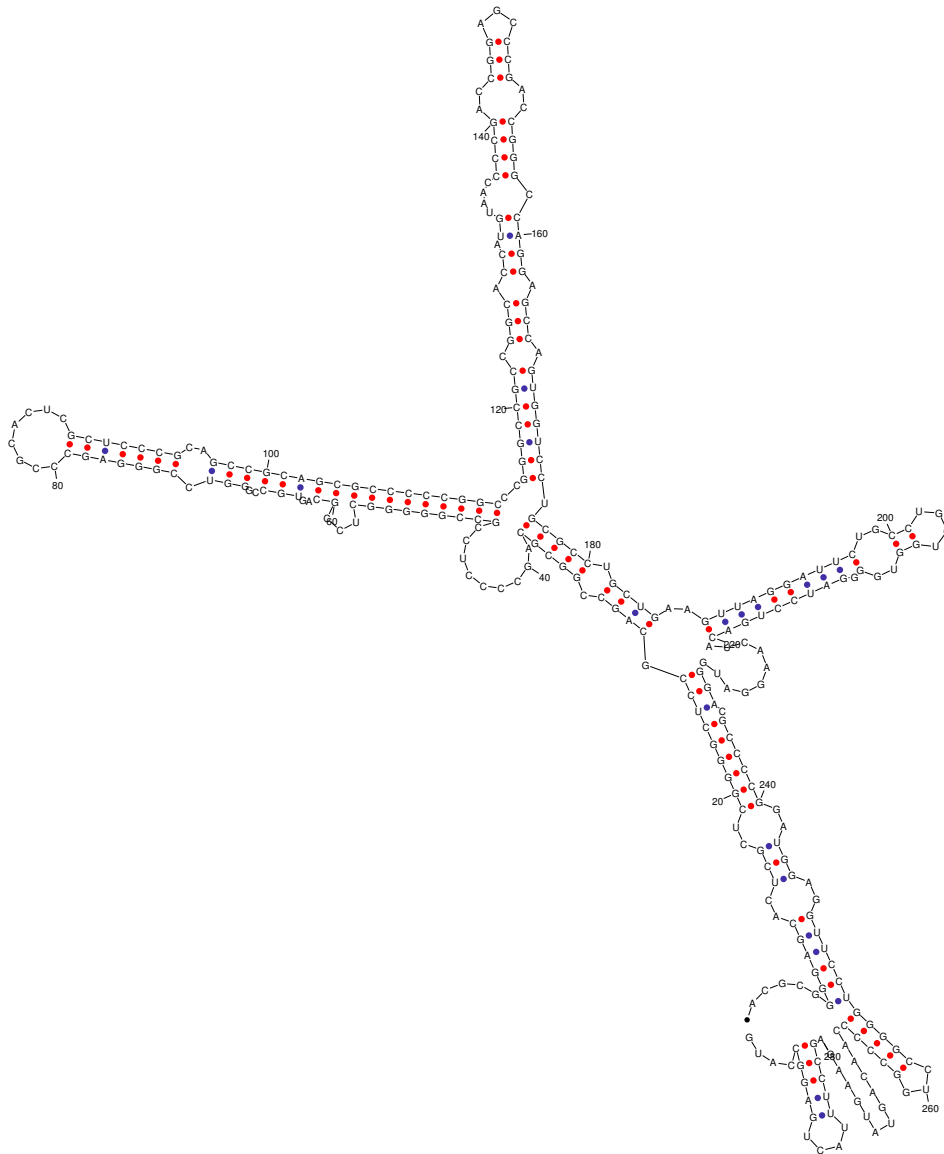


plt22ps by D. Stewart and M. Zuker  
© 2004 Washington University



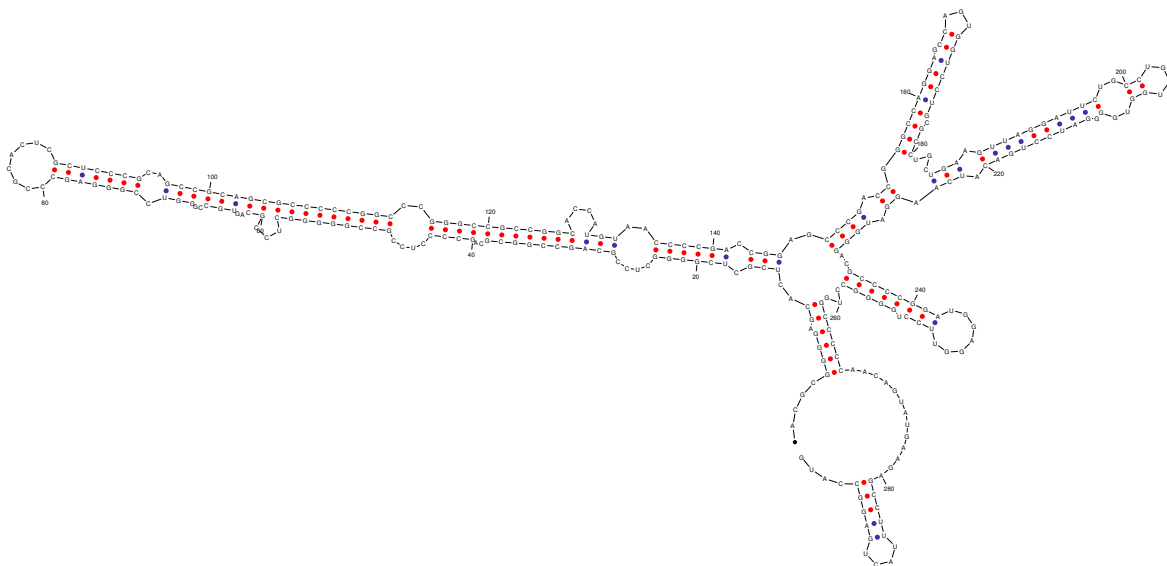
dG = -147.9 [initially -153.3] 04Sep12-02-13-04

plt22ps by D. Stewart and M. Zuker  
 © 2004 Washington University



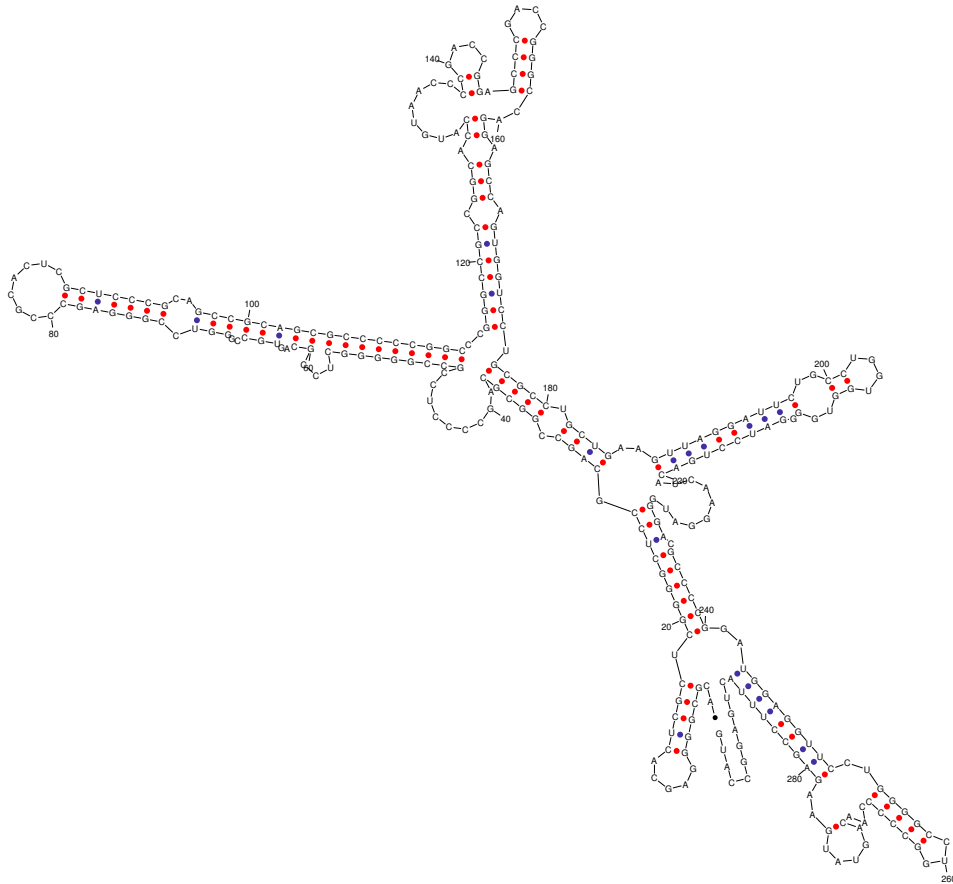
dG = -148.23 [initially -153.3] 04Sep12-02-13-04

plt22ps by D. Stewart and M. Zuker  
© 2004 Washington University



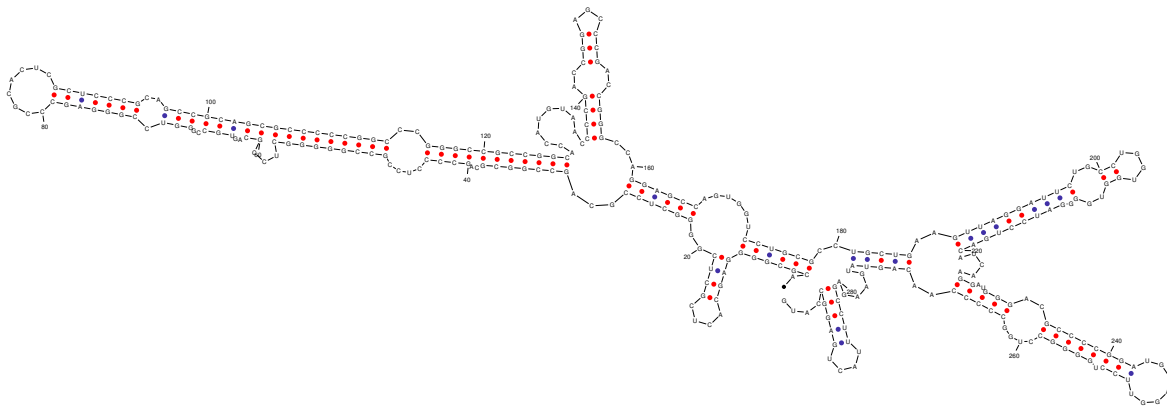
dG = -146.96 [initially -151.3] 04Sep12-02-13-04

plt22ps by D. Stewart and M. Zuker  
© 2004 Washington University



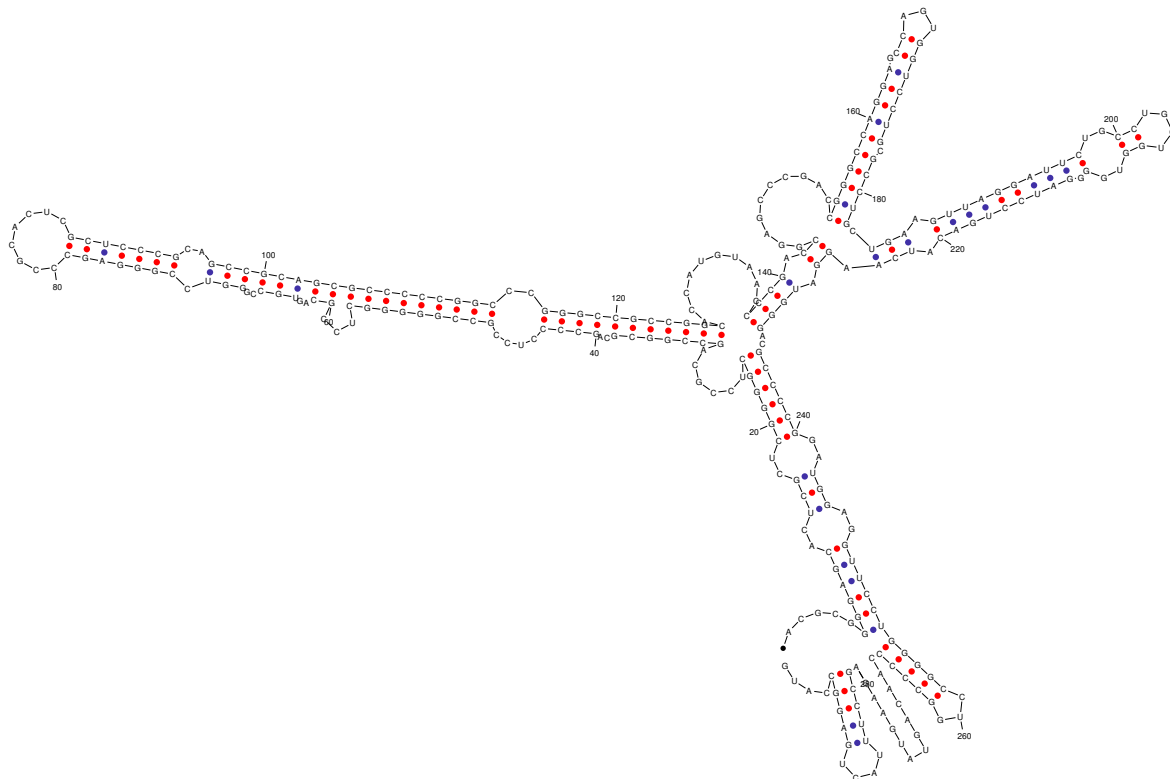
dG = -139.94 [initially -150.9] 04Sep12-02-13-04

plt22ps by D. Stewart and M. Zuker  
© 2004 Washington University



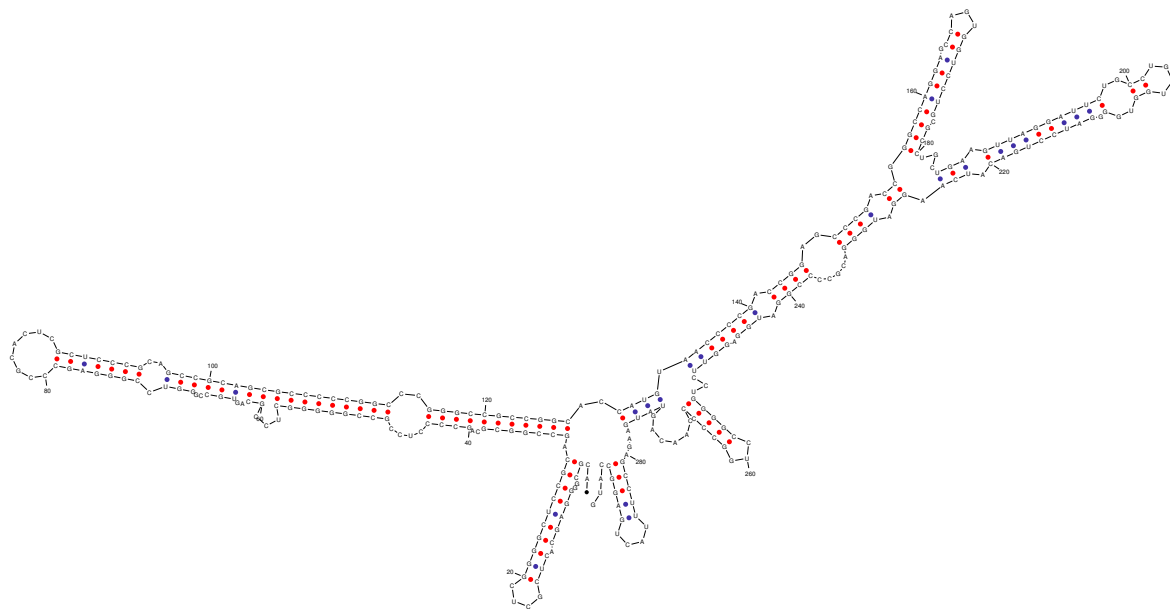
dG = -142.52 [initially -150.9] 04Sep12-02-13-04

plt22ps by D. Stewart and M. Zuker  
© 2004 Washington University



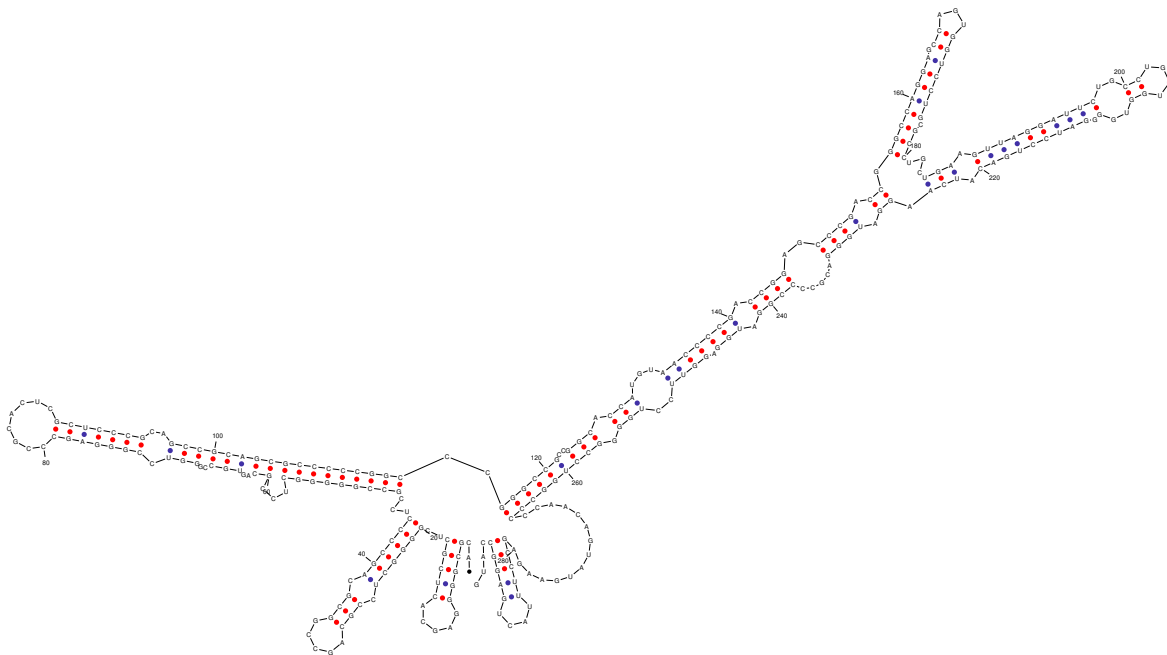
dG = -146.6 [initially -150.8] 04Sep12-02-13-04

plt22ps by D. Stewart and M. Zuker  
© 2004 Washington University



dG = -147.84 [initially -150.1] 04Sep12-02-13-04

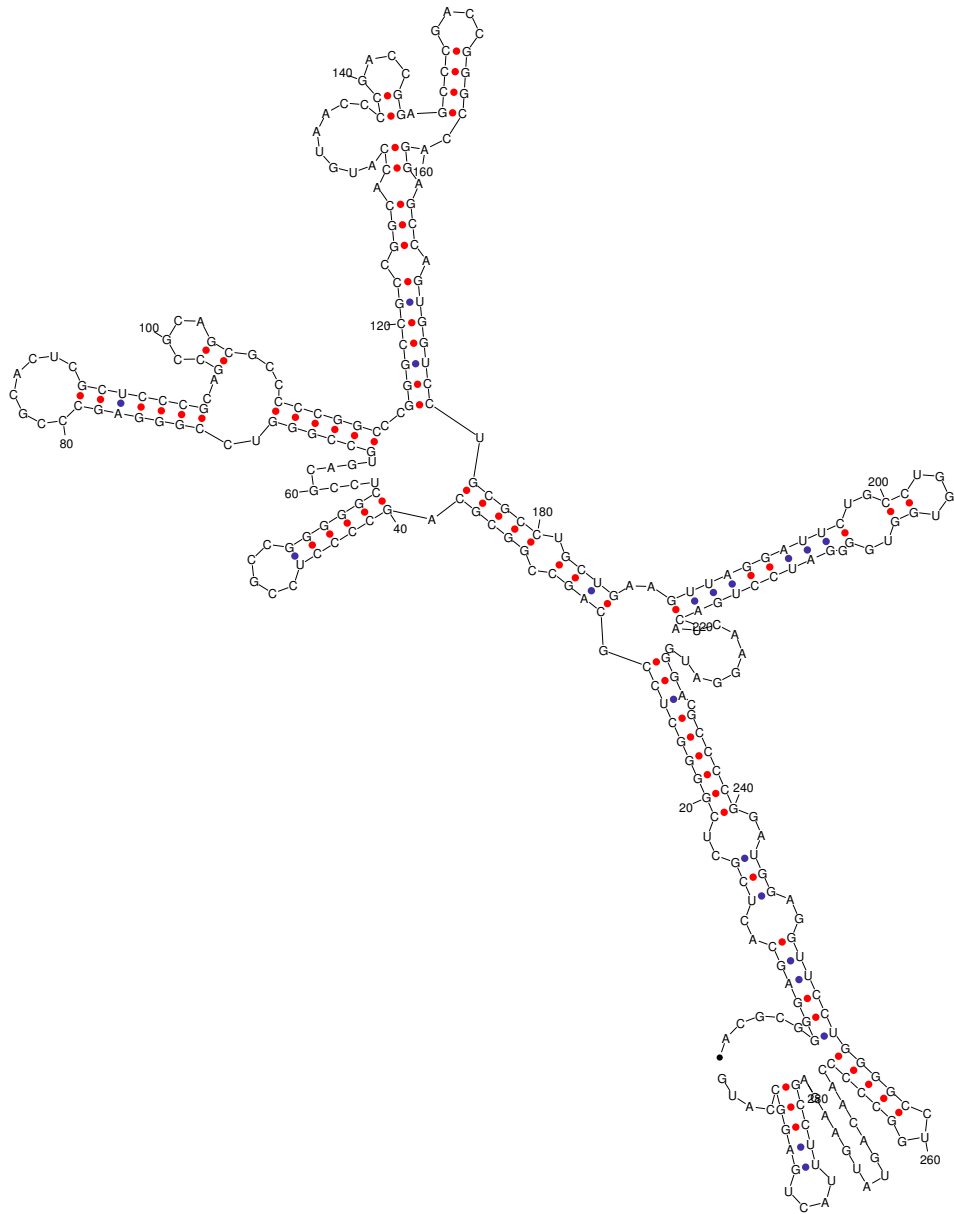
plt22ps by D. Stewart and M. Zuker  
© 2004 Washington University



dG = -147.8 [initially -150.1] 04Sep12-02-13-04

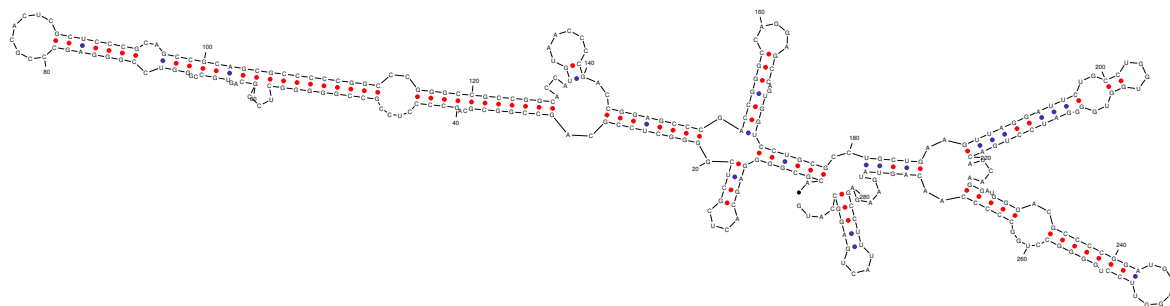


plt22ps by D. Stewart and M. Zuker  
 © 2004 Washington University



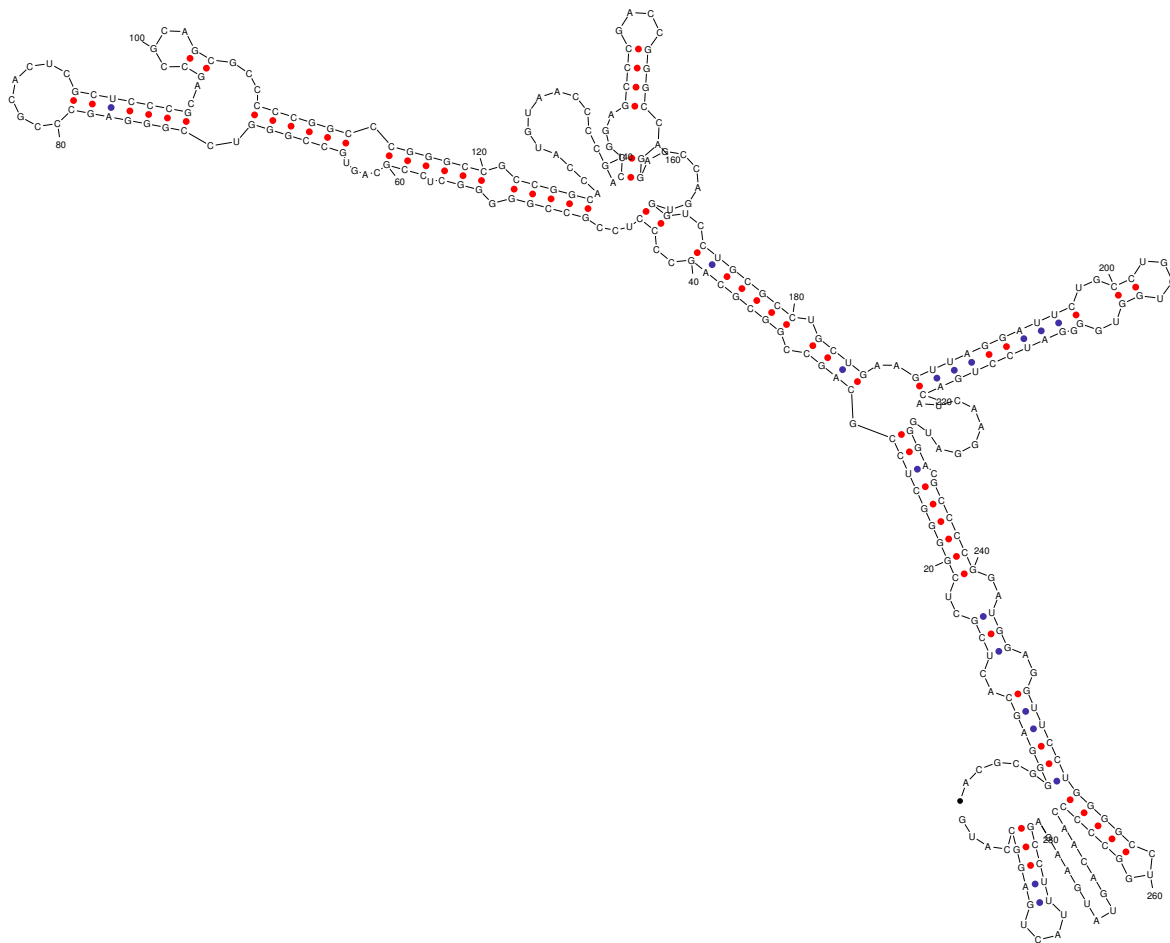
dG = -140.04 [initially -149.4] 04Sep12-02-13-04

plt22ps by D. Stewart and M. Zuker  
© 2004 Washington University



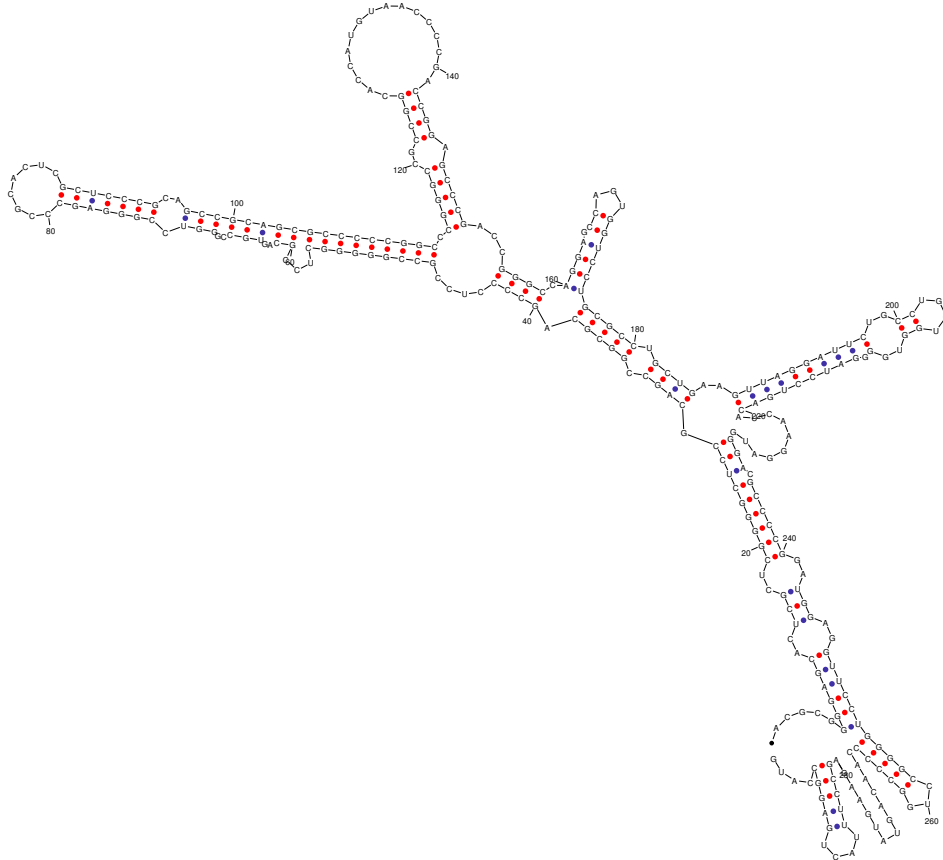
dG = -140.93 [initially -148.9] 04Sep12-02-13-04

plt22ps by D. Stewart and M. Zuker  
© 2004 Washington University



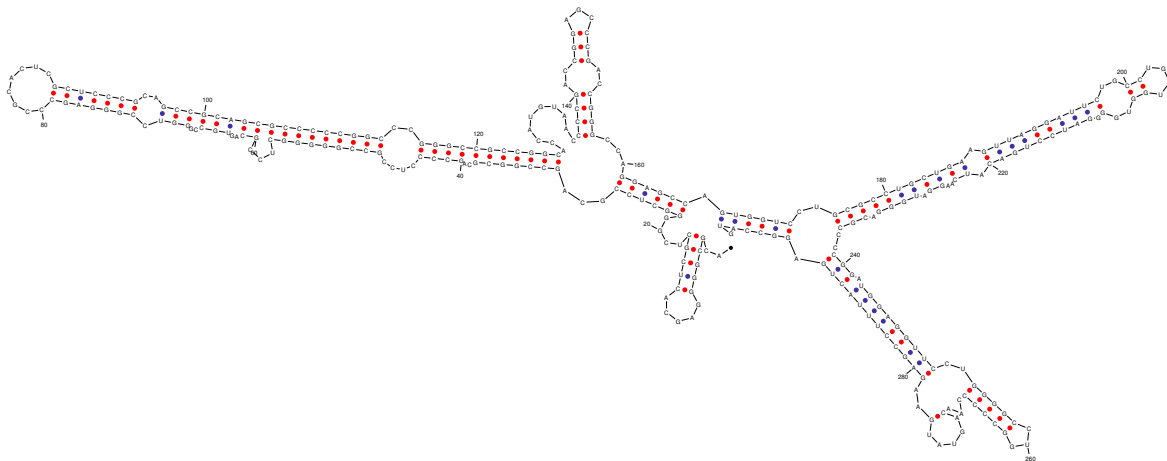
dG = -140.13 [initially -148.9] 04Sep12-02-13-04

plt22ps by D. Stewart and M. Zuker  
© 2004 Washington University



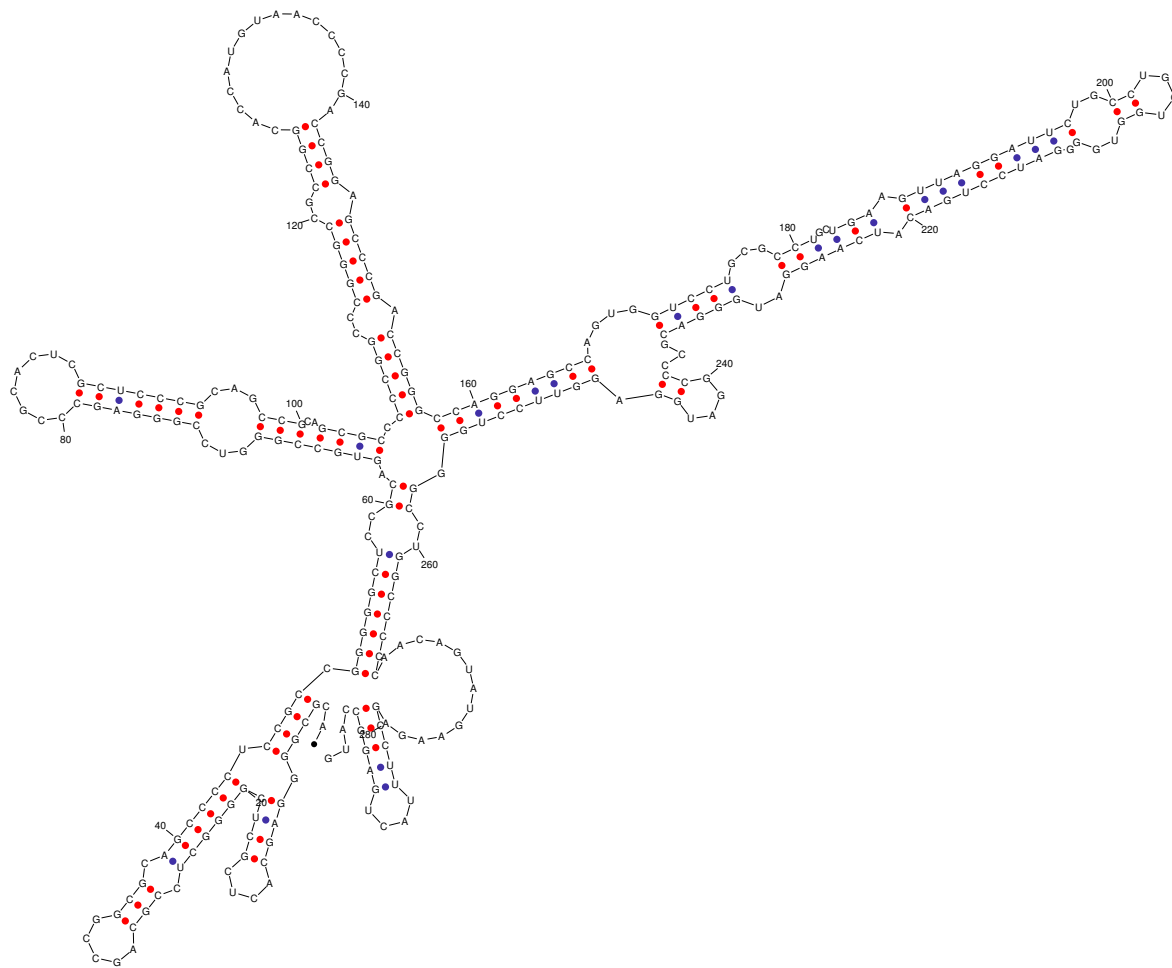
dG = -140.58 [initially -148.5] 04Sep12-02-13-04

plt22ps by D. Stewart and M. Zuker  
© 2004 Washington University



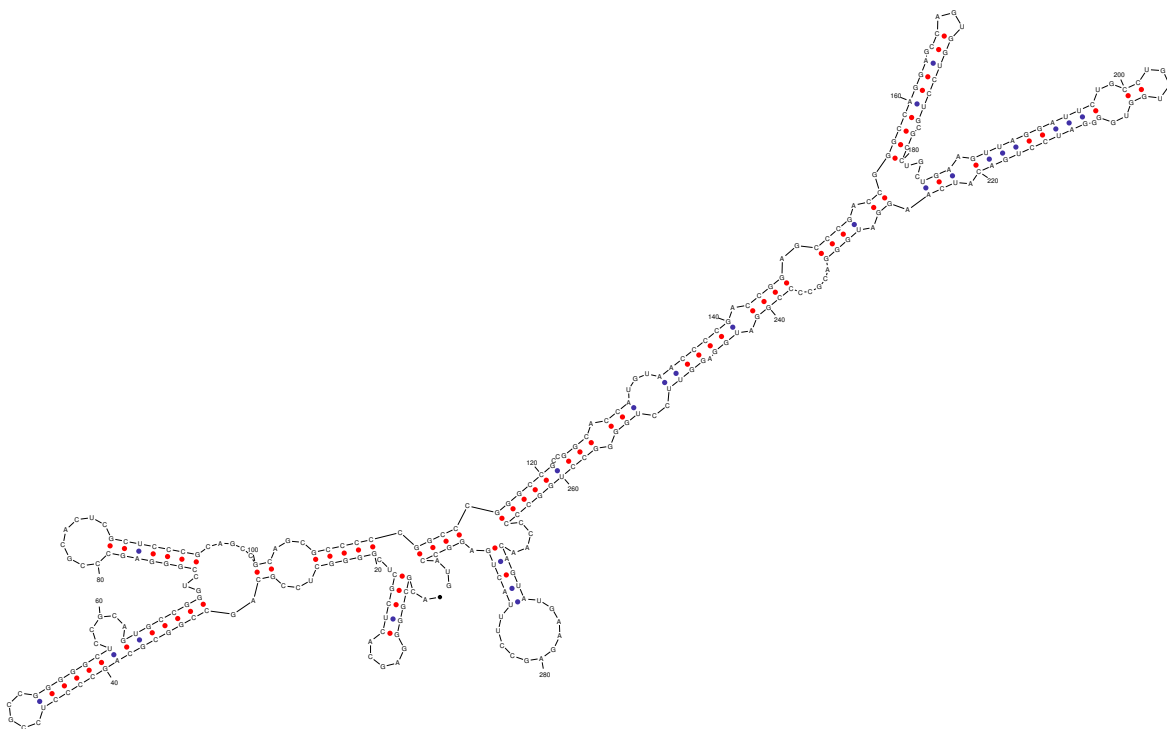
dG = -140.57 [initially -148.0] 04Sep12-02-13-04

plt22ps by D. Stewart and M. Zuker  
© 2004 Washington University



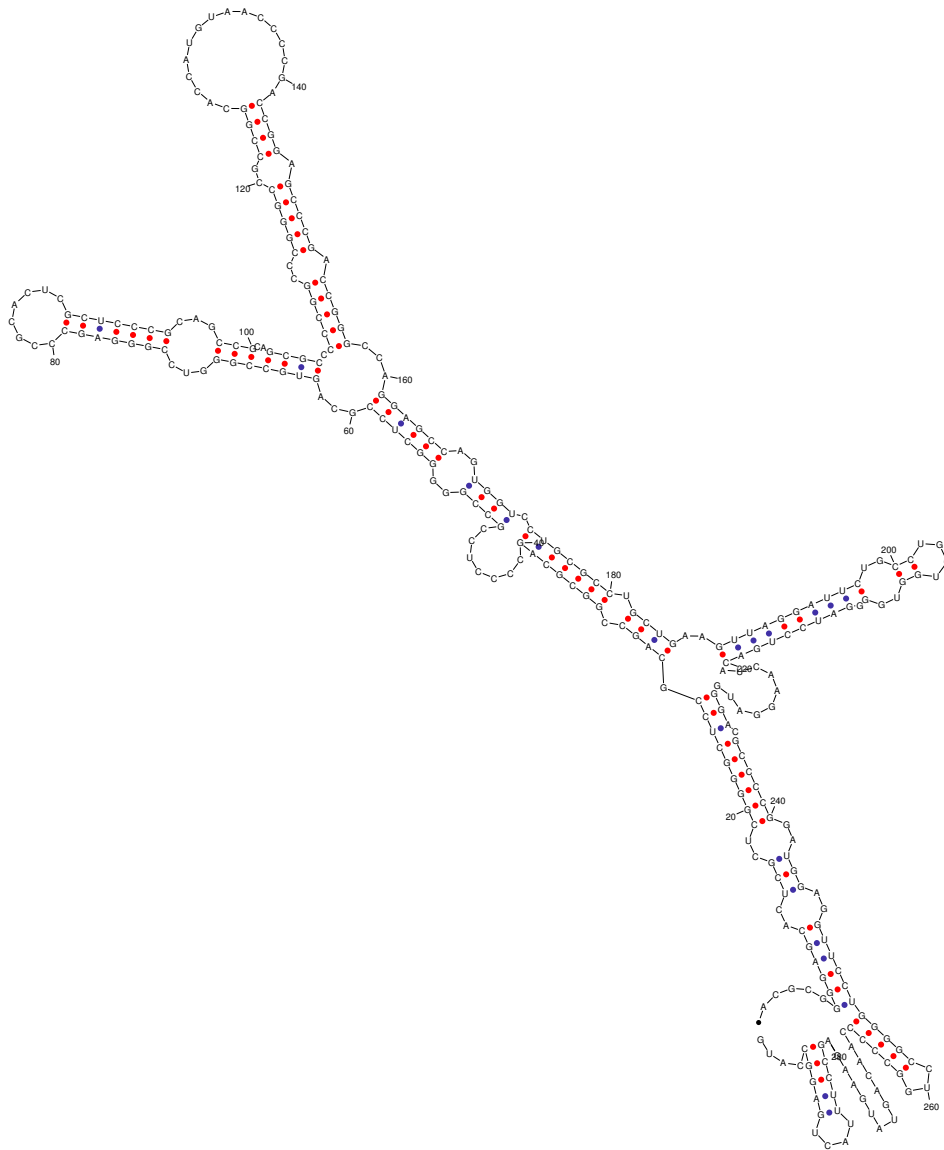
dG = -143.07 [initially -147.9] 04Sep12-02-13-04

plt22ps by D. Stewart and M. Zuker  
© 2004 Washington University



dG = -140.74 [initially -147.8] 04Sep12-02-13-04

plt22ps by D. Stewart and M. Zuker  
© 2004 Washington University



dG = -144.59 [initially -147.6] 04Sep12-02-13-04

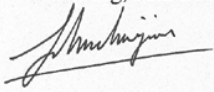


## Erklärung

Hiermit versichere ich, dass ich die vorliegende Arbeit selbständig und ohne fremde Hilfe verfasst, keine anderen als die angegebenen Hilfsmittel benutzt habe und die den verwendeten Werken wörtlich oder inhaltlich entnommenen Stellen als solche kenntlich gemacht habe.

Ferner versichere ich, dass ich mich zu keiner Zeit anderweitig um Erlangung des Doktorgrades beworben habe.

Hamburg, Mar 2006

A handwritten signature in black ink, appearing to read 'John Jia En Chua', written over a horizontal line.

John Jia En Chua